U S

Universitetet
i Stavanger

FACULTY OF SCIENCE AND TECHNOLOGY

MASTER'S THESIS

Study program/specialization: Master Offshore systems, Marine and subsea technology.	Spring semester, 2008 Open
Author: Thorgeir Anundsen	………………………………………… (signature author)
Supervisor: Arnfinn Nergaard	
Title of Master's Thesis: Operability comparison of three ultra-deepwater and harsh environment drilling vessels.	
ECTS: 30	
Subject headings: -Motion characteristics -Operation limitations -Harsh environment	Pages: ………………… + attachments/other: ………… Stavanger, ……………….. Date/year

Operability comparison of three ultra-deepwater and harsh environment drilling vessels.
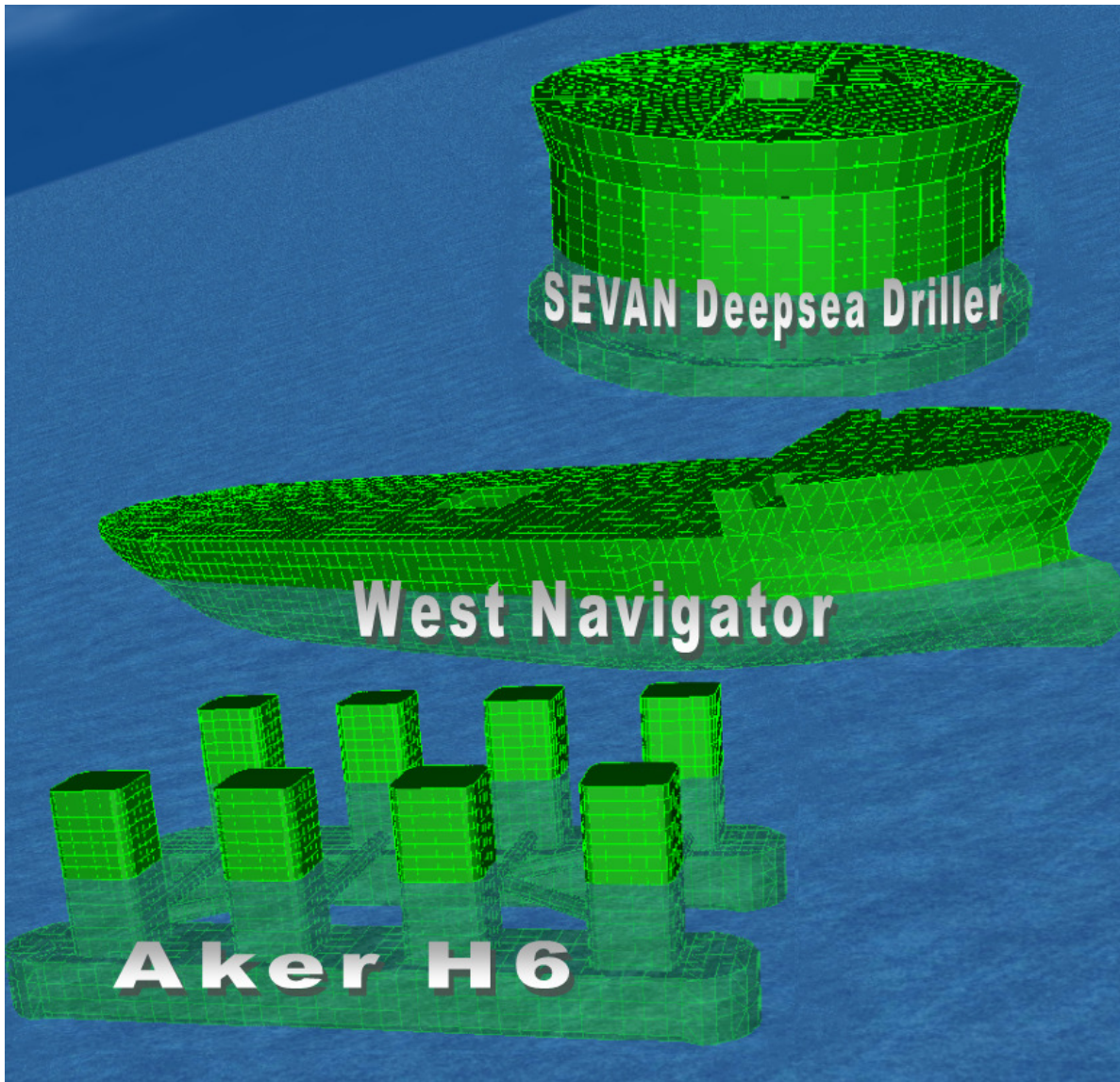
Thorgeir Anundsen

UiS

2008

Preface

Last semester I was given an assignment in the *Marine Technology* course which had the title: "Comparison of heave and roll behavior of a SEVAN platform, drillship and a semisubmersible". This spring I have continued the work on the subject, with emphasis on operability and harsh environments. The purpose of the project has been to gain knowledge on how different design principles of vessels contribute to the motion behavior, and to study the design principle's impact on the operability.

I am very grateful for the help offered by my supervisor

Dr. Eng. Arnfinn Nergaard, UiS

In addition I would like to thank Lars Rune Helland and Knut Holtan at Global Maritime for their help.

Stavanger June 2008

………………………..

Thorgeir Anundsen

Abstract

This report deals with how the design principles of different drilling vessels affect the motion characteristics and operability. Furthermore, the vertical heave limitation's influence on the operability has been analyzed. Drill strings and risers permit only minimal vertical relative motions between the vessel and the seabed. Seakeeping and wave load analyses are therefore very important in operability studies.

The motion behavior of the three analyzed vessel concepts can, due to the hull design, be described by very different characteristics. This manifests itself both in terms of natural periods, deck load capacities, waterline areas and dynamic amplification magnitudes. In addition, transit speed, price and build complexity are greatly affected by the design philosophy.

The operability of the vessels has been calculated for the "Southern Green Canyon" field in the Gulf of Mexico, the "Ormen Lange" field in the North Sea and for conditions typical for the west coast of Africa. The analyses show that all three vessels achieve a high operability in the Gulf of Mexico and west coast of Africa. In North Sea conditions, the SEVAN unit shows an unsatisfactory vertical response in the winter season, with a low operability as consequence. The operability in the mentioned areas can be seen in Table 1.

Vessel:	Total Operability (%)		
	North Sea	GoM	Africa
West Navigator:	96.4	100	100
SEVAN:	83.4	99.7	99.2
Aker H6:	98.2	100	100

Table 1: *Operability in three potential areas of operation.*

The operability can however be somewhat deceptive regarding indication of general motion behavior. In the most frequently encountered sea states the SEVAN unit performs better than the West Navigator in spite of lower operability. Furthermore, the West Navigator has in average twice the heave amplitudes compared to the Aker H6 under normal operational conditions.

Table of contents

Abbreviations

DDF	Deep Draft Floater
DOF	Degrees of Freedom
DP	Dynamic Positioning
FPSO	Floating Production Storage and Offloading
GM	Metacentric height
GoM	Gulf of Mexico
MODU	Mobile offshore drilling unit
PM	Pierson-Moskowitz
RAO	Response Amplitude Operator
Semi	Semisubmersible drilling rig
TLP	Tension Leg Platform
VCG	Vertical center of gravity
VDL	Variable deck load
WF	Wave Frequency

Symbols

a	Acceleration of fluid or structure
a	Distance from the axis of rotation to the centroid of the waterplane area.
A	Area
A_c	Cross section area column
A_{ij}	Added mass
A_w	Waterline area
b	Breath
B	Buoyancy center
B_0	Initial buoyancy center
b_0	Distance from centerline to centerline of hulls
b_c	Breath column
B_{ij}	Dampening coefficient
$B_{ij.critical}$	Critical dampening coefficient
C_A	Added mass coefficient
C_D	Drag coefficient
C_{ij}	Spring coefficient
d	Water depth
DAF	Dynamic amplification factor
F_3	Vertical excitation force

f_n	Natural frequency
g	Acceleration of gravity
G	Center of gravity
GM_0	Initial Metacentric height
G_ξ	Normalizing reference force
h	Height
H	Motion amplitude
$H(i\omega)$	Complex frequency response function
$H(\omega)$	Transfer function / RAO
H_s	Significant wave height
I	Moment of inertia
I_T	Transverse waterplane moment of inertia
$I_{T`}$	Transverse waterplane moment of inertia of individual element
k	Wave number
K_{ij}	Radius of gyration
l	Length
M	Metacenter
M_{ij}	Mass of structure
m_n	Spectral moments of order n
M_R	Restoring moment
N	Total number of cycles
n	Normal vector on the body surface pointing outwards into the fluid
n_o	Number of columns per hull
p	Pressure
r	Radius of gyration
$R(\omega)$	Response spectrum
S	Wetted Surface
$S(\omega)$	Wave spectrum
$s(\omega)$	Vessel elevation as a function of frequency
S_p	Average wave steepness
T	Time period / Duration
T_d	Damped natural period
T_p	Spectral peak period
T_R	Natural period
T_z	Zero-up-crossing period
u	Velocity
u´	Acceleration
u_0	Reference velocity

V	Volume
w	Width
w_c	Width column
z	Height from sea level
Δ	Displacement = ρ g $\forall$
$\forall$	Volume displacement of structure

Greek symbols

γ	Peak shape parameter
ζ	Damping level
ζ(t)	Water surface elevation
ζ_a	Wave amplitude
η_i	Displacement in *i* direction 1-6 (Surge, sway, heave, roll, pitch and yaw)
λ	Wave length
ρ	Mass density of water
σ	Spectral width parameter
Φ	Phase angle
Ω	Frequency ratio
ω_d	Damped natural frequency
ω_p	Spectral peak frequency
ω_R	Natural frequency

1 Introduction

High rig rates have led to an impressive newbuild program of vessels capable of operating in harsh environments and ultra deep waters, and global rig demand is expected to increase in the coming years. High oil and gas prices are positively influencing the demand, and as a result of the current low production capacity surplus and depleting reserves, oil and gas production from deepwater and harsh environment areas are expected to increase.

A unit designed for operation in both ultra deep and harsh environment needs to have both large deck load capacities and optimal motion characteristics. There is a possible conflict between increased drilling facility capacity and vessel motions required for operation in harsh areas. A large waterline area positively contributes to the drilling facility capacity, but often leads to reduced motion performance in severe weather.

Three vessels, which are designed to operate in both ultra deep water and harsh environments, will be analyzed in this report with respect to operability and general motion behavior: The semisubmersible *Aker H6*, the drillship *West Navigator* and the circular *SEVAN Deepsea Driller*. Will these rigs be both capable of operating in ultra deep water and harsh environments in an efficient manner?

In the past the deepwater drilling rig fleet was made up of semisubmersibles and drillships. Today, there is a new breed of circular drilling vessels, which combines the motion behavior of a semi with the deck load capacity of a drillship [24]. The distinctive circular hull design of the SEVAN unit has many benefits, and *SEVAN MARINE* claims that the unit has favorable heave and roll motions. If these claims are verified by the hydrodynamical analyses in the report, it would undoubtedly be a suitable platform for drilling operations.

The first chapters of the report will present the deepwater and harsh area markets and the wave theory behind the response analyses. The next sections concern general response of floating vessels, and is followed by the calculation procedure and operability limitations. The last chapter treats response behavior in specific weather conditions ranging from benign to very harsh.

The hydrodynamical loads and motion response have been calculated by use of the software package *MOSES*. In addition to this, a short- and long-term statistical model has been established in *Excel*. Hand calculations have been prepared in *Mathcad*. The files generated in these programs are enclosed on the CD attached to the report.

2 Deepwater and harsh area markets

The term deepwater in this thesis relates to water depths more than 300 meters. Very deep water refers to depths greater than 1000 meter, and ultra deep water refers to depths exceeding 2000 meter. About 58 billion barrels of oil equivalent total resources have been discovered in deep water from 18 basins on six continents, they report, with the majority of the resources from the Gulf of Mexico, Brazil and West Africa [20]. Only 25 percent of the total resources are developed or under development, and less than 5 percent have been produced, which illustrates the immaturity of deepwater exploration and production.

Offshore oil production is still dominated by benign and shallow water resources. Oil production from harsh environment areas currently represents approximately 7 % of the global production, while deepwater areas represent only 5% of the production. A breakdown of the world oil supply is shown in **Figure 2.1.**
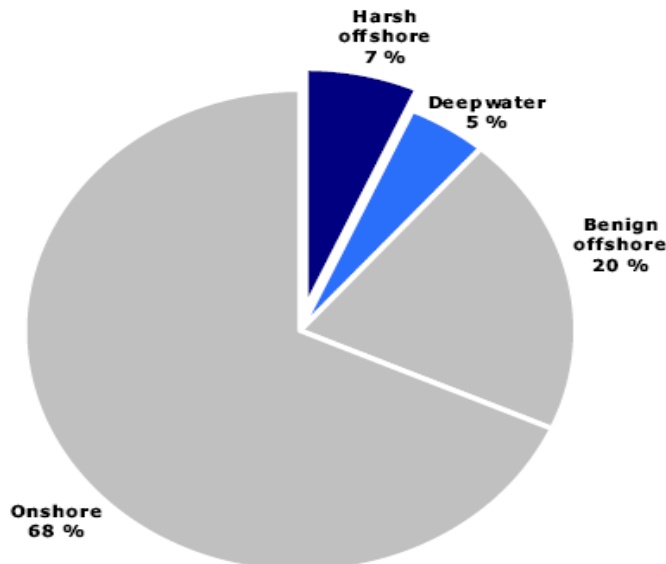
Figure 2.1: *World oil supply 2005. Source: Pareto, DTI, NPD and Douglas Westwood.*

Deepwater and harsh environment areas offer major growth prospects for producers to meet future oil and gas demands. Main areas of existing and prospective deepwater and harsh environment oil and gas resources include West Africa, Brazil, US Gulf of Mexico, North Atlantic/North Sea, Barents Sea, Sakhalin, East Canada/Greenland and Australia.

The growth within deepwater oil and gas production is expected to grow substantially during the next few years. Most of this growth will come from discoveries already made, as the lead-time to put new significant deepwater and harsh environment oil and gas fields on stream is substantial.

During the last couple of years, the world's deepwater reserves have more than doubled. Deepwater resources are currently one of the main areas of new offshore exploration efforts, as well as main areas for offshore production growth over the next few years. Drilling activity is planned in the Barents Sea, in the deepwater areas of the Norwegian Sea and in the North Sea. Global activity targeting deepwater reserves is therefore expected to result in a major growth in demand for offshore contractors.

In addition to deepwater resources, harsh environment areas may hold significant oil and gas reserves. Main areas include the Arctic region (Barents Sea and Kara Sea), the Norwegian Continental Shelf, Canada, the Atlantic margin and Greenland. According to US Geological Science, the Arctic region may hold as much as 75bn boe of reserves representing 25 per cent of world undiscovered oil and gas resources [20].

2.1 Potential areas of operation

All three vessels analyzed are ultra-deep water units, and three potential operating areas are analyzed: Southern Green Canyon in the Gulf of Mexico, west coast of Africa and the Ormen Lange field in the North Sea. Southern Green Canyon in the Gulf of Mexico and West coast of Africa are areas with relatively mild environment and very deep to ultra deep waters, whereas the Ormen Lange in the North Sea is a very deep area characterized as extremely harsh. Scatter diagrams for each area have been obtained, all of them describing the sea state by the parameters spectral peak period and significant wave height. Scatter diagrams for each location can be found in appendix 4.

2.1.1 North Sea – Ormen Lange

Figure 2.2: *Ormen Lange field (Google Earth).*

Ormen Lange is located 120 km North West of Kristiansund in the Norwegian Sea in 850 m to 1100 m water depth, and was the first true deepwater project in Norway, see **Figure 2.2**. Drilling operations where commenced by the West Navigator on 31st October 2004 and drilling will continue until 2013. The field is located in an area with extreme weather conditions and sub-zero water temperatures at the seabed [22]. The sea states in the area can be described by a JONSWAP spectrum with an average peak shape coefficient of 3.3.

2.1.2 GoM – Southern Green Canyon

The average water depth in the area is around 1350 m, and the sea states can be described by a JONSWAP spectrum with an average peak shape coefficient of 2. The environment is much less severe than in the North Sea, and one can experience long periods with very small waves.
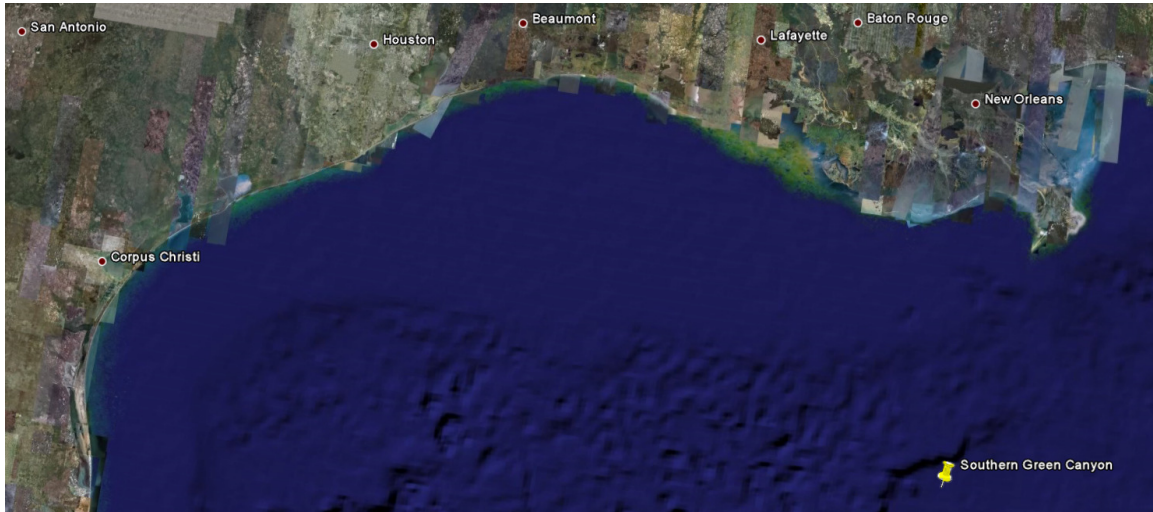
Figure 2.3: *Southern Green Canyon in the Gulf of Mexico (Google Earth).*

2.1.3 West coast Africa

The region has a benign weather environment with oilfields located in shallow to ultra deep water. However, one major concern in the area is occurrence of swells. These are waves arriving from a distant source, and since the wave length and period gradually increase along the path, the wave periods are high, usually between ten to twenty seconds.

In spite of relatively small wave amplitudes, these waves can cause heavy vessel oscillations due to wave periods being close to the vessel's natural periods. Special attention must be given to swell coming from a different direction than wind seas. This can for example cause heavy rolling of a drill ship, and must be taken into consideration in estimation of design loads. From an operability point of view it is however not easy to predict how much of the time the swell and wind seas have different directions, and they are therefore assumed to have the same bearing.

The sea states can be described by a JONSWAP spectrum with an average peak shape coefficient of 2.

3 Wave theory

Linear wave theory is normally sufficiently accurate for column-stabilized units like semi submersibles, and the other drilling units considered [6]. Furthermore should linear theory always be used in connection with stochastic response analysis, and relevant results are presented in equation 3.1 to 3.3 [9]. Since the vessels analyzed are intended for deepwater areas, only deepwater water particle behavior is considered. Figure 3.1 shows the properties of regular travelling waves.

Dynamic pressure:
$$\rho \cdot g \cdot \zeta_a \cdot e^{\frac{\omega^2}{g} \cdot z} \cdot \cos(kx - \omega t)$$
Equation 3.1

Vertical particle velocity:
$$\rho \cdot \zeta_a \cdot \omega \cdot e^{\frac{\omega^2}{g} z} \cdot \sin(kx - \omega t)$$
Equation 3.2

Vertical particle acceleration:
$$-\rho \cdot \zeta_a \cdot \omega^2 \cdot e^{\frac{\omega^2}{g} z} \cdot \cos(kx - \omega t)$$
Equation 3.3
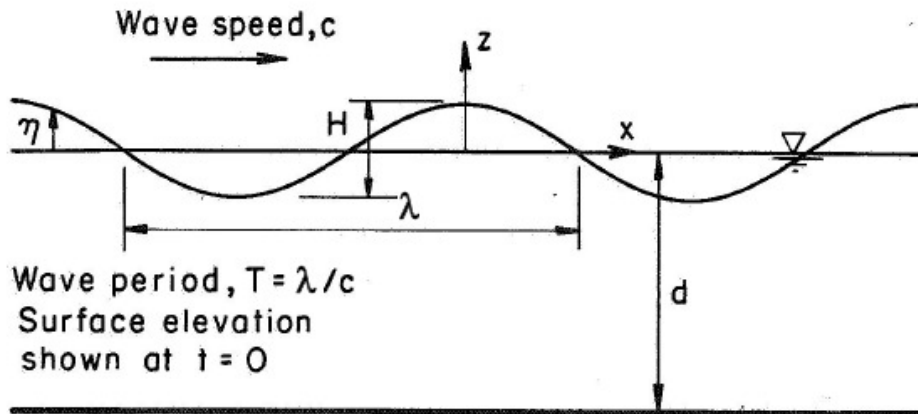
Figure 3.1: *Linear waves.*

3.1 Hydrodynamic forces

In order to make a fairly accurate estimate of the forces affecting a submerged body, it is important to classify the structure hydrodynamically. **Figure 3.2** can be a useful tool when judging whether viscous effects or different types of potential flow are most important.
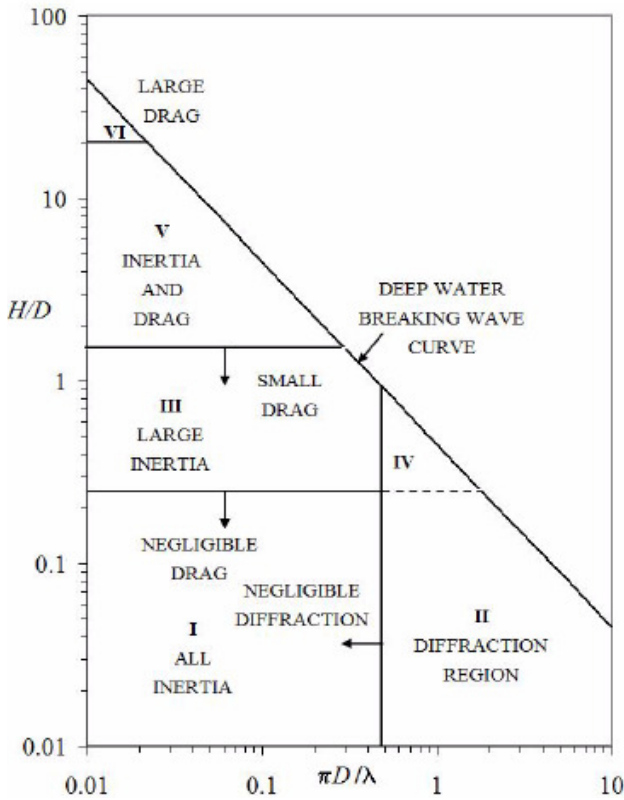
Figure 3.2: *Different wave force regimes [6].*

If the structural dimensions are small relative to the wave length, so that the incident wave is nearly undisturbed, the structure is classified as hydrodynamically transparent. To calculate forces on such structures, the Morison equation is introduced, which superposes inertia and drag forces. The magnitude of the respective forces depends on inertia and drag coefficients. DNV RP-C205 states that Morison's load formula is applicable when $\lambda > 5D$, where D is the diameter of the structure.

Structures having dimensions of the same order as the wave length, so that the incident wave field is significantly disturbed by the structure, are called hydrodynamically compact or large volume structures. The calculation of wave forces on these structures can be carried out using potential theory, as drag forces are of less significance.

Examples of large volume structures are GBS platforms, ships, FPSO`s, Spars and to a certain extent semisubmersibles. A semisubmersible may require a Morison load model for slender braces in addition to radiation/diffraction analyses [5].

Since it is possible to obtain results in irregular seas by linearly superposing results from regular wave components, it is sufficient from a hydrodynamical point of view to analyze the structure in incident regular sinusoidal waves of small wave steepness [1].

The hydrodynamical forces on a floater can be divided into two sub categories:

A: Forces on the body when it is restrained from oscillating and there are incident regular waves. These forces are called *excitation forces*.

B: Forces on the body that arises from the oscillation of the body with the same frequency as the incident waves in sub-problem *A*. There are no incident waves. The hydrodynamic loads are called *added mass, damping* and *restoring forces.*

Due to the linearity assumption the forces *A* and *B* can be superposed in estimation of the total hydrodynamic load.

3.1.1 Wave exciting inertia forces

The wave exciting inertia forces consist of two different inertia loads. One effect comes from the unsteady pressure induced by the undisturbed wave, and is called the Froude-Krylov force. In addition to the Froude-Krylov force that originates from the undisturbed wave pressure, a hydrodynamic mass diffraction force acts on the structure. This force is obtained by integration of the pressure field arising from the relative acceleration between the structural component and the wetted surface. This inertia force is superposed on the Froude-Krylov force in presence of wave induced pressure field.

The Froude-Krylov force can be expressed as [9]

$$F_{FK} = -\int p\mathbf{n}\,dS$$

<div align="right">**Equation 3.4**</div>

where

$\mathbf{n}$ = The normal vector on the body surface pointing outwards into the fluid
p = Pressure
S = Wetted surface

If all surfaces of the body are wetted, and the diameter of the structure $\ll \lambda$, the Froude-Krylov force can be approximated to a product of displaced water mass and water particle acceleration.

$$F_{FK} = \rho \cdot \forall \cdot a$$

<div align="right">**Equation 3.5**</div>

For all structures which penetrate the water surface, the pressure integration has to be performed according to equation 3.4. Froude-Krylov forces depend exclusively upon the acceleration of the external flow, while the hydrodynamic mass force is proportional to the relative acceleration between the external flow and the moving body.

The hydrodynamic mass term is not a physical mass as such, but is caused be a rise in the undisturbed pressure because of the presence of the submerged body, and arises exclusively from the relative acceleration between structure and fluid.

3.1.2 Added mass, damping and restoring terms

The added mass and damping loads are steady-state hydrodynamic forces and moments due to forced harmonic rigid body motions, with no incident waves [1]. However, the forced vertical oscillation of the vessel generates outgoing waves. The heave motion causes fluid to oscillate which means that there is a pressure field in the fluid.

The restoring term is related to the relative change in buoyancy, due to the vertical displacement of the vessel. The force can be associated with the spring force in a mass-damper-spring system.

Added mass is often misunderstood to be a finite amount of water that oscillates rigidly connected to the body. This is not the case, and fluid will oscillate with different amplitude throughout the fluid, and decay far away from the body. The added mass term can be derived from pressure distribution, and the equivalent amount of oscillating mass is dependent on the frequency of oscillation.

As mentioned earlier, the Morison equation superposes inertia and drag forces. The drag part of the Morison equation is dependent on the drag coefficient, the relative velocity and the projected area. The Morison equation for horizontal forces on a vertical rigid cylinder can be written as

$$F_{Morison} = \frac{1}{2} \cdot \rho \cdot C_D \cdot D \cdot |u| \cdot u + \frac{1}{4} \cdot \pi \cdot \rho \cdot C_M \cdot D^2 \cdot u' \qquad \textbf{Equation 3.6}$$

3.1.3 Forces on hydrodynamical compact structures

When forces on hydrodynamically transparent structures are calculated, water particle velocity and acceleration in the region of the structure are assumed not to differ from the values at the cylinder axis. With large structural diameters, usually for $D > \lambda/6$, the incident wave is significantly disturbed by the structure. According to potential theory, the pressure distribution and the corresponding forces can be calculated from the velocity potential. This method of calculation can be quite complex, and appropriate numerical solutions have been developed.

The most common numerical methods for solution of potential flow is boundary element method, where the velocity potential in the fluid domain is represented by a distribution of sources over the mean wetted body surface [6].

3.1.4 Non-linear wave effects

The earlier discussed wave loads are all forces that oscillate with the same frequency as the wave elevation. Different hydrodynamic effects are important for each floater type, and must be taken into account in the analysis and design. The wave frequency motions are mainly linearly excited motions in the wave-frequency range of significant wave energy. Higher order wave loads yield high frequency resonant motions, springing and ringing of TLP`s and gravity based structures. They are excited by non-linear wave effects. Similar non-linear effects cause low frequency drift motions. For a moored structure it occurs in surge, sway and yaw. Some of the effects can be linearised and included in a so-called frequency domain approach, while others are highly non-linear and can only be handled in time-domain. These analyzing techniques will be explained in chapter 6.1 and 6.2.

An example of a non-linear force is the drag load acting on the braces of a semi submersible. The drag part of the Morison equation can in a simplified form be expressed as

$$F_d = C_d \cdot \frac{\rho}{2} \cdot A \cdot u \cdot |u|$$

Equation 3.7

where A is the projected area of the braces.

If we introduce the local orbit velocity and a reference velocity u_0 the non linear drag term can be obtained as

$$F_d = C_d \cdot \frac{\rho}{2} \cdot A \cdot u_0^2 \cdot \cos(\omega t) \cdot |\cos(\omega t)|$$

Equation 3.8

The term $\cos(\omega t) |\cos(\omega t)|$ can be developed into a series and we obtain the approximate drag force [9]:

$$F_d = \left(\frac{8}{3\pi} \cdot \cos(\omega \cdot t) + \frac{8}{15 \cdot \pi} \cdot \cos(3\omega \cdot t) \right) \cdot C_d \cdot \frac{\rho}{2} \cdot u_0 \cdot A$$

Equation 3.9

The drag force thus consists of a linear component with the same frequency as the wave elevation, and an additional term with the triple frequency. In reality it also contains higher order (5ω, 7ω etc.) components which normally are of less significance. This phenomenon can be of great significance for offshore structures, since a lower frequency wave can produce higher frequency resonance.

The drag force must be linearised if the dynamic equation of motion is to be solved in the frequency domain. Only then can solutions be arbitrarily superposed. If a linearized drag coefficient is introduced, the drag force can be expressed as

$$F_{dl} = C_{dl} \cdot \frac{\rho}{2} \cdot A \cdot u \qquad\qquad \textbf{Equation 3.10}$$

where the linearized drag coefficient, C_{dl} can be given as

$$C_{dl} = \frac{8}{3\pi} \cdot C_d \cdot \zeta_a \cdot \omega \cdot e^{kz} \qquad\qquad \textbf{Equation 3.11}$$

If the structural component in addition moves harmonically with velocity *s* in the wave field, then the relative velocity is to be introduced and we obtain

$$C_{dl} = \frac{8}{3\pi} \cdot C_d \cdot (u(z) - s) \qquad\qquad \textbf{Equation 3.12}$$

The linearized drag force corresponds to the first term of equation 3.9. Since the superimposed motion *s* is unknown, the solutions must be obtained by iteration, for which special algorithms exist.

When the vessel's response characteristics are calculated in the hydrodynamical software package MOSES, viscous damping is added for all vessels, although it is not so important for the drill ship since it is dominated by radiation damping. Especially the semisubmersible would have an extremely high RAO peak at resonance without viscous damping, due to low radiation damping. By default MOSES linearizes harmonically via the linearization technique above, but can also perform a spectral linearization if it is told to do so. In this report the described harmonic linearization technique is used.

4 Statistical description of waves

The sea surface consists of a pattern of waves with various periods, heights and phase angles. The water surface elevation $\xi(t)$ at a fixed location in the sea is a random process which can be modeled as a long-term non-stationary process over a period of years [16]. However, for short term intervals, of the order of some hours, the surface elevation can be approximated as a stationary process. That is a sea state in which the significant wave height and mean wave period are assumed constant during the time considered.

The long term variation of a wave climate can be described in terms of generic distributions or in terms of governing sea state parameters. Long term statistics are associated with non-stationary processes occurring over a period of months and years, and long term data for wave conditions are commonly given in the form of a scatter diagram. A scatter diagram provides the frequency of occurrence of a given parameter pair (e.g. T_p and H_s).

The second-order statistics of a stationary surface elevation process are described by the mean square spectral density function $S(\omega_n)$. In this study $\xi(t)$ is considered to be a zero mean, Gaussian, stationary process and is represented by a linear summation of an infinite number of sinusoids with phase angles randomly distributed between 0 and 2π.

Since the wave profile is assumed to be the sum of sine and cosine functions, the wave process can be described by a Fourier series. We neglect non-linear effects and make use of linear superposition.

The water surface is given as [16]:

$$\xi(t) = a_0 + \sum_{n=1}^{N} \left(a_n \frac{\cos \cdot 2n\,\pi}{T} \cdot t + b_n \cdot \sin \cdot \frac{2n\,\pi}{T} \cdot t \right) \qquad \textbf{Equation 4.1}$$

where T is the time interval investigated

The constants a_0, b_n and a_n can be given as

$$b_n = \frac{2}{T} \cdot \int_{-\frac{T}{2}}^{\frac{T}{2}} \xi(t) \cdot \frac{\sin \cdot 2n\,\pi}{T}\, dt \qquad a_0 = \frac{1}{T} \cdot \int_{-\frac{T}{2}}^{\frac{T}{2}} \xi(t)\, dt \qquad a_n = \frac{2}{T} \cdot \int_{-\frac{T}{2}}^{\frac{T}{2}} \xi(t) \cdot \frac{\cos \cdot 2n\,\pi}{T}\, dt \quad \textbf{Equation 4.2}$$

Since we assume that $\xi(t)$ has its origin at mean sea level $a_0=0$ and $\xi(t)$ can be written as

$$\xi(t) = \sum_{n=1}^{N} \left(a_n \cdot \cos \cdot \omega_n \cdot t + b_{n\omega} \cdot \sin \cdot \omega_n \cdot t \right)$$

Equation 4.3

This function can also be expressed as

$$\xi(t) = \sum_{n=1}^{N} \left(\xi_n \cdot \cos \left(\omega_n \cdot t - \theta_n \right) \right)$$

Equation 4.4

where

$$\theta_n = \tan^{-1} \left(\frac{a_n}{b_n} \right) \qquad\qquad \xi_n = \sqrt{a_n^2 + b_n^2}$$

Equation 4.5

The energy in a harmonic wave is proportional to the amplitude squared, and the energy density function is given as

$$S(\omega_n) = \frac{1}{2} \cdot \frac{\zeta_n^2}{\Delta\omega}$$

Equation 4.6

where $\Delta\omega$ is the increment in frequency, $2\pi/T$. In **Figure 4.1** the energy distribution for 7 wave components is shown.
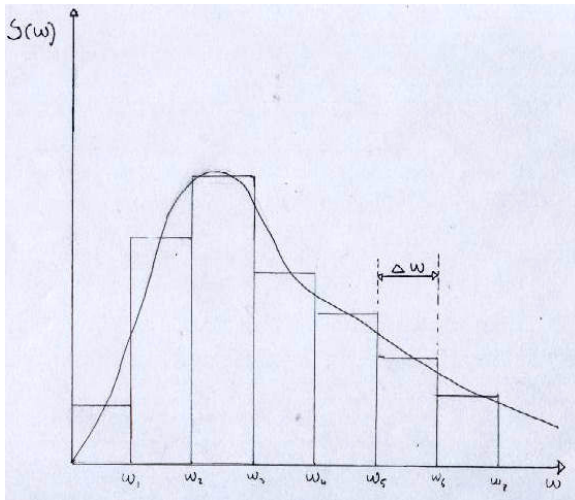
Figure 4.1: *Energy distribution over discrete frequency intervals*

If we let the period of observation, T, increase, then $\Delta\omega$ will decrease. If we let T→∞, $\Delta\omega$→0, and S(ω) becomes a continuous function.

The phase angles θ_n for the n different components, are more or less randomly distributed from 0 to 2π. If we undertake a new investigation immediately after T/2 with a duration of T, we can make a new calculation of S(ω) and θ_n. If we compare the new surface elevation function, $\xi(t)$, with the previous, we realize that they are completely different. However, the wave spectrum S(ω) related to the two periods will be similar.

If we compare the phase spectra's for the two periods, we find that they are entirely different, which indicates that the waves are statistical by nature, and therefore can be described by statistical methods.

A stationary sea state can be characterized by a set of environmental set of parameters such as *significant wave height H_s* and the *peak period T_p*. The significant wave height is defined as the average height of the highest one-third waves in the indicated time period. The peak period T_p is the wave period determined by the inverse of the frequency at which a wave energy spectrum has its maximum value. The *zero-up-crossing period T_z* is also used some times. It describes the average time interval between two successive up-crossings of the mean sea level, and can in combination with a JONSWAP spectrum be given as [6]:

$$T_z = T_p \left(0.6673 + 0.05037\,\gamma - 0.006 \cdot \gamma^2 + 0.0003341 \cdot \gamma^3 \right)$$

Equation 4.7

The significant wave height is an important parameter in statistical analysis for several reasons. The statistical distribution of wave heights and most energy spectrum analyses are related to the significant wave height, and the major portion of the wave energy surrounds it [10].

The wave conditions in a sea state can be divided into two classes: *wind seas* and *swell*. Wind seas are generated by local wind while swells have no relationship to the local wind. Swells are waves that have traveled out of the areas where they were generated. Note that several swell components may be present at a given location.

4.1 Wave Spectra

Wave spectra describe the power spectral density of the vertical sea surface displacement. Wave spectra can be given in table form, as measured spectra, or by a parameterized analytic formula. The most appropriate wave spectrum depends on the geographical area with local bathymetry and severity of the sea state.

Under the design stage of an offshore structure, spectra describing the actual sea state in the relevant area of operation are not always available. We can however make us of standardized analytical wave spectra. Two of these spectra are:

- Pierson-Moskowitz spectrum
- JONSWAP spectrum

Various idealized spectra are used to describe the sea state. The Pierson-Moskowitz spectrum (PM) and JONSWAP spectrum are frequently applied for wind induced seas. The PM was originally proposed for fully-developed sea, and the JONSWAP (Joint North Sea Wave Project) spectrum extends to include fetch limited seas. Both spectra describe wind sea conditions that often occur for the most severe sea states. A two peak spectrum may be used to account for both wind generated sea and swell, like the Torsethaugen spectrum.

A Pierson-Moskowitz wave spectrum representing fully developed seas is applicable when the growth of the waves is not limited by the size of the generation area. Unless the spectrum peak period is close to a major peak in the response transfer function (e.g. a resonance peak) the Pierson-Moskowitz spectrum is assumed to give acceptable results [6]. The Pierson-Moskowitz spectrum can be given as

$$S_{PM}(\omega) = \frac{5}{16} \cdot H_s^2 \cdot \omega_p^4 \cdot (\omega)^{-5} \cdot e^{\left[-\frac{5}{4} \cdot \left(\frac{\omega}{\omega_p} \right)^{-4} \right]}$$

Equation 4.8

where $\omega_p = 2\pi/T_p$ is the angular spectral peak frequency.

The JONSWAP wave spectrum is a peak enhanced Pierson-Moskowitz spectrum and takes into account the imbalance of energy flow in a sea state when the waves are in the process of growing under strong winds; i.e. the seas are not fully developed. This is the case for extreme wave conditions in the North Sea. The JONSWAP wave spectrum is usually applied for ultimate strength analyses of structures operating in harsh environments. The JONSWAP spectrum is a modified PM spectrum and can be given as

$$S_J(\omega) = S_{PM}(\omega) \cdot A_\gamma \cdot \gamma^{e^{\left[-0.5 \left(\frac{\omega - \omega_p}{\sigma \cdot \omega_p} \right)^2 \right]}}$$

Equation 4.9

where

γ = Peak shape parameter
A_γ = Normalizing factor
σ = Spectral width parameter

Figure 4.2 shows the difference between a Pierson-Moskowitz spectrum and a JONSWAP spectrum with a peak shape parameter γ of 3.33. For $\gamma = 1$ the JONSWAP spectrum reduces to the Pierson-Moskowitz spectrum.
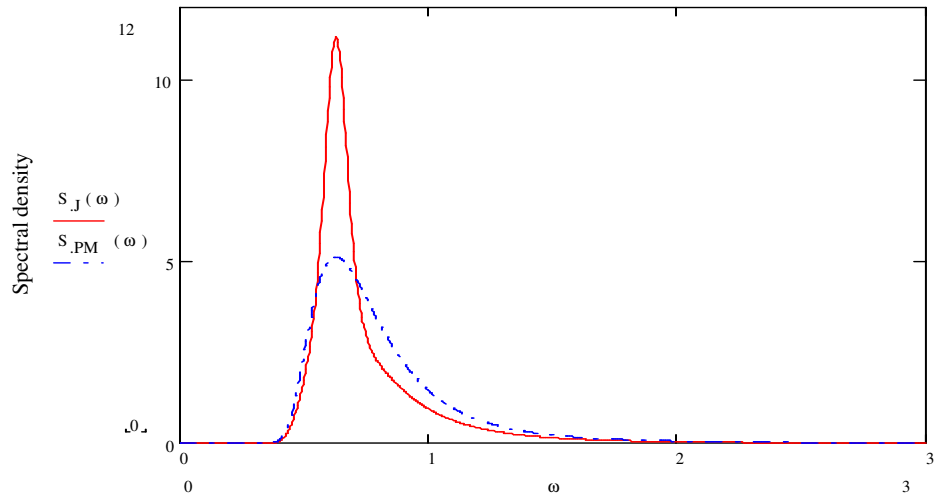
Figure 4.2: *Comparison of a Pierson-Moskowitz and a JONSWAP spectrum.*

5 Definition of motions

The vessels motions are important in relation to operating capabilities, helicopter operations and personnel comfort. In addition to this, vessel accelerations affect equipment and cargo aboard by introducing an inertia load. The cargo is also affected by the rotation of the vessel, as the rotation changes the direction of gravity relative to the structure.

A floating structure may respond with motions in three different time scales; wave frequency motions, low frequency motions and high frequency motions [5]. The oscillatory rigid-body translatory motions are referred to as surge, sway and heave, and are motions in the x-, y- and z-axis respectively. The oscillatory angular motions around the x-, y- and z- axis are referred to as roll, pitch and yaw respectively, see **Figure 5.1**.

A right-handed coordinate system is used, and the translatory displacements in the x-,y- and z-directions are called η_1, η_2, and η_3 respectively. This means that η_1 is surge, η_2 is sway and η_3 is the heave displacements. Furthermore, η_4, η_5, and η_6 are the angular displacement around the x-, y- and z- axis respectively.

The orientation of the vessels relative to the prevailing sea is indicated with an angle, as shown in **Figure 5.1**.
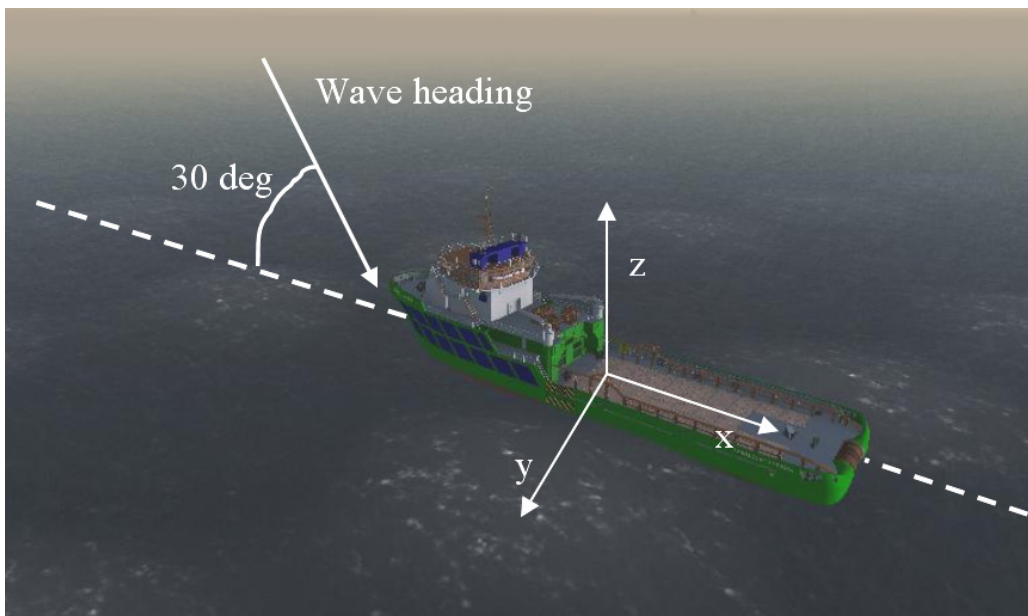
Figure 5.1: *Supply ship with waves coming in at 30 deg "off bow".*

In MOSES the system of axes is rotated 180 degrees, which means that head seas is coming from 180 deg and beam seas is coming from 90 degrees. This is because of the vessel definition with the x-axis running from fore to aft.

6 Dynamic equation of motion

Under effect of harmonic excitation forces, floating structures experience rigid-body oscillations, which depend on their total mass, damping and restoring forces. These terms can be illustrated in a simplified damped spring-mass idealization of the system, see **Figure 6.1**. A vessel oscillating in vertical direction can be described as a linear system of one degree of freedom, which consists of a spring, damper and a mass. The total mass, M_{33}, includes the mass of the structure, the "trapped" water mass enclosed by structural components, and the hydrodynamic mass which results from the relative acceleration between structure and fluid.
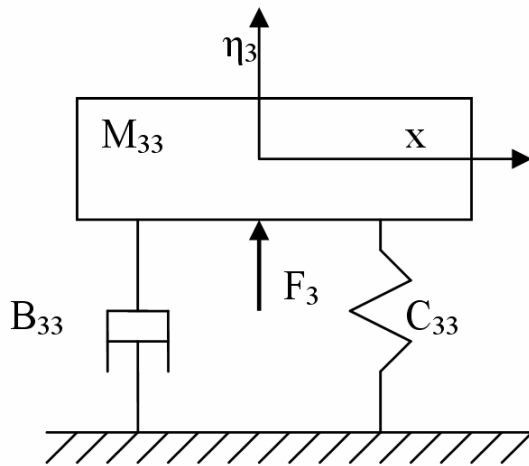
Figure 6.1: *Simplified single degree of freedom model.*

The damping force, $B_{33*}\dot{\eta}_3$, can be related to either structural damping or fluid damping, the latter associated with drag and wave radiation. Finally, the restoring forces, $C_{33*}\eta_3$, arise from relative change of buoyancy forces compared to the structure's displacement.

The dynamic equation of motion is written as [2]:

$$M_{33} \cdot \frac{d^2}{dt^2} \eta_3 + B_{33} \cdot \frac{d}{dt} \cdot \eta_3 + C_{33} \cdot \eta_3 = F_3(t)$$

Equation 6.1

There are two completely different ways to solve equation 6.1

- Frequency domain analysis
- Time domain analysis

The most common representation of signals and waveforms in general is in the time domain. However, many signal analysis techniques work only in the frequency domain. Frequency domain is a term that is used to describe the analysis of signals or

mathematical functions with respect to frequency. **Figure 6.2** shows the connection between frequency domain and time domain representation of a certain sea state [1].
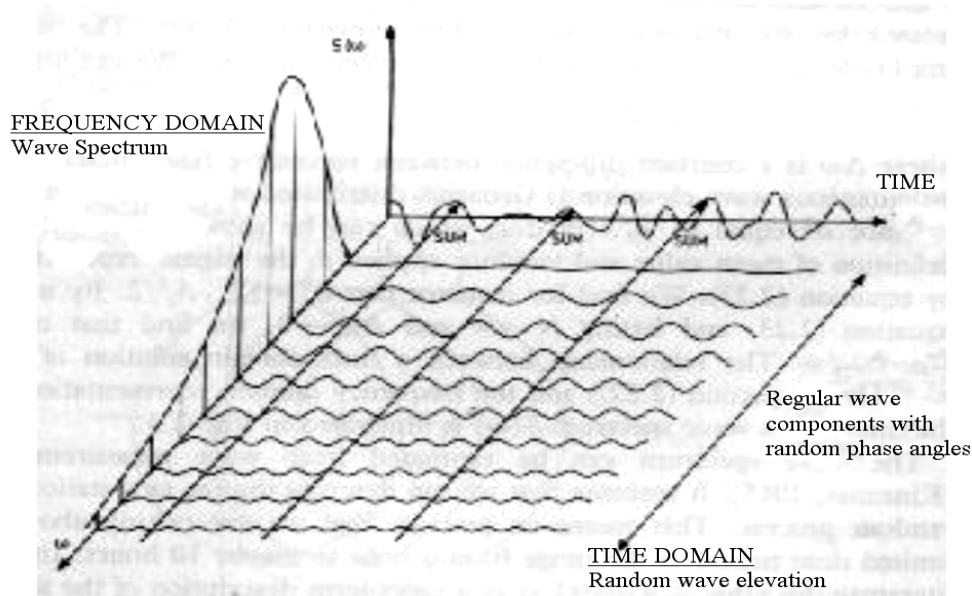
Figure 6.2: *Figure illustrating the connection between a frequency domain and time domain representation of waves in a long-crested short term sea state [1].*

6.1 Frequency domain analysis

Frequency domain analysis is used extensively for floating units, including analysis of both motions and forces. The main advantage of this method is that the computations are relatively simple and efficient compared to time domain analysis methods. The equation of motion can in a complex form be represented as

$$M_{33} \cdot \frac{d^2}{dt^2}\eta_3 + B_{33} \cdot \frac{d}{dt} \cdot \eta_3 + C_{33} \cdot \eta_3 = F_0 \cdot e^{i\omega t}$$

Equation 6.2

The harmonic load function, F(t), can be given in complex form as

$$F(t) = F_0 \cdot e^{i\omega t}$$

Equation 6.3

where F_0 is the load amplitude. The particular solution is assumed to be in the form

$$\eta_3(t) = H \cdot e^{i\omega t}$$

Equation 6.4

where H is the motion amplitude, and we obtain by substituting equation 6.4 into equation 6.2.

18

$$M_{33} \cdot \left(-\omega^2\right) \cdot H \cdot e^{i\omega t} + B_{33} \cdot i \cdot \omega \cdot H \cdot e^{i\omega t} + H \cdot C_{33} \cdot e^{i\omega t} = F_0 \cdot e^{i\omega t}$$

Equation 6.5

$$\left(-M_{33} \cdot \omega^2 + B_{33} \cdot i \cdot \omega + C_{33}\right) \cdot H \cdot e^{i\omega t} = F_0 \cdot e^{i\omega t}$$

Equation 6.6

Introducing the damping factor $\xi = B_{33}/B_{33.critical} = B_{33}/2*M_{33*}\omega_n$ and the frequency ratio $\Omega = \omega/\omega_R$, the equation can be written as [2]:

$$\frac{C_{33} \cdot H}{F_0} = \frac{1}{\left(1 - \Omega^2 + i \cdot 2 \cdot \zeta \cdot \Omega\right)} = H(i\omega)$$

Equation 6.7

where $H(i\omega)$ is known as the complex frequency response function of the system. The absolute value of $H(i\omega)$ is given by $|H(i\omega)|$ and denotes the magnification factor.

$$|H(i\omega)| = \left|\frac{C_{33} \cdot H}{F_0}\right| = \frac{1}{\sqrt{\left(1 - \Omega^2\right)^2 + (2 \cdot \zeta \cdot \Omega)^2}}$$

Equation 6.8
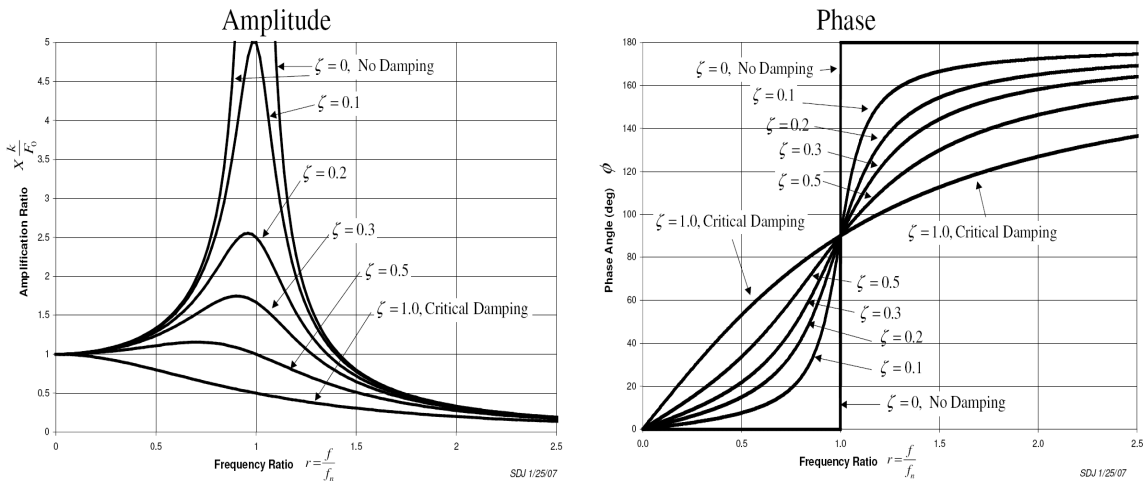
Figure 6.3: *Dynamic amplification and phase diagram.*

The magnification factor with the corresponding phase diagram is illustrated in **Figure 6.3**. It shows that the response is in phase with the exciting force at frequencies lower than $\omega = \omega_R$, and in anti-phase for higher frequencies. The steady-state solution can be given as $\eta_3(t)$, where Φ is the phase angle [2]:

$$\eta_3(t) = \frac{F_0}{C_{33}} \cdot |H(i\omega)| \cdot e^{i(\omega t - \phi)}$$

Equation 6.9

6.2 Time domain analysis

Time domain analysis is mainly used when a frequency domain approach is not possible, or when more detailed answers are needed [12]. A time domain analysis offers great insight into the behavior of a system at the cost of time consuming calculations. This analysis method is for instance more applicable for varying damping, nonlinear load or nonlinear behavior of the structure.

When the time domain approach is used, the dynamic equation of motion is solved with respect to time. There are several methods available, but all integration methods have two fundamental characteristics. First, they are not intended to satisfy the governing differential equations at all time t but only at discrete time intervals Δt apart. Secondly, a suitable type of variation of displacement, velocity and acceleration is assumed within each time interval. The time duration T, in which the solution is sought, is divided into n equal time steps so that $\Delta t = T/n$.

In comparison with frequency domain analysis, the advantage of a time domain analysis is that it can easily capture higher order load effects. In addition, a time domain analysis can predict the maximum response without making assumptions regarding the response distribution.

Examples of effects that should be analyzed in the time domain are; simulation of slow drifts motions, coupled floater and mooring response, "ringing" and transient slamming response.

7 Global response

In this thesis calculations will be done only in the frequency domain, and an important tool in analyzing the linear behavior of offshore structures in the frequency domain is the transfer function. Given linear behavior, a structure responds to the harmonic excitation of an elementary wave of frequency ω_n with a phase-shifted harmonic output signal of equal frequency. The ratio of output signal to the input signal is called the transfer function, $H(\omega)$, also called the Response Amplitude Operator.

$$H(\omega) = \frac{s(\omega)}{\zeta(\omega)}$$

Equation 7.1

The ratio of the spectral energy density of the output and input signals is proportional to the square of the ratio of corresponding amplitudes of the response components and the elementary waves, which is equal to the square of the magnitude of the transfer function. The structural response, $S_R(\omega)$, is related to the sea spectrum as [9]:

$$S_R(\omega) = \left(\left|H(\omega)\right|\right)^2 \cdot S(\omega)$$

Equation 7.2
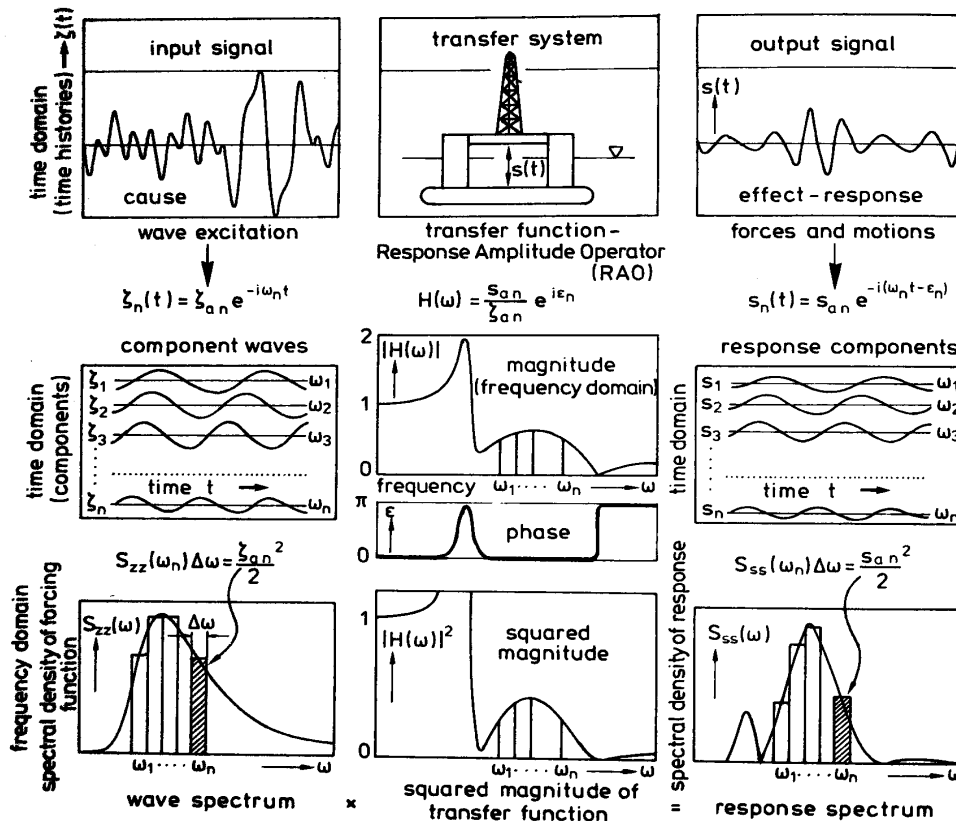
Figure 7.1: *Response of offshore structures in random seas [9].*

An important parameter in relation to the statistical description of the response is the spectral moment of order n, which can be given as [6]:

$$m_n = \int_0^\infty \omega^n \cdot S_R(\omega)\, d\omega$$

This parameter is used when determining the most probable largest heave and roll motions. When the response spectrum is known, statistical parameters can be calculated and the same statistical approach as for wave statistics can be used. The use of this method requires linear wave forces and linear relationship between structural response and load. This method can therefore be inconvenient for nonlinear effects like drag loads, time varying geometry, horizontal restoring forces and variable surface elevation. However, in many cases these non-linearities can be satisfactorily linearised.

Since the short-term random wave field is generally represented as stationary and Gaussian, it can be concluded, due to linearity, that the response will also be stationary and Gaussian. This allows the response statistics to be fully determined by a frequency domain analysis where efficient numerical methods are available.

Provided that transfer functions have been derived for all six motion components (roll, pitch, yaw, sway, surge and heave) for a vessel at a defined reference point (often at the centre of gravity, or amidships at the waterline), then RAOs can be readily be calculated for any location on the vessel. This data can be combined with wave climate data and limiting motion criteria to derive quantitative downtime estimates.

8 Velocity and Acceleration spectra

The operability criterion in this thesis is solely based on maximum roll and pitch angles, and heave amplitudes related to the maximum stroke length on the heave compensating equipment. The operability indicates how much of the time the vessel can continue its operation, without being forced to interrupt because of the heave amplitude is exceeding the maximum allowable value. As long as the heave motions are below the limit, the vessel can operate. However, the operability does not tell you about comfort level for personnel, acceleration induced forces on equipment and cargo, safety level for helicopter operations and so on.

The vessel's vertical motion, velocity and acceleration, given a sinusoidal vertical oscillation, can in the simplest form be given as

$$\eta_3 = \frac{H}{2}\cdot\sin(\omega t) \qquad \eta'_3 = \omega\cdot\frac{H}{2}\cdot\cos(\omega t) \qquad \eta''_3 = -\omega^2\cdot\frac{H}{2}\cdot\sin(\omega t) \qquad \textbf{Equation 8.1}$$

This means that the velocity and especially the acceleration are very dependent on the frequency that the vessel is oscillating with. The response spectra for the motion, velocity and acceleration can be written as

$$R_{motion} = \left(\left|\frac{\eta_3}{\zeta_a}\right|\right)^2\cdot S(\omega) \qquad\qquad \textbf{Equation 8.2}$$

$$R_{vel} = \left(\left|\omega\cdot\frac{\eta_3}{\zeta_a}\right|\right)^2\cdot S(\omega) = \left(\left|\frac{\eta_3}{\zeta_a}\right|\right)^2\cdot\omega^2\cdot S(\omega) \qquad\qquad \textbf{Equation 8.3}$$

$$R_{acc} = \left[\left|(-\omega)^2\cdot\frac{\eta_3}{\zeta_a}\right|\right]^2\cdot S(\omega) = \left(\left|\frac{\eta_3}{\zeta_a}\right|\right)^2\cdot\omega^4\cdot S(\omega) \qquad\qquad \textbf{Equation 8.4}$$

Figure 20.6 in appendix 7 displays the heave motion, velocity and acceleration response spectra for a sea state with spectral peak period of 8 seconds, and a significant wave height of 7 meters. The values used were chosen for convenience and are not intended to represent any part of the world. The most probable largest heave motion, velocity and acceleration can be derived from the area underneath the corresponding spectra. For velocity and acceleration especially, this leads to the RAO values having a larger impact on the response spectrum for high frequencies, due to the ω^2 and ω^4 terms in equation 8.3 and 8.4. Since the cargo forces and personnel comfort directly relates to the acceleration,

a vessel with a high natural period and low magnification at small wave periods is desirable.

Personnel comfort is very dependent on lateral acceleration induced by pitch and roll. This can be seen in Figure 8.1, where criteria for different activities are given. The accelerations where the personnel is located, e.g. in the accommodation area, depend on the location, both longitudinally and transversely, and how the vessel's heave, roll and pitch accelerations combine at this location. The level of personnel comfort will not be calculated, since it can not directly be related to the operability of the vessels. However, being aware of the acceleration magnitudes on the rig are very important, both regarding to structural integrity and personnel comfort.

Root mean square criterion

Vertical acceleration	Lateral acceleration	Roll	Description
$0.20g$	$0.10g$	$6.0°$	Light manual work
$0.15g$	$0.07g$	$4.0°$	Heavy manual work
$0.10g$	$0.05g$	$3.0°$	Intellectual work
$0.05g$	$0.04g$	$2.5°$	Transit passengers
$0.02g$	$0.03g$	$2.0°$	Cruise liner

Figure 8.1: *Acceleration and roll criteria (NORFORSK 1987).*

9 Main characteristics of floaters

Common for all types of floaters is that they utilize excess buoyancy to support deck payload. Floating structures are used in all fields of marine technology, particularly in exploration work. Depending on the task the vessel is going to perform, the heave restrictions can limit the operability. A diminished operability is often related to resonance phenomena, and **Figure 9.1** shows the typical natural periods for offshore floaters.

Floater Mode	Natural periods (seconds)			
	FPSO	DDF	TLP	Semi
Surge	> 100	> 100	> 100	> 100
Sway	> 100	> 100	> 100	> 100
Heave	5 – 12	20 – 35	< 5	20 – 50
Roll	5 – 30	50–90	< 5	30 - 60
Pitch	5 – 12	50 –90	< 5	30 - 60
Yaw	> 100	> 100	> 100	> 100

Figure 9.1: *Typical natural periods of deep water floaters (DNV RP-F205)*

9.1 Drillship

In general drillships have a high block coefficient, or a high ratio of displacement to the product of length, width and draft. In comparison with other drilling platforms, drillships have a high storage capacity, especially on the deck area [9]. They do not need anchor vessels, and can cover long distances in a relatively short time. A drillship also benefits from a low hull steel weight per volume of displacement with a lower net initial cost and lower operating cost per meter of operating depth.

For drillships and FPSO`s, due to their large superstructures and their active or passive weather-vaning ability, wind forces are often dominant relative to current forces. Drillships can experience significant low frequency response in the horizontal plane. They may be particularly sensitive to surge excitation due to low viscous hull damping.

9.2 Semisubmersible

A semisubmersible is a multi-hull column-stabilized structure, which consists of a deck structure with large diameter support columns attached to submerged pontoons. Semisubmersibles have small waterplane areas, which give vertical natural periods above 20 seconds, usually outside the range of the high energy wave periods in severe weather.

A semi submersible is very sensitive to weight changes and has low flexibility with respect to deck load and oil storage. Semisubmersibles have three characteristic drafts [9]:

-*Transit draft* is used when moving between sites. In this draft only the pontoons are submerged. This insures minimum wave resistance and maximum waterplane area for high stability and seaworthiness.

-*Operating draft* is used during drilling, and the structure is semi submerged by flooding the ballast tanks in the pontoons. The waterline area is now limited to cross sections of the surface piercing columns. As explained in detail in chapter 11.1, the completely submerged pontoons experience a downward excitation force below the crest of a wave, compensating for the upward force the columns are experiencing. Motion characteristics of semi submersibles are favorable in arbitrary irregular seas compared to other vessels, and are therefore an ideal platform for floating drilling operations.

-*Survival draft* is an emergency draft with improved stability used in extremely heavy seas. Compared to the operating draft, the pontoons are closer to the surface, and this yields and in-phase motion of the platform in long-period waves, which heavy seas mainly consists of. Because of this phenomenon the platform follows the wave elevation to some extent, and allows a 100-year wave to pass under the deck structure.

The heave natural period of the semi is above the range of natural wave periods. Despite this fact, wave frequency motions are significant, especially in extreme conditions. Large semi submersibles, like the heavy lift vessels, with displacement of 100000 tons or more are generally less sensitive to wave frequency action. Low frequency response may be more dominant in roll and pitch motions [5].

The advantage of their excellent motion characteristics has to be set against the disadvantages of limited variable deck load capacity owing to low buoyancy reserves and static stability, as semis are characterized by a small waterline area and a high center of gravity under operating conditions.

9.3 SEVAN stabilized platform

In 1986 Arne Smedal, the founder of Sevan Marine, came up with a unique idea of a circular FPSO unit. However, the time was not right and the idea impossible to commercialize. Today the "Sevan Piranema" FPSO is producing oil in the Brazilian Piranema field. The diameters of the buoys are 60 meter for the smaller units and 106 meter for the biggest buoy. At drafts between 17 m and 33 m respectively, the huge buoys reach displacements of 55.000 tons to 305.000 tons, providing a storage capacity between 0.3 million bbl and 2 million bbl.

Construction of the first SEVAN *drilling* unit has begun and is scheduled for delivery in the first half of 2009. The first drilling unit will work for Petrobras America Inc. in the

very deep waters of the US section of the Gulf of Mexico, under a six year contract. The main benefits of the SEVAN design are the high deck load capacity and stability reserves. The unit's variable deck load capacity is more than 15000 metric tons, which is approximately twice the capacity of latest generation semis and similar to the capacity of a deepwater drillship. The unit has high stability reserves, which means that heavy equipment can be stacked on at higher levels than on a semisubmersible rig, and the extra deck load capacity will thus reduce the need for supply boats. The SEVAN unit can also store oil, and there is no need for weathervaning. Because of its compact design most of the typical fatigue damage typical for floaters is eliminated.

Sevan Marine claims that the unit has favorable heave and roll motions because of the circular shape and a motion damping bilge box, see **Figure 9.2**. Additionally they state that due to the immense size the pressure field on the lower surface shows saddle-type distributions, with the consequence that the oscillating vertical forces, and hence the heave motions remain small. If these claims are verified by the hydrodynamical analysis made in this thesis, it would undoubtedly be a suitable platform for drilling as well as production operations.
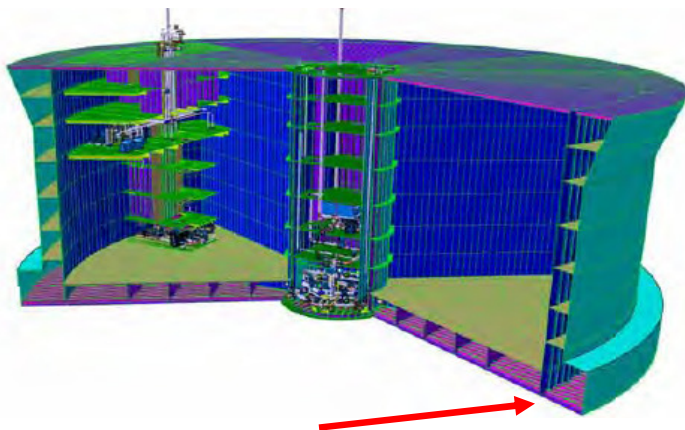
Figure 9.2: *Bilge box on a SEVAN FPSO*

Another advantage with the Sevan Stabilized Platform is the prize. According to Sevan's vice president Fredrik Major, the all-in delivery cost is $ 430 million, compared to $ 500-800 million for typical sixth generation semisubmersibles and top of the range drillships. The internal storage capacity, a feature not shared by semisubmersibles, enables the unit to conduct extended well testing, including in environmentally sensitive areas like the Barents Sea.

10 Background for selection of compared vessels

The main focus in the thesis is to make a realistic estimate of the operability of different floating drilling vessels for operation in harsh and deepwater areas. The three concepts analyzed are a conventional monohull drillship with a single moonpool, a 6th generation semisubmersible drilling rig and the circular drilling unit of the SEVAN design. The term

generation indicates the time the semisubmersible is built and, to a certain extent, the semi's water depth and deck load capabilities.

It is not easy to choose the parameters that shall form the basis when deciding which vessels to compare. All vessels shall be capable of drilling in ultra deep water, and the water depth capability is therefore most important. Factors such as deck load capacity and deck area are bound to be different, due to the design principles of the various vessels. The same goes for parameters concerning different fluid storage capacities, price, transit speed and operating displacement. Therefore it was decided to compare vessels that are intended to perform the same tasks at the same locations; drill wells in harsh environment and ultra deep areas. Many different drillships and semisubmersibles could be analyzed but the motion characteristics of the vessels within each category are similar. The compared vessels are the SEVAN Deepsea Driller, the Aker H6 and the West Navigator. The main particulars of the vessels are described on the following page.

10.1 Vessel Main particulars

SEVAN Driller:

Operational draft: …………….…..15 m

Operational displacement: ....65 000 mt

Variable deck load capacity: ….15000 mt

Maximum water depth: ………....3600 m

Hull diameter: ………………….……75 m

Deck diameter: ……………………...80 m

Figure 10.1*: SEVAN Deepsea Driller*

West Navigator:

Operational draft: …………..……...13 m

Operational displacement:… 100 000 mt

Variable deck load capacity: .... 9000 mt

Maximum water depth: …...……2500 m

Length:……………………..……253 m

Breath: ………………...……….42 m

Figure 10.2: *West Navigator*

Aker H6:

Operational draft: …………..……...23 m

Operational displacement: ....64500 mt

Variable deck load capacity: ….7000 mt

Maximum water depth: ………..3000 m

Length main deck: ………………..90 m

Breath main deck: ………….……..70 m

Figure 10.3: *Aker H6*

11 General motion characteristics

The motion behavior of the vessels can, due to the hull design, be described by very different characteristics. This manifests itself both in terms of natural periods, waterline areas and dynamic amplification magnitudes.

The motion behavior of semisubmersibles is thoroughly described in the following section. It is essential to be aware of the complex force picture affecting the semisubmersible in order to fully understand its behavior. The other vessels' behavior is less complicated, and hence one does not need to study their excitation mechanisms as much to achieve the same understanding of the motion behavior.

11.1 Motion of semi submersibles

Knowing the forces acting on arbitrary structures, it is possible to calculate the seaway motions of a semisubmersible, and to analyze the influence of the most significant parameters. A semisubmersible, the Aker H6, with fore-and-aft symmetry will be analyzed for deep water operations. The heave motions in beam seas will be studied, and drag forces will be neglected in this preliminary strip-theory response study. Interaction effects between columns and pontoon and end effects are not taken into account in the calculations. It must therefore be emphasized that this preliminary study is only meant to explain the excitation mechanisms acting on the vessel, and do not intend to realistically estimate the forces affecting the semisubmersible.

The forces on semisubmersibles can be divided into forces acting on columns, and forces affecting the main hulls. The only excitation force on the columns is the Froude-Krylov force. The small hydrodynamic added mass for the columns should strictly speaking also be included, but as this is not possible to do in a simple manner it will be neglected herein. Since the columns are partly submerged, the force has to be derived from pressure integration of the wetted surface. This force is equal to the product of the pressure from the undisturbed incident wave at the depth h_c, and the water line area, see **Figure 11.1**.
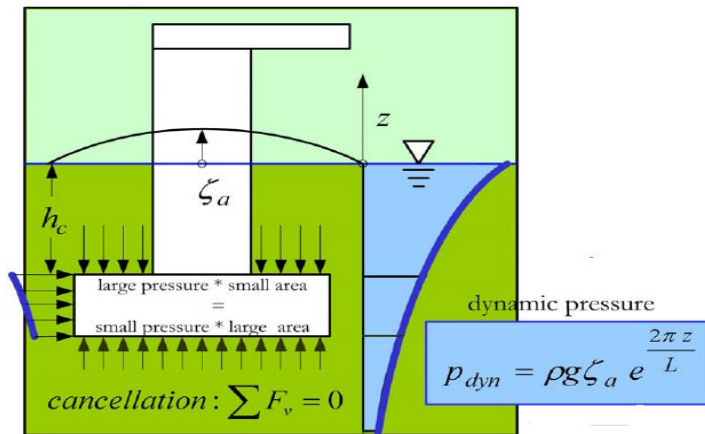
Figure 11.1: *Pressure distribution on the pontoon [3].*

The excitation forces affecting the main hulls are the sum of Froude-Krylov forces and the hydrodynamic mass force. Both these forces can be integrated in the inertia part of the Morison formula, and are proportional to the water particle acceleration.

There are no forces acting on the columns as such, but the "column force" is rather a correction for the calculated force acting on the main hulls. Forces on the pontoons are calculated with Morison's formula, but this method requires that the entire surface is wetted. The area corresponding to the non-wetted surface is the cross section area of the columns. This corrective force is therefore referred to as the force acting on the columns. But in reality, the force acting on the very column gives no axial contribution, as it only acts normal to the column.

The dynamic pressure decays with both depth and wave frequency. As seen from the formula for wave induced dynamic pressure, equation 3.1, the wave action decays with increasing draft. At $z/\lambda = 0.5$ only 4.3% of wave action is observed.

The upper left diagram on **Figure 11.2** shows the force on one column as a function of frequency. It is in phase with the wave elevation, and decreases exponentially with increasing frequency. The forces in **Figure 11.2** are normalized by a reference force, so that the maximum excitation force on 4 columns is equal to 1 and is non-dimensional. The complete calculation can be seen in appendix 8.
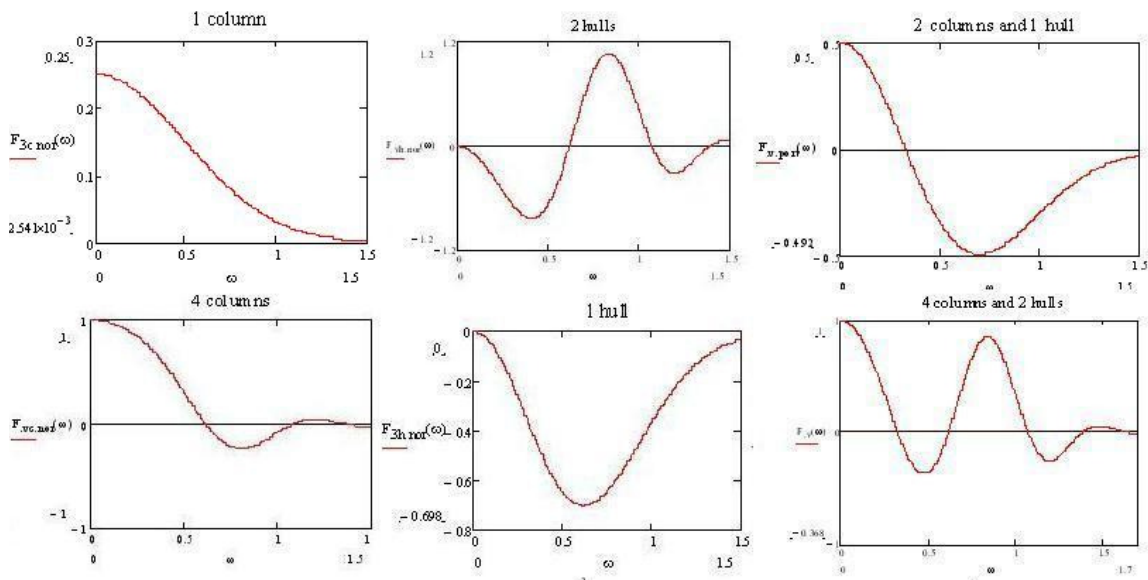
Figure 11.2: *Vertical forces on hulls and columns of a semi submersible. Calculated in Mathcad.*

Semisubmersibles are wide structures, and benefits from this regarding to stability and heave motions in "medium" wave conditions. At wave lengths $\lambda = 2b\ldots(2b)/3\ldots(2b)/5\ldots$ the vertical forces on the respective sides of the semi submersible are in anti-phase, and hence no heave motions are observed, see Figure 11.3.

The consequence of this can be seen in Figure 11.2, where the 4 columns of the semi submersible experiences *geometrical cancellation* because of the anti-phase effect shown in Figure 11.3. However, these wave lengths induce large roll motions.
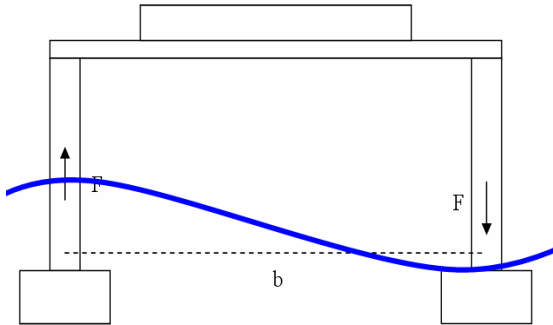
Figure 11.3: *Geometrical heave cancellation.*

If we observe the dynamic behavior of a single main hull, we observe an anti-phase force corresponding to the associated water particle acceleration. This inertia force is proportional with the water particle acceleration, and is visualized in the lower mid diagram, **Figure 11.2**. Similar to the column force behavior, two main hulls also experiences *geometrical cancellation* at certain frequencies in beam seas.

Considering one side of the structure, the upper right diagram shows that the total vertical inertia force is cancelled at a selected frequency, because of the phase-shifted forces on columns and hull. This frequency is called the *cancellation frequency* and is determined by the waterline area compared to the lower surface area of the hull. If both sides of the structure are taken into consideration, the total excitation force is obtained. This force is visualized in the lower right diagram of **Figure 11.2**. The first cancellation frequency follows from superposition of the effects of columns and hulls, and the zero-points at higher frequencies are related to the spacing of columns.

Figure 11.4 shows the Response Amplitude Operator for the semi submersible in beam seas. In addition to this it also illustrates the corresponding phase. It must be emphasized that the above relations only apply for undamped motion under exclusive action of inertia forces. From this it follows that the heave response is infinite at $\omega = \omega_R$ and zero at $\omega = \omega_C$. In this limited frequency range, the velocity-dependent viscous force also has to be considered. Another consequence of the neglected drag force is that the motion of the semi submersible is either in phase with the wave elevation, or π radians out of phase as seen in **Figure 11.4**. The reason for the semi submersible responding in this particular phase pattern can be derived from the lower right diagram in **Figure 11.2**. This diagram shows the combined vertical force on the semi submersible, and the frequency of the zero-points in this diagram corresponds to the phase-shifting frequencies in **Figure 11.4**. When the total force is positive, the force is in phase with wave elevation.

As seen in **Figure 6.3** the response of an undamped system is in phase with the exciting force at frequencies lower than $\omega = \omega_R$, and in anti-phase for higher frequencies. For frequencies higher than $\omega = \omega_R$, the phase will be governed by whether the total vertical

force is positive or not. For frequencies higher than $\omega = \omega_R$, the semi submersible will follow the wave elevation when the total exciting force is negative, and move in the opposite direction of the wave elevation when the force is positive.
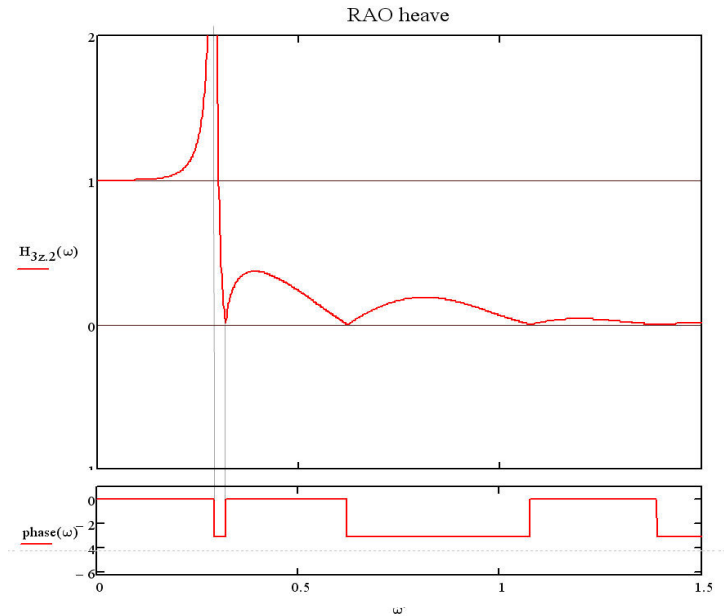
Figure 11.4: *Heave response of a semi submersible in beam seas.*

At lower frequencies the effect of the columns dominates, while at higher frequencies the effect of the main hulls prevails. At values of $\Omega < 0.3$, dynamic effects are negligible, and the motion behavior is dominated by the restoring force, and the structure follows the wave. In the resonance frequency domain $0.3 < \Omega < 2$, the dynamic behavior is mainly governed by damping, while for $\Omega > 2$ the system is called mass dominated.

For offshore activities aboard a semi submersible it follows that for the most frequently encountered wave periods (T<10s), heave will be less than 10% of the wave elevation. For the highest possible 100-year wave, periods lie in the region of 14-17 s [9], and heave motion reaches approximately 40 % of the wave elevation. If we consider a 20 meter high wave at a period of 16 s, the semi submersible will rise 4 m as the 10 m wave crest passes (linear theory is assumed). This means that the relative motion between the water level and the main deck is only 6 m. Consequently, the air gap and overall height can be significantly reduced. This contributes positively to the stability of the platform and it can therefore be made smaller and at less cost.

The added mass in heave for Aker H6 is calculated in Mathcad to 86350 tons, based on an added mass coefficient, C_A, for the pontoons of 1,8, see appendix 8. This results in an equivalent oscillating mass of 150850 tons in heave, which gives an undamped natural period of about 22 seconds in heave. This is a well established method to estimate the natural frequencies of floating vessels, but strictly speaking the procedure is not correct. The mass in the equations of motion for a ship in the frequency domain depends on frequency. Thus, there can not exist a classical natural frequency as such. When referring to a natural frequency of a floater, the reference is in reality made to the frequency where

the response peaks [22]. The added mass in heave for Aker H6 is shown in **Figure 11.5**, and the values in the diagram are gathered from the output file in Moses. It shows that the added mass is not constant, and tells us that the added mass calculated in Mathcad was slightly overestimated. The deviation in added mass is probably caused by the assumption of infinite length of pontoon in the hand calculations, and by not taking the effect of the columns into account.
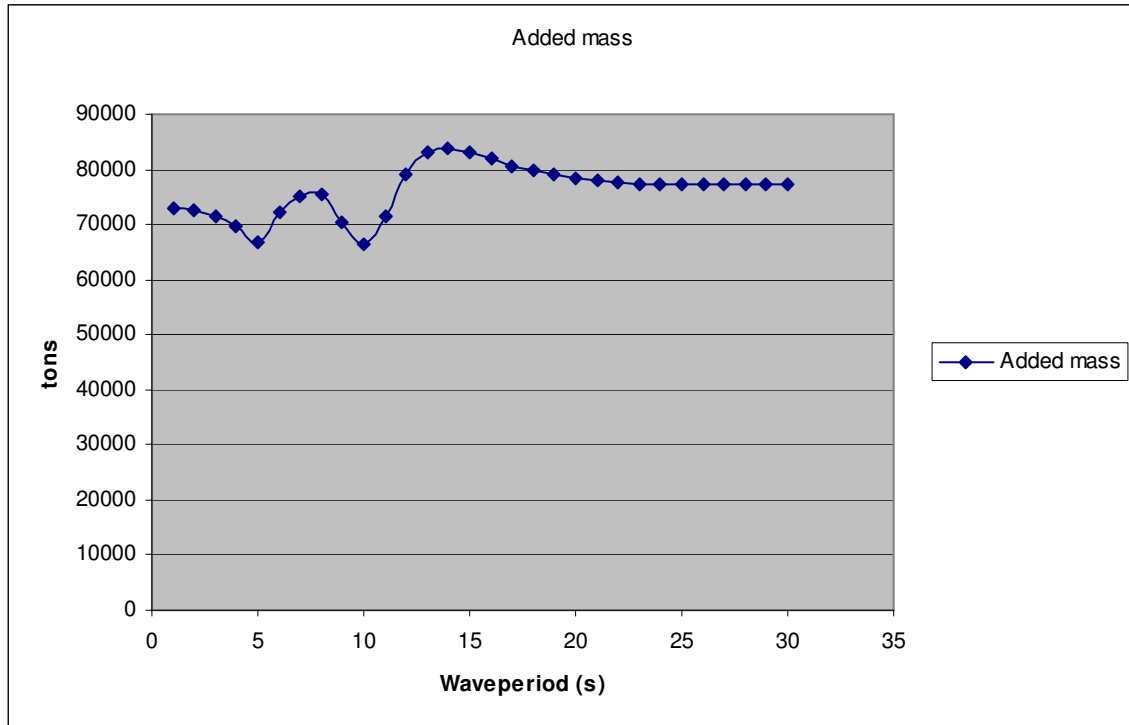
Figure 11.5: *Added mass Aker H6*

12 Hydrostatics and stability

Roll motions, -speeds and –accelerations are analogous heave response very important regarding excessive forces on cargo, discomfort for personnel, helicopter operations etc. To fully understand the rotational response of a floating structure, it is important to be aware of the concept of static stability. When we earlier analyzed the effect of the waterplane area of floating structures, results showed that a small area positively contributed to the vertical motion response. However, a decrease of the waterplane area reduces the stability, and hence the deck capacity of the vessel. A brief argumentation is given below:

The buoyancy force corresponds to the weight of water displaced by the structure and acts on the centroid of displaced fluid volume. When a vessel is in static equilibrium, the line between the buoyancy center B_0 and the center of gravity G, is vertical. When the vessel is slightly rotated about the x-axis, as in **Figure 12.1**, the center of buoyancy B is displaced to a new position. The new action line of buoyancy force intersects the previous one at the metacenter M.
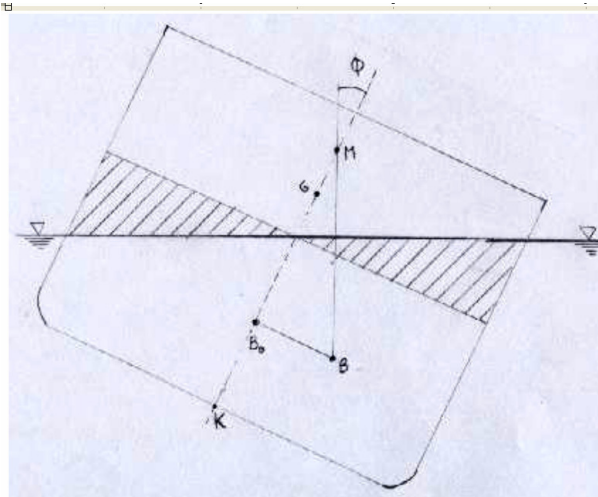
Figure 12.1: *Stability of a mono hull vessel*

The resulting "righting moment" M_R rotates the structure back to its original position if the metacenter is above the center of gravity. V denotes the volume of the displaced water.

$$M_R = \rho \cdot g \cdot V \cdot GM_0 \cdot \sin\phi \qquad\qquad \textbf{Equation 12.1}$$

In the calculation of the resonance periods for the vessel in roll, we assume small angles of rotation which results in the approximation [7]:

$$C_{44} = \Delta GM \qquad\qquad \textbf{Equation 12.2}$$

It can be seen from Figure 12.1 that GM = BM - BG. GM is an expression of the vessels stability. Equation 12.3 states that the rotational eigenperiod decreases with increasing values of GM.

$$\omega = \sqrt{\frac{\Delta GM}{I}} \qquad \omega = \sqrt{\frac{A_w \cdot D \cdot \rho \cdot g \cdot GM}{m \cdot r_1^2}} = \sqrt{\frac{GM \cdot g}{r_1^2}} \qquad \textbf{Equation 12.3}$$

BM is equal to the transverse waterplane moment of inertia, I_T, divided with the vessels displacement. I_T is given as

$$I_T = \int_0^l \int_{-\frac{B}{2}}^{\frac{B}{2}} y^2 \, dy \, dl = \int_0^l \frac{B^3}{12} \, dl \qquad \textbf{Equation 12.4}$$

With equation 12.4 we obtain for a vessel with volume displacement Length*Breath*Draft:

$$BM = \frac{\frac{L \cdot B^3}{12}}{L \cdot B \cdot D} = \frac{B^2}{12 \cdot D} \qquad \textbf{Equation 12.5}$$

For multi-element structures, the water plane moment of inertia can be calculated in a modified way, depending on the geometry of the surface-piercing elements and their distance from the heeling axis. This procedure of calculation is referred to as the Steiner formula, where $I_{T'}$ is the columns water plane moment of inertia and *a* is the distance from the axis of rotation to the centroid of the waterplane area.

$$I_T = n \cdot \left(A_c \cdot a^2 + I_{T'} \right) \qquad \textbf{Equation 12.6}$$
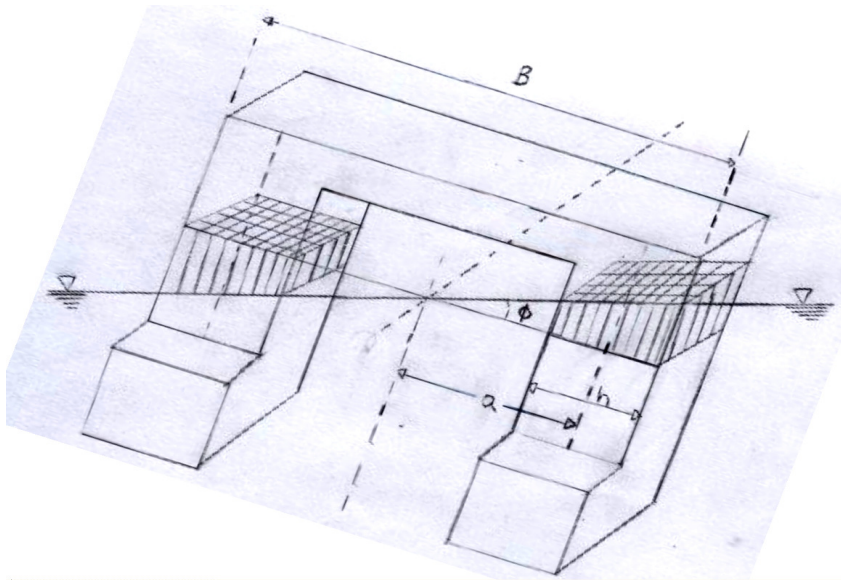
Figure 12.2: *Stability of multi hulled vessel*

The stability behavior of semi submersibles is very complex and the above given equations is only valid for small heel angles. However, it gives a simple understanding of the various parameters' contribution to the resonance period in roll. The same method can be used to determine the vessels pitch response. In chapter 17.2 the knowledge of hydrostatics and stability will be very useful, when analyzing the rotational response of the vessels.

13 Operation limitations

On a floating platform moving in the seaway, the vertical relative motion between the stationary well and the platform needs to be compensated for by a number of hydraulic devices [9]:

-The heave compensator, which is located between the hook and the rotary swivel, carries the drill string and compensates for vertical motions up to a double amplitude of 7.62 m (25 ft)

-The riser tensioner maintains a high tensile force in the riser pipe, in order to minimize wave and current induced bending deflections. Vertical motions with a double amplitude of 15.25 m (50 ft) can be taken up by the telescopic slip joint.

-The guidelines are also held under tension by the guideline tensioner, again up to a maximum vertical motion of 15.25 m.

The stroke length on the compensating system and the sensitivity of the operation governs the limiting heave amplitude. **Table 2** shows typical maximum allowed single amplitudes for offshore drilling vessels. There is also a limiting *rotation* amplitude to prevent excessive stress on equipment and collisions in the moonpool etc.

Activity	Limiting Heave amplitude(m)	Limiting Rotation ampl.(deg)	Duration (%)
Drilling/Tripping	3	4	56.1
Running casing	2.75	4	12.5
Running BOP and Riser	1.25	2	10
Cementing	2	3.5	5.5
Logging	2.75	4	5.5
Disconnect	4	5	
Other	3	4	10.4

Table 2: *Typical limiting **single** amplitudes and duration of operations (Clauss et al)*

The total operability of the vessels is based on the limiting amplitude of the specific operations they are going to perform, and the duration (%) of these operations. The activity is assumed to be an independent variable, and therefore the crew of the vessel does not choose which operation to perform based on the given wave conditions. This assumption is considered to be reasonable, due to the natural sequence of performing the various tasks.

The limiting amplitudes are values characteristic for the latest generation of drilling vessels. The drilling equipment and compensation systems are similar, regardless of the vessel type they are mounted on. The duration of each operation is gathered from ref [9], and are only typical values. With today's drilling and completion technology the distribution could look slightly different, but the difference in resulting operability between the vessels would probably not be significantly affected.

If the limiting motions are exceeded, the activity has to be interrupted and the riser uncoupled. The rig floor limiting amplitudes are equal for all types of drilling vessels, provided identical capacity and performance of the compensation system. The rig floor amplitudes can through the RAO and statistics be converted to a maximum operating condition. **Figure 13.1** shows typical operation and survival limits of a 5th generation semisubmersible drilling rig. The next chapter explains in more detail how these limits are obtained.

Conditions	Wind (m/s)	Wave, Hs (m)	Mean current (m/s)	Heave Amplitude (m)	Surge Amplitude (m)	Pitch Amplitude (°)	Roll Amplitude (°)
Operating Conditions	32	8.5	0.6	3	3.5	4.5	4.0
Survival Conditions	41	19	0.75	13	12	9	8

Figure 13.1: *Typical drilling rig limits*

14 Calculation procedure

The availability of the different vessels are calculated in an excel document developed for this specific project. The calculation procedure is shown in **Figure 14.1,** where all phases of the calculation process are illustrated. The transfer function (RAO) is established in MOSES, a hydrodynamical software package described in chapter 15. The transfer function is input to the excel document where wave spectrum, scatter diagram and seakeeping criteria are chosen. Based on the response spectrum, a most probable maximum motion within a given period of time is estimated by use of a Rayleigh distribution. This provides the operational limits for the vessel which is compared with the sea states in the wave scatter diagram for the relevant location. The number of sea states in the scatter diagram which exceeds the operational limits for the vessel are added together, and form a basis for estimation of the total operability.

The most probable largest heave motion is based on the number of wave cycles corresponding to a three hours time interval, see equation 14.1. This is a common duration in short term wave statistics, but other values could also represent a reasonable time period to base the operability calculations on. An adjusted duration would however not represent any major difference in the extreme value distribution, due to the $\sqrt{\ln(N)}$ term in equation 14.1.

$$\eta_{3max} = \sqrt{2 \cdot m_0 \cdot \ln(N)}$$ **Equation 14.1**

The number of cycles, N, relates to the duration T and zero-up-crossing period T_z in the following way

$$N = \frac{T}{T_z}$$ **Equation 14.2**

The most probable largest motions, velocities and accelerations could also have been calculated directly in MOSES. This would however make the total calculation process more time consuming, due to lack of long term wave calculation capabilities. With the developed calculation method, one can by feeding the excel program with the RAOs and choose the area of operation and the desired spectrum, obtain the operability automatically. This makes the developed program useful also in future operability assessments.

All vessels are assumed positioned by DP, due to the water depth in the areas they are intended to operate. The wave headings used to generate the operability results are 45 deg "off bow" for Aker H6 and 25 deg "off bow" for West Navigator. The Sevan Deepsea Driller's response is independent of the heading, and the operability is therefore valid for all wave headings.
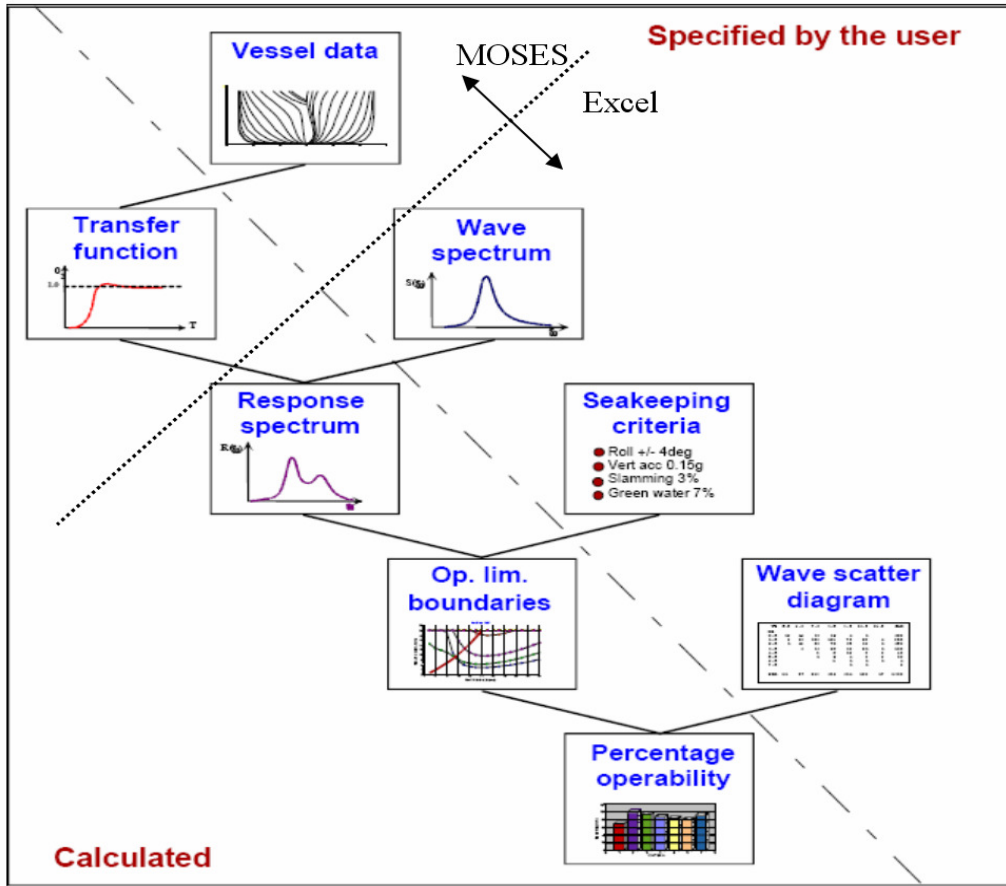
Figure 14.1: *Calculation method.*

15 Introduction to MOSES

The hydrodynamic loads and motion response have been calculated by using the software package MOSES (Multi-Operational Structural Engineering Simulator). This program was developed by Ultramarine Inc. in Houston Texas, and is an integrated hydrostatic, hydrodynamic and structural analysis package. Hydrodynamic calculations can be performed using either one or a combination of the different theories; Morison's equations, 2-D strip theory, or 3-D diffraction theory. MOSES can perform static, frequency domain and time domain simulations. Structural analyses can be carried out for beam and plate structures. In addition to the potential damping established by diffraction analysis, it is also possible to include viscous damping contributions to the model. MOSES is ideally suited for calculating the motional responses of semi submersibles, ships and units like the SEVAN buoy.

There are two ways that MOSES can compute hydrodynamic forces on a mesh; With a two dimensional approximation (Strip Theory), or with a three dimensional diffraction theory. While the details of what is required for a strip theory model differ a bit from the general theory, the basic result is the same. Normally one can use strip theory for "ship like" vessels, but three dimensional diffraction theory should be used for semi submersibles, spar structures or things for which length and breadth are approximately equal. *Ultramarine* emphasizes that strip theory can be used for most monohull analyzes, but diffraction theory should be used when surge and sway effects also are important.
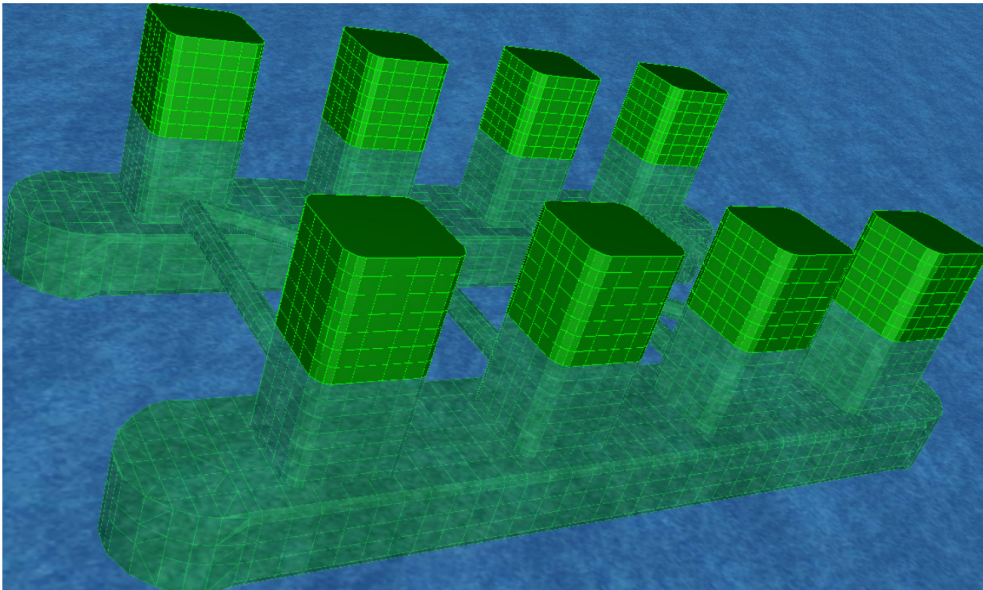
Figure 15.1: *Screen dump of the Aker H6 model in MOSES.*

16 MOSES models

All vessels have been modeled using 3D diffraction panels, where panels represent the outer geometry of the structures. The wetted surface of the models has been discretisized into 3400 panels in average with panel sizes about 2.5 x 2.5 m or less. This means that the hydrodynamic pressure load can be derived without being underestimated down to wave periods around 3-4 seconds. DNV RP F-205 recommends that the diagonal of the panel should be less than 1/6 of the smallest wave length considered. This will insure the accuracy of the pressure distribution. The number and size of the panels determine the accuracy of the results [5]. The computational effort required is of course quite sensitive to the number of panels, so one should constantly be seeking for a good compromise between fidelity and efficiency.

MOSES has linearized the equations for RAO computations by using a specified wave steepness. MOSES uses this steepness to calculate a "real" wave amplitude for linearization for each period and heading. A default wave steepness of 1/20 is used.

The waves are assumed to be long crested, which leads to a small overestimation of motion amplitudes compared to response in conditions with shorter wave crests.

16.1 Aker H6

The model consists of 5785 diffraction panels, which makes the analysis rather time consuming. The calculation time increases with the number of panels squared, and fairly accurate pressure results could have been reached with fewer panels. In spite of this, calculations were performed with a high amount of panels, especially around edges and corners to capture various flow separation effects.
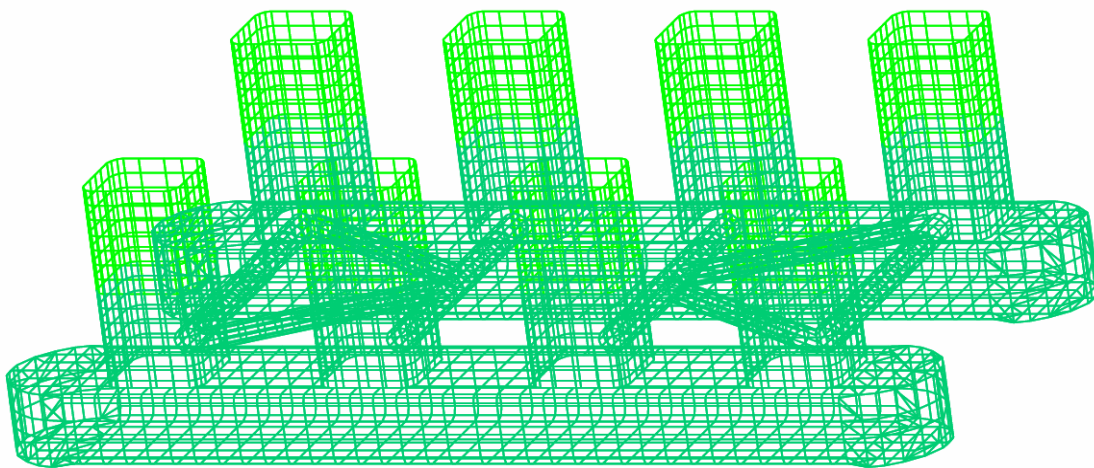
Figure 16.1: *Hydrodynamical model of Aker H6*

The drag factor of the plates in the model is adjusted so that the heave peak around the natural period of the rig has a value of approximately 1.4. This corresponds with the peak response of the heave RAO published on the Aker Drilling website. This RAO is shown in **Figure 16.2**, and acts as a verification of my results. Fortunately their heave RAO is almost identical to the one produced in MOSES, **Figure 17.1**.
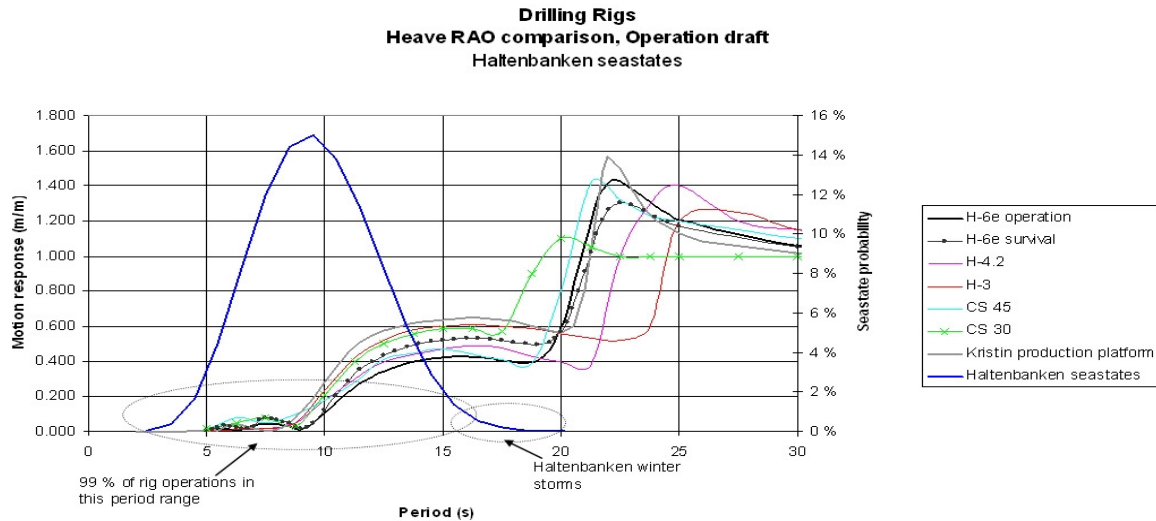
Figure 16.2: *RAO published on the AKER Drilling website.*

The desired damping level has been achieved by introducing a general damping for each plate. This was done by using the "cs_curr" function in Moses with a drag coefficient of 0.35. The heave damping level for the Aker H6 has little effect on the operability, since the heave natural- and cancellation periods are much higher than expected wave periods in severe weather. For roll and pitch damping plays a significant role, due to lower natural periods in these modes.

The vessel's GML and GMT are governed by the vertical center of gravity, which is dependent on the loading case. Normally one can experience GM values from 1 m to approximately 5 m. According to equation 12.3 the rotational natural periods are varying with the square root of GM, hence the selected GM value has a significant impact on the roll and pitch natural periods. A GMT value of 3 m is selected to represent an average loading condition, and the corresponding longitudinal GM is 6 m. The radii of gyration are estimations based on values from similar semisubmersibles.

Vessel	Draft (m)	VCG (m)	GML (m)	GMT (m)	Kxx (m)	Kyy (m)	Kzz (m)
Aker H6	23	20.6	6	3	30	40	45

16.2 West Navigator

The model is made up of 3004 diffraction panels, which give a good representation of the outer hull relative to the geometrical description of the hull that was available. Both

heave, pitch and roll have natural periods in vicinity of the high-energy wave period range, and waves can therefore excite resonant oscillations in these degrees of freedom.

Heave motions are heavily damped by radiation damping but roll is not. Therefore, viscous damping was added to achieve reasonable values of magnification in roll. No information regarding the vessels motion characteristics is published, and because of this it will not possible to tune in the damping level accordingly. Hence, default damping values has to be used. The radii of gyration are estimated based typical values given in [1].
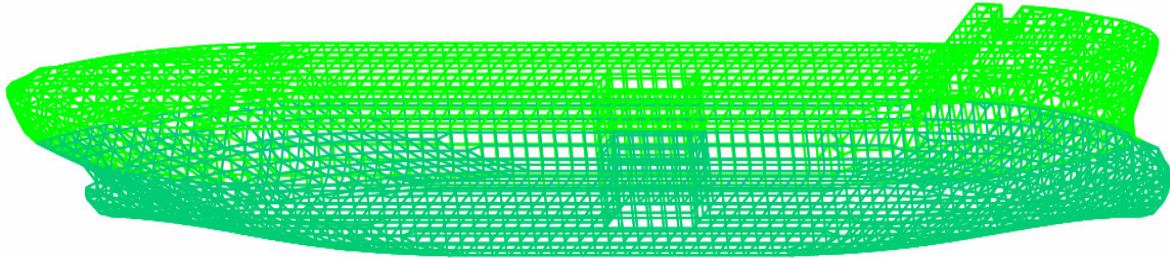
Figure 16.3: *Hydrodynamical model of West Navigator*

The vertical center of gravity is set to 14.5 m to achieve a natural period of approximately 18 seconds in roll, which is common for this type of vessel. This VCG gives the West Navigator a transverse GM of 3.5 m.

Vessel	Draft (m)	VCG (m)	GML (m)	GMT (m)	Kxx (m)	Kyy (m)	Kzz (m)
West Navigator	13	14.5	306	3.5	15.9	56	56

16.3 SEVAN Deepsea Driller

The model consists of 1477 diffraction panels. This is considered sufficient regarding the hydrodynamical pressure distribution. The SEVAN Deepsea Driller outer hull was modeled based on geometrical data given by Sevan Marine. The draft, GM and radii of gyration were given by the company too. Information regarding moonpool details or the natural periods could not be extracted from them. However, my own produced RAO`s were examined by Sevan Marine engineers, who found them in accordance with their own results.
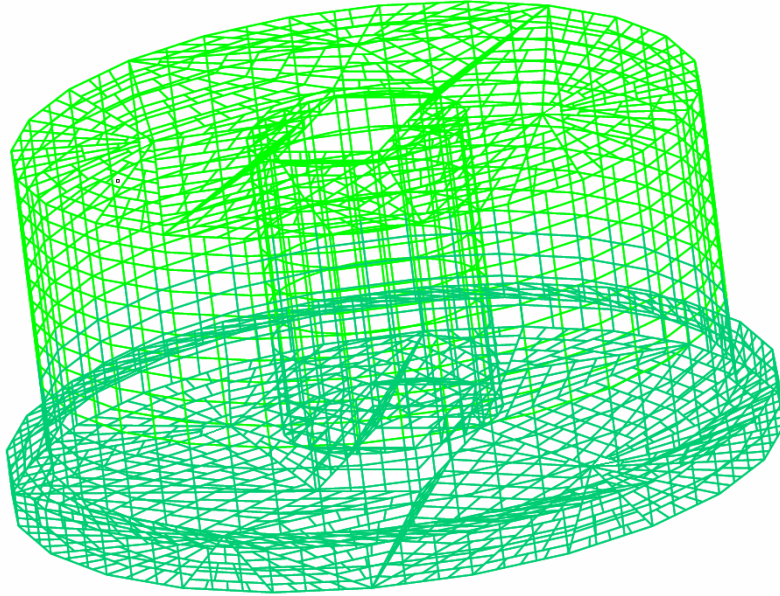
Figure 16.4: *Hydrodynamic model of SEVAN Deepsea Driller*

Vessel	Draft (m)	VCG (m)	GML (m)	GMT (m)	Kxx (m)	Kyy (m)	Kzz (m)
SEVAN Driller	15	20	10.4	10.4	23	23	32

17 Response characteristics

The most probable largest heave motion can be derived from the response spectrum, and the RAO`s are therefore key indicators to interpret the vessel's motion behavior. Response amplitude operators have been established for several headings to get a realistic picture of the vessels operating in different wave headings. All RAOs represent the behavior in the moonpool. It must be emphasized that the heave RAO in the moonpool includes both heave motions in the center of gravity of the ship and pitch induced heave motions. For Aker H6 and SEVEN Deepsea Driller the pitch induced heave will not give a significant contribution, whereas for the West Navigator it can be important, due to the moonpool not being located in the longitudinal center of the ship.

17.1.1   Aker H6

As shown in **Figure 17.1** the heave response for the Aker H6 is not drastically affected by the wave heading, showing only a minor rise in RAO values for off bow headings. This is a great advantage and means that weathervaning is not required for satisfactory heave response. **Figure 17.1** and **Figure 17.2** show the difference between the heave RAO calculated by hand in Mathcad and the one obtained in MOSES. It must be emphasized that the RAO in **Figure 17.2** is an undamped RAO based on simplifying

assumptions. The most obvious difference between the figures is the dynamic amplification at the resonance and cancellation periods. Without damping the amplification is infinite at resonance and zero at the cancellation period. The undamped RAO shows the same behavior at the lower *geometrical* cancellation periods also.
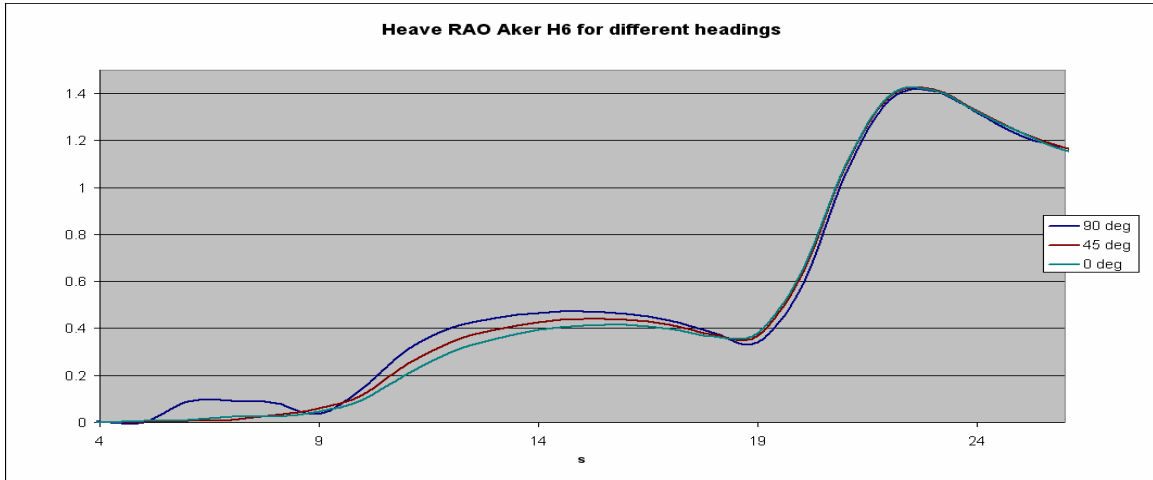
Figure 17.1: *Heave RAO Aker H6.*

Another distinct difference between the damped and undamped RAO is the natural period. In land based constructions with a low level of damping, the damped natural period will not be significantly higher than the undamped. The Aker H6 has a maximum amplification factor of 1.42 which corresponds to a damping level of approximately 35 % according to **Figure 6.3**. The damped eigenfrequency can be given as

$$\omega_d := \omega_R \cdot \sqrt{1 - \zeta^2}$$ **Equation 17.1**

By introducing a damping level of 35 % in equation 17.1 the natural period is theoretically displaced approximately from 22 to 23 seconds, which is in accordance with the results from MOSES.
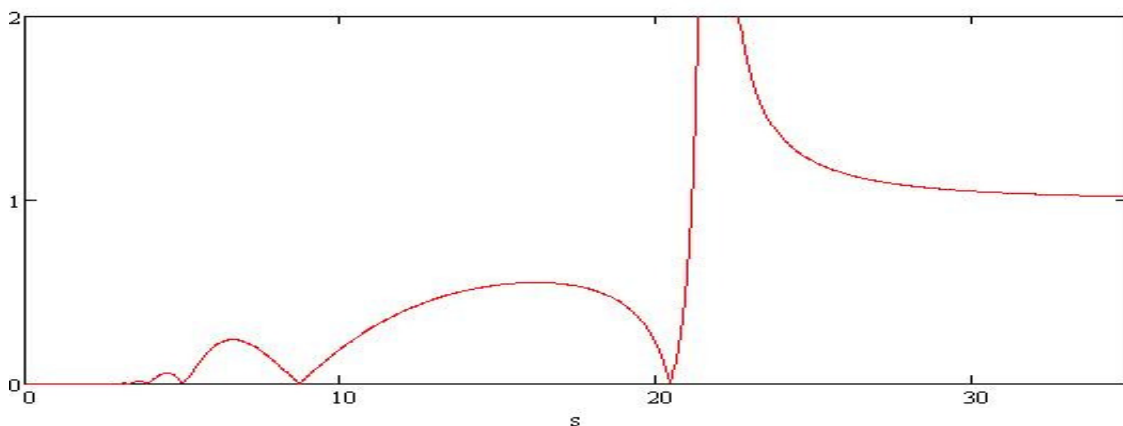
Figure 17.2: *Heave RAO Aker H6 in beam seas. Calculated by hand in Mathcad.*

17.1.2   West Navigator

The operability of the West Navigator is extremely dependent on the vessel's orientation relative to the incoming waves. **Figure 17.3** shows the dynamic amplification for several wave headings and illustrates that the motion behavior can be considerably improved by orienting the ship into prevailing sea. The RAO for beam seas shows that the West Navigator has a natural period of approximately 10 seconds, and has a dynamic amplification of 1.35 at this wave period. When the vessel is oriented into the prevailing seas, the ship's length in the wave direction is at its maximum, and the lower hull surface shows saddle-type pressure distribution. The consequence is that the oscillating vertical forces, and hence the heave motions remain small.
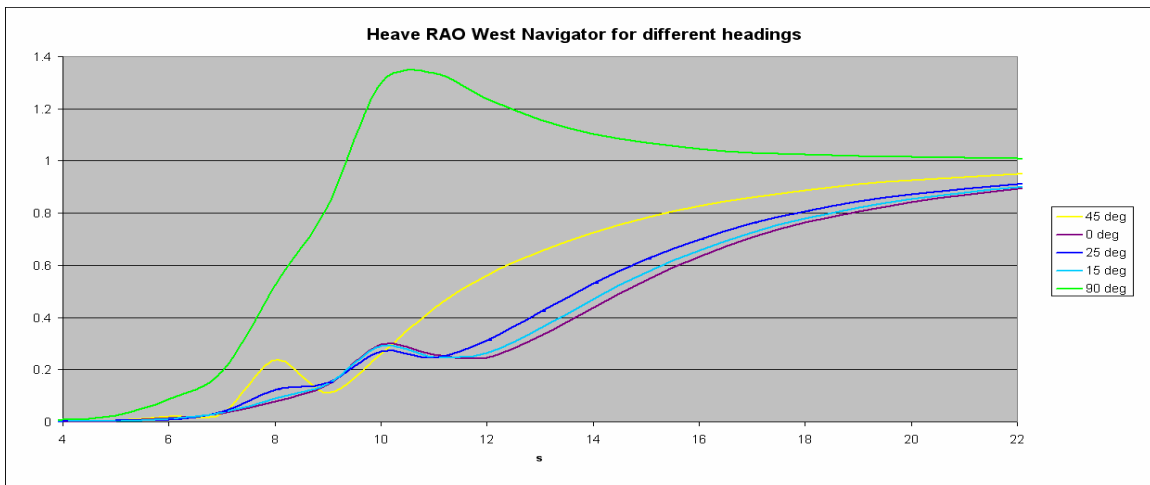
Figure 17.3: *Heave RAO West Navigator.*

For wave headings between 0 and 90 degrees, the RAO is composed by a mixture of the beam and head RAOs. For headings less than 15 degrees off bow the operability is almost the same as for head seas. A verification of the heave RAO is presented in appendix 6.

If one fails to orientate the ship into the incoming waves or if the sea state is composed by wind induced waves and swells coming from different directions, the operability will be dramatically reduced. A critical condition is the combination of head sea and beam swells. Significant roll accelerations may occur and thus have impact on topside structure and equipment, riser system and mooring system etc. **Figure 17.4** shows an example of a typical worst case weather spread for a drill ship and a SEVAN unit. Under these conditions drillships suffer from poor response characteristics for beam seas, in addition to the excessive loads applied to the mooring system.
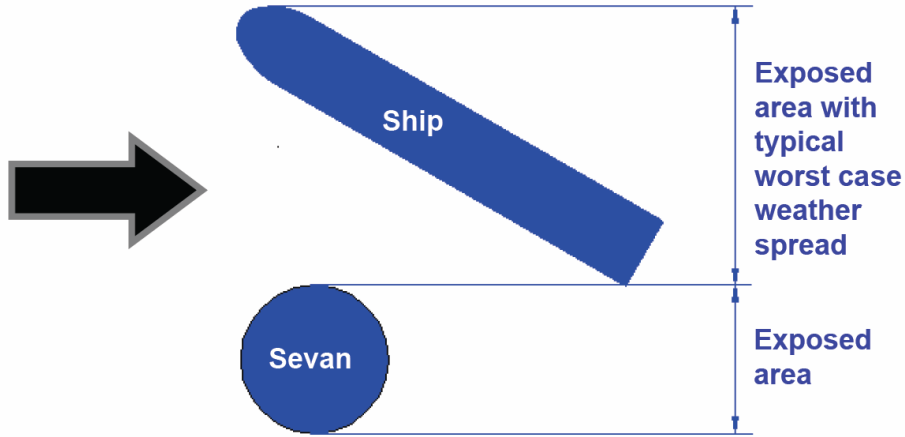
Figure 17.4: *Exposed area in worst case weather spread (From SEVAN MARINE)*

17.1.3   SEVAN Deepsea Driller

The SEVAN unit is characterized by its circular shape and profits from this by having equal motion behavior for all wave headings, hence there is no need for weathervaning and all the costly swivel- and turret arrangements involved. For wave periods lower than 10 seconds the SEVAN Deepsea Driller has excellent heave motions, due to the large dimensions and its bilge box. This can be seen in **Figure 17.5** where the dynamic amplification is practically zero for values lower than 8.5. The blue graph shows the result of removing the bilge box from the vessel.
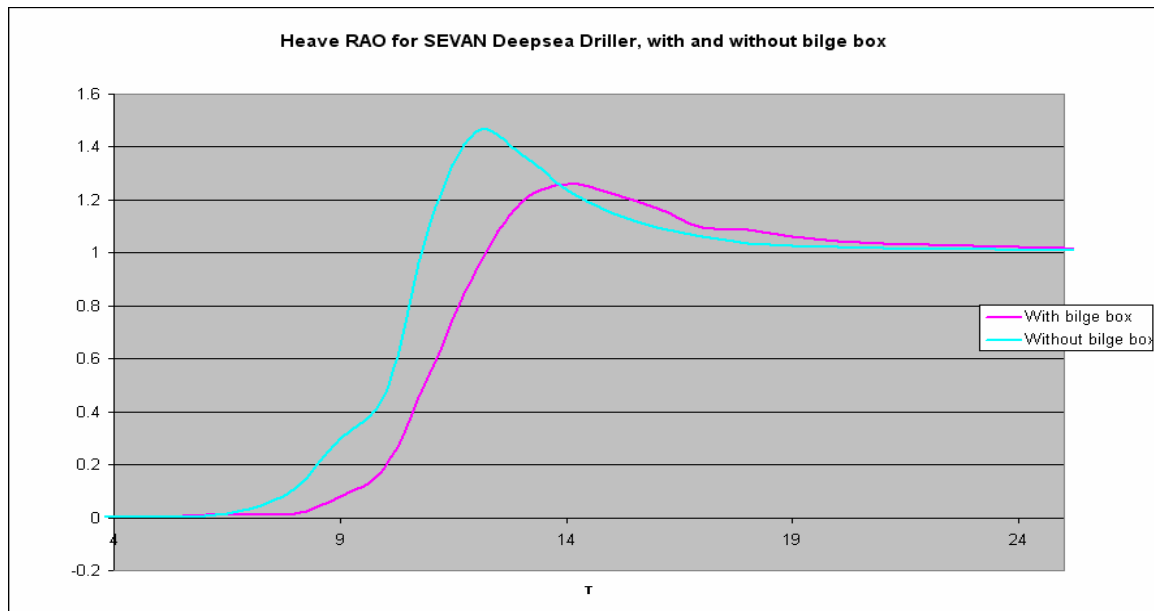
Figure 17.5: *Heave RAO SEVAN Deepsea Driller, with and without bilge box.*

The SEVAN Deepsea Driller has a natural period of about 14 seconds. The maximum dynamical amplification is less then 1.3 due to both radiation damping and viscous damping related to the bilge box. The bilge box also increases the added mass, and thereby increasing the natural period.

Figure 17.6 illustrates the bilge box's influence on the added mass A_{33} in heave, and shows an average increase in the added mass of approximately 25 0000 tons. This rises the natural period in heave from 12 to 14 seconds, and thereby enhances the motion performance significantly. If an average added mass is put into equation 17.2, one obtains an eigenperiod of 11.94 s without a bilge box and 13.86 s with a bilge box.

$$T_n = \frac{2 \cdot \pi}{\sqrt{\dfrac{\rho \cdot g \cdot A_w}{M_{33.sevan} + A_{33.sevan}}}}$$

Equation 17.2

This is in accordance with results acquired in MOSES and validates the results, given correct added mass estimated in MOSES.
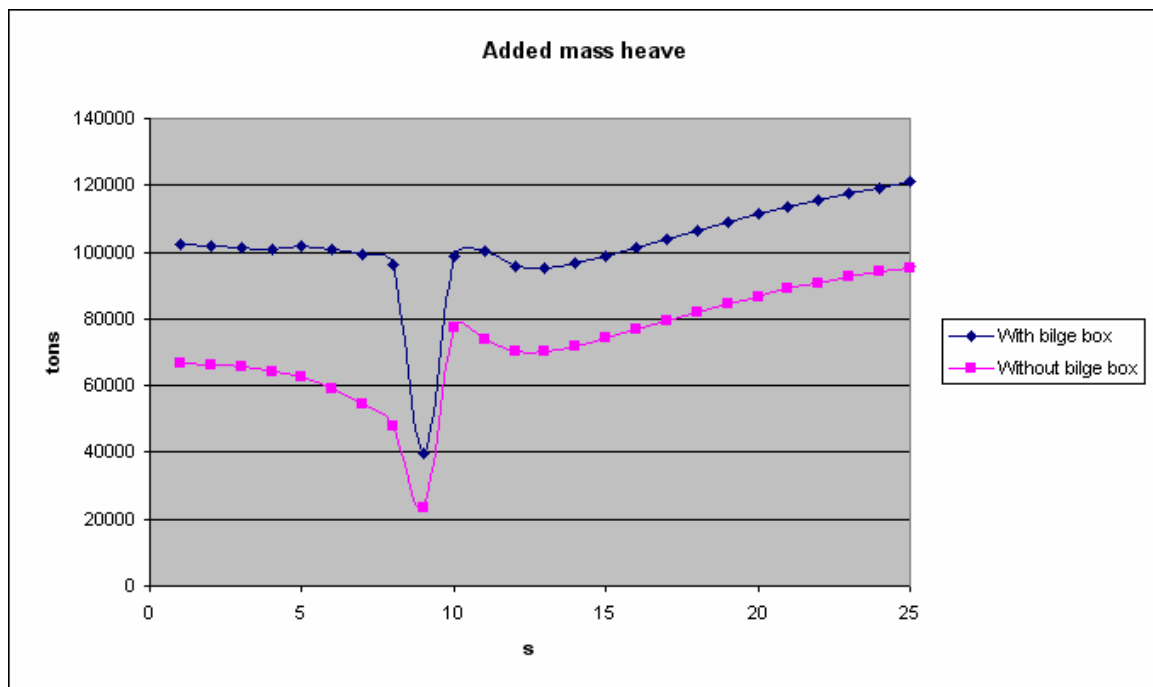
Figure 17.6: *The bilge box's influence on the added mass in heave.*

Figure 17.6 shows that there exists a so-called irregular frequency at a wave period of 9 seconds. This is a numerical phenomenon where the computational algorithm breaks down at particular frequencies. In essence, these are natural frequencies at which water would slosh inside the vessel [22]. Examples of hull shapes that are vulnerable to this numerical phenomenon are vessels having a cross section looking like an upside down T,

like the SEVAN unit. Here we have a horizontal vessel surface in close proximity to the water surface, and this can cause negative added mass.

The presence of the irregular frequency does not cause any problems concerning the motion response in this case. This can be seen in **Figure 17.5**, where the RAO is not significantly affected by the singularity in the numerical algorithm. If the irregularity however would have caused any problems, the offending periods could have been removed, and the results for these periods interpolated. There are many research papers and books written on this topic, where one of the more useful ones is [1].

17.2 Rotational response characteristics

Most tasks performed by drilling vessels have an operational limit of 4 degrees rotation in roll and pitch. Given the wave headings used in the operability analysis, one of the rotational modes are more likely to cause the vessel to rotate beyond the operational limit than the other one. Primarily this depends on the rotational natural periods and the damping levels in the corresponding degree of freedom. **Figure 17.7** shows the RAO for the most critical rotational mode for each vessel. RAOs for all degrees of freedom can be seen in appendix 6. The natural period in roll and pitch are dependent on the loading condition, as explained in chapter 12. The vessels operate in a specific operational draft, and to maintain this draft with varying deck loads, it must compensate with its ballast system. A heavy loaded condition results in a low GM and high natural period, and a light loaded condition results in a high GM and low natural period. The RAOs in **Figure 17.7** are based on the loading conditions defined in chapter 16.
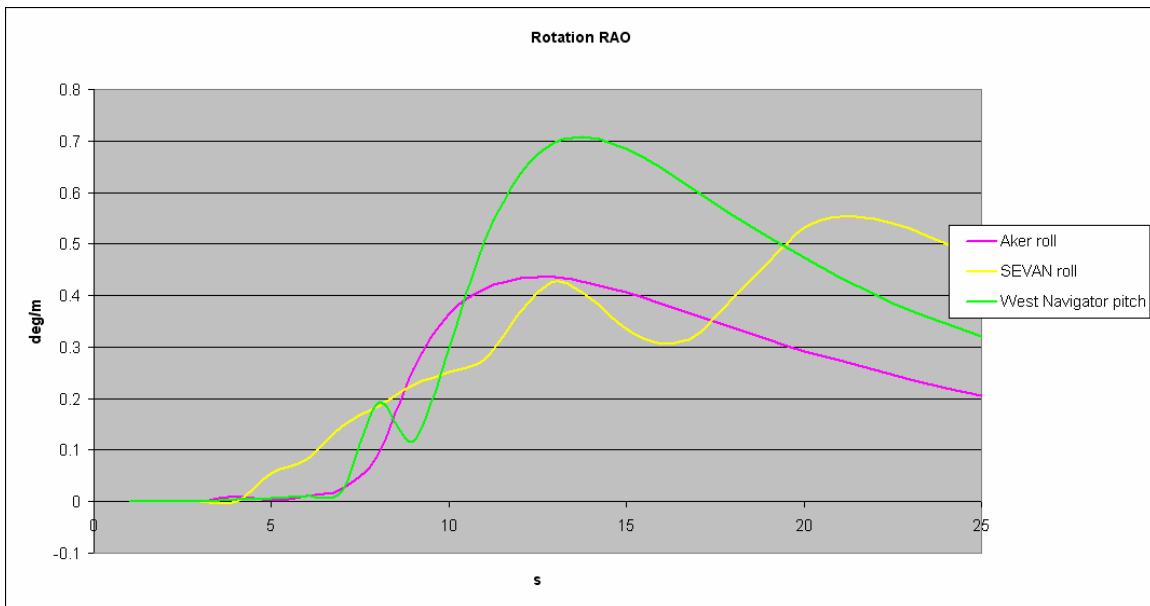
Figure 17.7: *Rotational RAOs.*

The rotational response will not be described as thoroughly as the vertical response, due to insignificant impact on the operability compared to heave motions. The West Navigator could however, analogous to the behavior in heave, experience considerable roll motions if not oriented correctly, or with wind seas and swells coming from different directions. This phenomenon is left out due to insufficient long term meteorological data.

17.3 Operational limitations

The maximum significant wave height in which the vessel can operate is very much dependent on the wave peak period. Generally speaking, the vessel can operate in larger wave heights when the wave periods are small, due to the vessels favorable response behavior at wave periods lower than its natural period.

The relationship between the wave length and height can be characterized by the wave steepness. The ratio between the wave *period* and height is closely related to the wave's steepness, and hence the steepness indicates what wave heights one can expect for a given wave period. **Figure 17.8** indicates the maximum significant wave height in which the vessel can drill, based on a maximum allowable double amplitude of 6 meters. A similar diagram has been established for each activity, with the corresponding rig floor limiting amplitudes.

The reason for the operability curves not exceeding 12.75 m in significant wave height can be related to the wave scatter diagrams which have significant wave height values ranging from 0.25 m to 12.75 m. The heave scatter diagrams, which the operability curves are based on, are calculated with the same parameter range as the wave scatter diagrams, hence the upper limitation of 12.75 m in the figure. In reality this is not a problem, since none of the vessels can operate in significant wave heights over 10 to 11 meters.
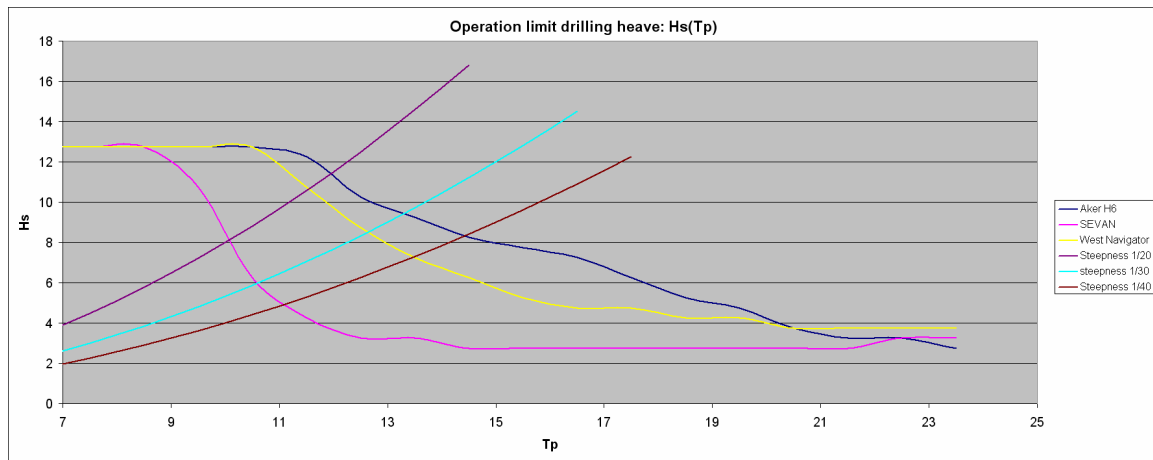
Figure 17.8: *Maximal significant wave height in which the vessels can operate.*

It can be difficult to determine a criterion for a maximum sea state in which to operate based on the blue, pink and yellow curves in **Figure 17.8.** To ease the interpretation of the figure, different average wave steepness curves are added. The formula for average wave steepness, S_p, is obtained from DNV RP C205 and can be seen in equation 17.3**.**

$$S_p = \frac{2 \cdot \pi}{g} \cdot \frac{H_s}{T_p^2}$$

Equation 17.3

Based on a selected steepness, one can define a maximum significant wave height criterion. It is however not easy to decide which wave steepness to base the criterion on, and the intersection between the selected steepness- and operability curves only acts as a rough indication. It must also be stressed that the operational criteria in **Figure 17.8** are only theoretical, and does not take DP capabilities, safety factors or wind/current loads into account. The wave headings used to generate the operability results are 45 deg off bow for Aker H6 and 25 deg off bow for West Navigator. The Sevan Deepsea Driller's response is independent of the heading, and the operability curve is therefore valid for all wave headings.

The curves in **Figure 17.8** are based on a heave scatter diagram established for each vessel. The heave scatter diagrams can be seen in appendix 3 and displays the most probable largest heave motion (m) for significant wave heights ranging from 0.25 m to 12.75 m and wave peak periods from 2.5 s to 23.5 s. The uppermost cell for each wave period in the heave scatter table which has a value larger than the operational limit for the task considered, creates the operational limit. As an example the maximum significant wave height the Aker H6 can operate in is 10.25 m, provided a peak period of 12.5 seconds. This is based on a maximum rig floor single amplitude of 3 meters, and is in accordance with **Figure 17.8.**

17.4 Operability results

The motion behavior of the vessels will depend on the location in which they are going to operate. Some areas around the world are characterized by having very short and deep waves as the Mediterranean Sea. The Pacific Ocean has a reputation of the opposite, and offshore Australia or New Zealand are known for very long wave periods, in the order of 1-2 minutes or more [21]. As seen in Figure 17.8 the operational limit depends on the wave period, hence the wave periods in the area of operation has a significant impact on the operability. In addition to this, the general harshness of the prevailing sea state varies a lot, with the environmental characteristics ranging from benign to harsh.

In the following operability results for Southern Green Canyon, Ormen Lange and west coast of Africa are presented. The monthly operability results for the Ormen Lange field are however omitted due to layout considerations, but can be seen in appendix 5.

The operability in the following tables is only related to "waiting on weather". "Downhole downtime", planned maintenance and rig equipment downtime are not taken into consideration.

Operability - Gulf of Mexico, Southern Green Canyon

Operability drilling/tripping:			GoM
	Heave	Rotation	Total
Aker H6:	1.000	1.000	1.000
SEVAN:	0.999	1.000	0.999
West Navigator:	1.000	1.000	1.000

Operability running casing:			GoM
	Heave	Rotation	Total
Aker H6:	1.000	1.000	1.000
SEVAN:	0.998	1.000	0.998
West Navigator:	1.000	1.000	1.000

Operability logging:			GoM
	Heave	Rotation	Total
Aker H6:	1.000	1.000	1.000
SEVAN:	0.998	1.000	0.998
West Navigator:	1.000	1.000	1.000

Operability miscellaneous:			GoM
	Heave	Rotation	Total
Aker H6:	1.000	1.000	1.000
SEVAN:	0.999	1.000	0.999
West Navigator:	1.000	1.000	1.000

Operability running BOP/riser:			GoM
	Heave	Rotation	Total
Aker H6:	0.999	0.999	0.999
SEVAN:	0.988	1.000	0.988
West Navigator:	0.997	0.999	0.997

Operability cementing:			GoM
	Heave	Rotation	Total
Aker H6:	1.000	1.000	1.000
SEVAN:	0.995	1.000	0.995
West Navigator:	1.000	1.000	1.000

Operability TOTAL:			GoM
	Heave	Rotation	Total
Aker H6:	1.000	1.000	1.000
SEVAN:	0.997	1.000	0.997
West Navigator:	1.000	1.000	1.000

Downtime TOTAL:			GoM
	Heave	Rotation	Total
Aker H6:	0.000	0.000	0.000
SEVAN:	0.003	0.000	0.003
West Navigator:	0.000	0.000	0.000

Table 3: *Operability Gulf of Mexico.*

Operability – All year Ormen Lange

Operability drilling/tripping:			Ormen yearly
	Heave	Rotation	Total
Aker H6:	0.994	1.000	0.994
SEVAN:	0.861	1.000	0.861
West Navigator:	0.981	0.993	0.981

Operability running casing:			Ormen yearly
	Heave	Rotation	Total
Aker H6:	0.991	1.000	0.991
SEVAN:	0.846	1.000	0.846
West Navigator:	0.973	0.992	0.973

Operability logging:			Ormen yearly
	Heave	Rotation	Total
Aker H6:	0.991	1.000	0.991
SEVAN:	0.846	1.000	0.846
West Navigator:	0.973	0.992	0.973

Operability miscellaneous:			Ormen yearly
	Heave	Rotation	Total
Aker H6:	0.994	1.000	0.994
SEVAN:	0.861	1.000	0.861
West Navigator:	0.981	0.992	0.981

Operability running BOP/riser:			Ormen yearly
	Heave	Rotation	Total
Aker H6:	0.894	0.959	0.894
SEVAN:	0.667	0.978	0.667
West Navigator:	0.846	0.897	0.846

Operability cementing:			Ormen yearly
	Heave	Rotation	Total
Aker H6:	0.968	0.999	0.968
SEVAN:	0.768	0.999	0.768
West Navigator:	0.941	0.982	0.941

Operability TOTAL:			Ormen yearly
	Heave	Rotation	Total
Aker H6:	0.982	0.996	0.982
SEVAN:	0.834	0.998	0.834
West Navigator:	0.964	0.983	0.964

Downtime TOTAL:			Ormen yearly
	Heave	Rotation	Total
Aker H6:	0.018	0.004	0.018
SEVAN:	0.166	0.002	0.166
West Navigator:	0.036	0.017	0.036

Table 4: *Operability Ormen Lange*

Operability – Typical West coast of Africa conditions

Operability drilling/tripping:			Africa
	Heave	Rotation	Total
Aker H6:	1.000	1.000	1.000
SEVAN:	1.000	1.000	1.000
West Navigator:	1.000	1.000	1.000

Operability running casing:			Africa
	Heave	Rotation	Total
Aker H6:	1.000	1.000	1.000
SEVAN:	1.000	1.000	1.000
West Navigator:	1.000	1.000	1.000

Operability logging:			Africa
	Heave	Rotation	Total
Aker H6:	1.000	1.000	1.000
SEVAN:	1.000	1.000	1.000
West Navigator:	1.000	1.000	1.000

Operability miscellaneous:			Africa
	Heave	Rotation	Total
Aker H6:	1.000	1.000	1.000
SEVAN:	1.000	1.000	1.000
West Navigator:	1.000	1.000	1.000

Operability running BOP/riser:			Africa
	Heave	Rotation	Total
Aker H6:	1.000	1.000	1.000
SEVAN:	0.922	1.000	0.922
West Navigator:	0.998	1.000	0.998

Operability cementing:			Africa
	Heave	Rotation	Total
Aker H6:	1.000	1.000	1.000
SEVAN:	0.993	1.000	0.993
West Navigator:	1.000	1.000	1.000

Operability TOTAL:			Africa
	Heave	Rotation	Total
Aker H6:	1.000	1.000	1.000
SEVAN:	0.992	1.000	0.992
West Navigator:	1.000	1.000	1.000

Downtime TOTAL:			Africa
	Heave	Rotation	Total
Aker H6:	0.000	0.000	0.000
SEVAN:	0.008	0.000	0.008
West Navigator:	0.000	0.000	0.000

Table 5: *Operability West coast of Africa.*

17.5 Discussion of operability results

The total operability in the GoM is as expected very good for all vessels; 100 % for the West Navigator and the Aker H6, and 99.7 % for the SEVAN Deepsea Driller. Furthermore, all vessels achieve a high operability in the west coast of Africa. West Navigator and Aker H6 can operate in all sea states typical for the west coast of Africa, while the SEVAN unit in this area has a total operability of 99.2 %. In spite of very low significant wave heights in the area, the SEVAN unit exhibits some vertical motions due to resonance effects.

The operability in the Ormen Lange field is very satisfactory for the Aker H6 and the West Navigator, respectively 98.2 % and 96.4 %. "Offshore structures" by Clauss et al states that the operational efficiency of large drillships with dynamic positioning compares well with large semisubs. Considering this statement, the operability results where as anticipated. The SEVAN Deepsea Driller is according to the hydrodynamical results **not** very suitable for North Sea conditions, with an all year operability of 83.4%. However the SEVAN unit shows an acceptable operability in the summer season from April to September, see **Figure 17.9**. During the winter season the operability for the SEVAN unit is much to low, and it would spend much time waiting on weather.
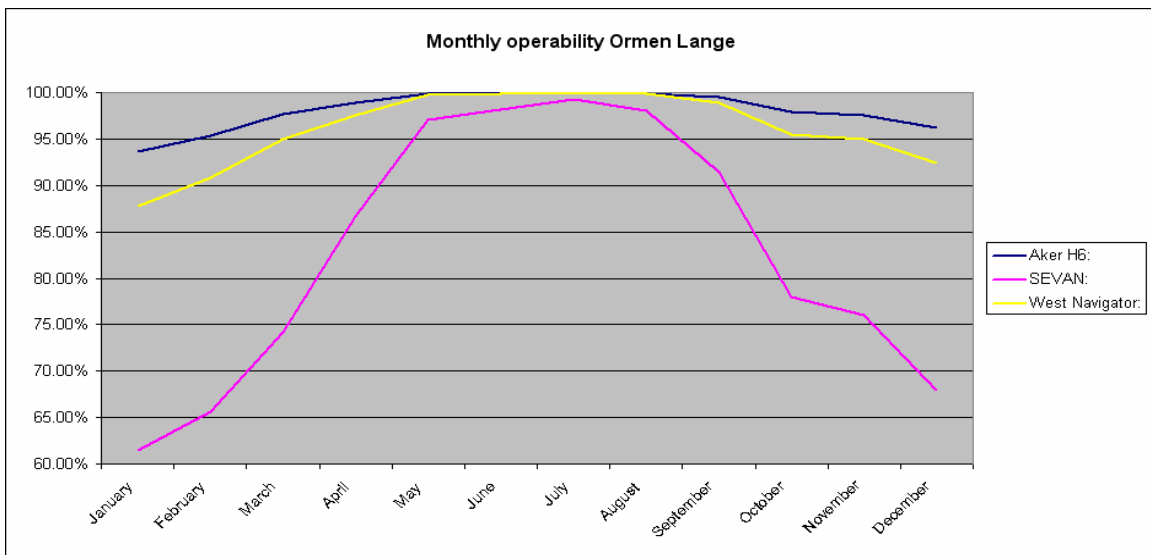
Figure 17.9: *Monthly total operability Ormen Lange*

The operability can however be somewhat deceptive regarding indication of general motion characteristics. It tells you how much of the time the vessel can operate, but it does not tell you in what fashion it operates. In spite of the operability of the West Navigator being just 1.8 % under the operability of the Aker H6 in North Sea conditions, it does not mean that the motion amplitudes in general are 1.8 % lower.

17.5.1　Response in sea states with low to medium peak periods

Figure 17.10 shows the most probable largest heave motions for Hs = 5.75 meters at different wave periods. The wave height is selected for convenience, and since there is assumed a linear correlation between the wave height and the motion response the wave height is irrelevant and the results can be linearly scaled up to a desired wave height. A PM spectrum was used in this particular case to calculate the heave motions. Figure 17.10 reveals some interesting motion characteristics at low wave peak periods.

Spectral peak period (s)	2.5	3.5	4.5	5.5	6.5	7.5	8.5
Aker H6:	0.00	0.00	0.02	0.03	0.08	0.19	0.39
West Navigator:	0.00	0.01	0.03	0.09	0.24	0.49	0.74
SEVAN Driller:	0.00	0.00	0.02	0.04	0.09	0.31	0.81

Figure 17.10: *Most probable largest heave values for Hs = 5.75 m and Tp = 2.5 – 8.5 s*

In spite of low operability in the North Sea, the SEVAN Deepsea Driller shows good motion behavior at low wave peak periods. If we consider wave periods between 4.5 and 8.5 seconds, which **98 %** of the sea states in the Gulf of Mexico consist of, the SEVAN unit performs better than the West Navigator, as seen in **Figure 17.11.** The Aker H6 has in average approximately half the motion amplitudes of the West Navigator in sea states with peak periods less than 10 seconds.
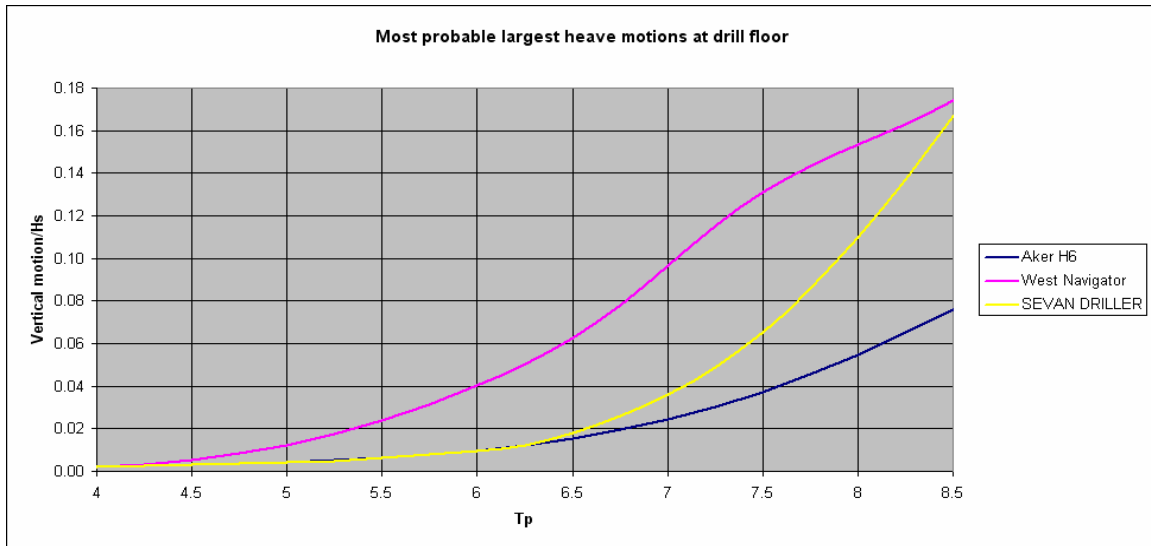
Figure 17.11: *Most probable largest heave motions at drill floor in sea states with low peak periods.*

Figure 17.11 reveals that the SEVAN Deepsea Driller and the Aker H6 have identical heave characteristics in sea states with peak periods lower than 6.5 seconds, which 82 % of the sea states in the Gulf of Mexico consist of. The West Navigator has significantly higher heave amplitudes in these sea states.

17.5.2　Response in sea states with high peak periods

In terms of operability, the most important wave period range is around eight to fifteen seconds. Waves with periods higher than fifteen seconds have seldom large energy, and waves with periods under eight seconds are rarely any threat concerning large dynamic amplification. This is why values between only eight and fifteen seconds are included in the diagram published by Aker Drilling, seen in **Figure 17.13**.
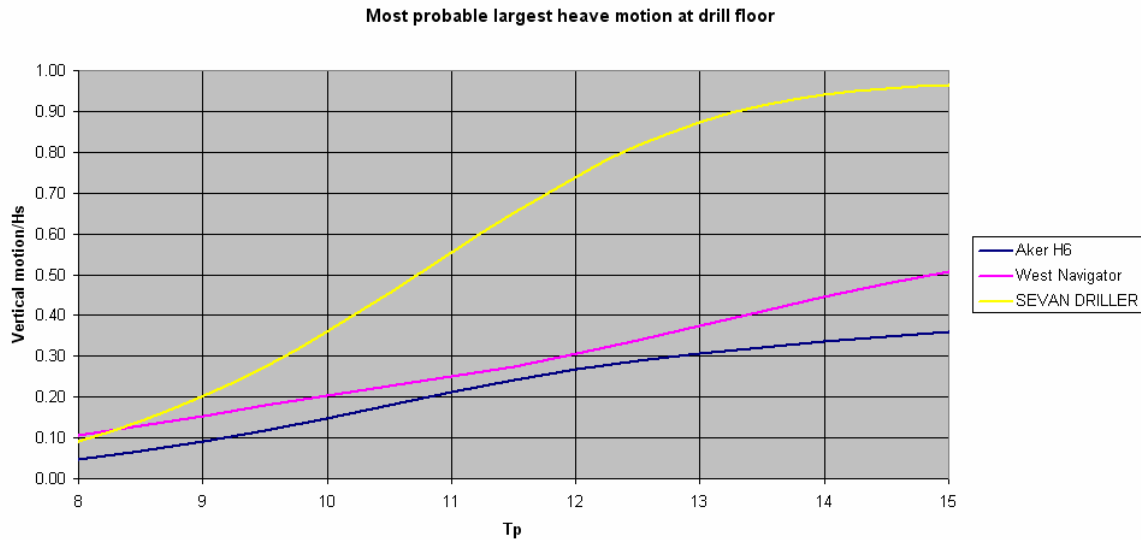
Figure 17.12: *Most probable largest heave motions as a function of peak period.*

In sea states with peak periods over 8.5 seconds, the West Navigator has less heave motions than the SEVAN Deepsea Driller. This is illustrated in **Figure 17.12**. The unfavorable heave motions of the SEVAN unit in this period range can be ascribed its heave natural period of about 14 seconds. The natural period in heave for the West Navigator is actually about 10 seconds, but it does not suffer from this if oriented correctly. The saddle-type dynamic pressure distribution along its long hull prevents the response from peaking at the natural period and the heave motions remain relatively small.

Figure 17.13 shows the most probable largest heave motions for Aker H6, and is based on a figure published on Aker Drilling's website. Everything in **Figure 17.13** is in original state except from the yellow broken line, which represents the response magnitudes calculated in this thesis. The figure confirms that the results are in accordance with Aker's, and therefore acts, together with **Figure 16.2**, as a verification of my own results. The small deviation at lower wave periods, are most probably caused by the wave heading used. The calculated motion amplitudes are based on a 45 deg off bow heading, while the heading used in **Figure 17.13** is not indicated. Regarding the operability the deviation is not significant, since wave conditions with peak periods lower than 10 seconds normally do not cause any excessive motions for the Aker H6.
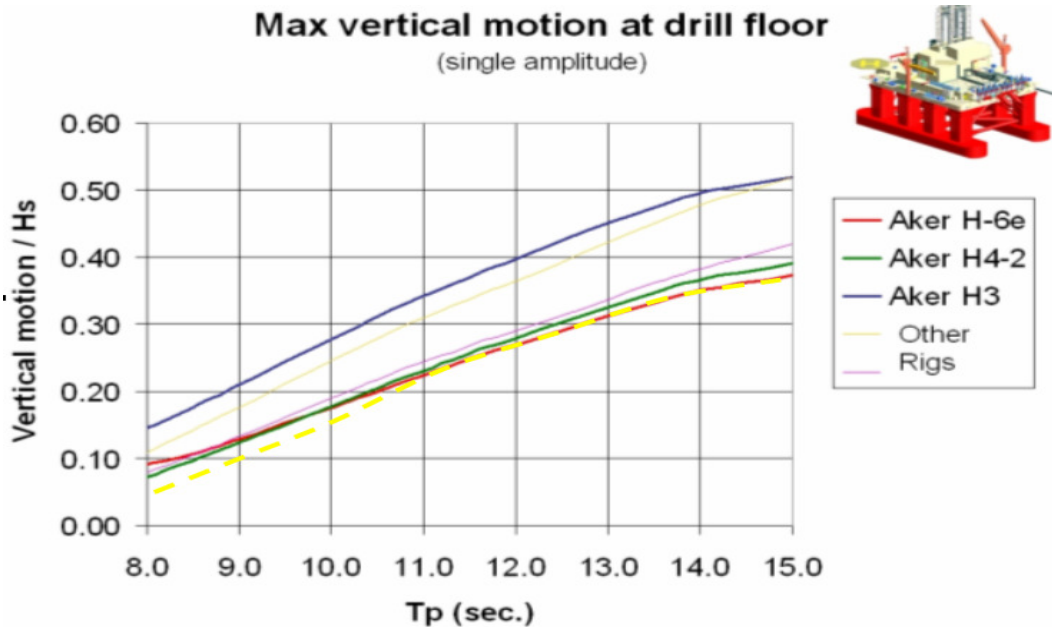
Figure 17.13: *Most probable maximum vertical motion at drill floor (From Aker Drilling's Website).*

17.5.3   Response in sea states with extreme peak periods

From an operability point of view, the vessel's behavior in peak periods over 14-15 seconds is less important than the behavior in peak periods from 8 to 15 seconds. In a harsh environment area like the Ormen Lange, only 2 % of the sea states consist of peak periods exceeding 14.5 s. Much of the difference in operability for Aker H6 and West Navigator can however be ascribed motion response in sea states with peak periods exceeding 14.5 seconds.

If we only consider drilling/tripping, there is a 1.3 % difference in operability between the two mentioned vessels, see **Table 4**. If we compare the heave- and wave scatter diagrams carefully, we find that as much as 0.9 % of the difference in operability can be ascribed the heave response in sea states with peak periods exceeding 14.5 s. This is quite remarkable, considering that only 2 % of the sea states contain peak periods over 14.5 seconds. The reason for extreme peak periods having such a large impact on the operability results, especially for the Aker H6 and the SEVAN unit, can probably be explained by Figure 17.8. It shows that both vessels can drill in all sea states with peak periods under 12 to 15 seconds, depending on the wave steepness. The *difference* in operability is therefore directly related to behavior in wave periods exceeding this range. The most probable largest heave motions in extreme sea states can be seen in **Figure 17.14**.
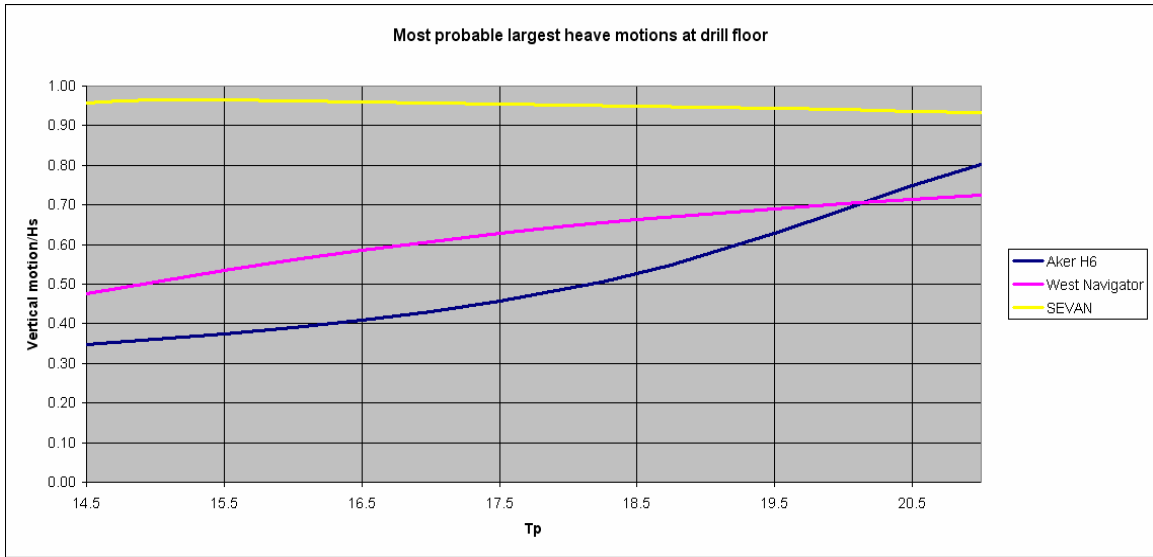
Figure 17.14: *Most probable largest heave motions in extreme sea states*

17.5.4 The heave limitation's influence on the operability

The heave limitations used in the operability analysis are typical values for the latest generation of drilling vessels, and depending on the sensitivity of the operation, the heave limitation can vary a lot. In **Figure 17.15** the operability in the Ormen Lange field is displayed as a function of limiting heave amplitude, and the curves show that Aker H6 has the highest operability for all heave limits. The West Navigator also has a high operability, except for very strict heave limitations, where the SEVAN unit performs better than the West Navigator. Operability in this heave limitation range is however more academically than practically interesting, as drilling- and completion operations seldom require heave restrictions of less than 2 meters.
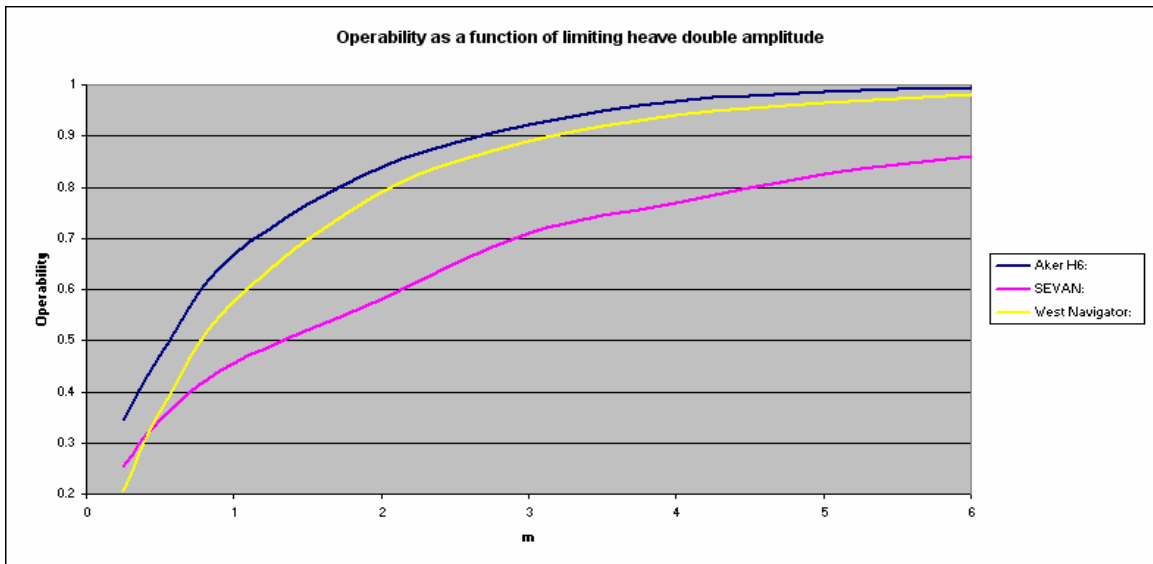
Figure 17.15: *Operability as a function of limiting heave amplitude. Based on the Ormen Lange "all year" scatter diagram.*

60

17.6 Optimizing the SEVAN hull for harsh environment

SEVAN MARINE is focusing on areas like the GoM, West Africa, Brazil, India and Southeast Asia in the marketing of the drilling unit. In the North Western Europe the company is until now not focusing on drilling, but rather on FPSO`s and "Gas to Wire" offshore powerplants. At the same time they are marketing the SEVAN Deepsea Driller as a vessel capable of operating in harsh environment, but hydrodynamical analysis shows that it has a low operability in severe weather due to resonance in heave.

The SEVAN unit is within *SEVAN MARINE* called SEVAN DRILLER #1, and was designed to operate in the ultra deep waters in Gulf of Mexico. Since the SEVAN DRILLER # 1 was designed to operate in an area with relatively mild conditions, they chose not to sacrifice fluid- and deck-load capacity for lower heave motions in high wave periods. This results in a poor operability in the North Sea during the winter season.

They have not announced any concrete plans to design a drilling rig *particularly* designed for North Sea winter conditions, but through the communication with the company, one can assume that there is a possibility for a future circular drilling rig, SEVAN DRILLER #2, specially designed for severe weather. There are many parameters than can be tuned to achieve better heave motion characteristics in severe weather, such as operational draft, water line area and bilge box diameter. These parameters also have an impact on building costs, freeboard requirements, stability, DP requirements, structural integrity, surge motions and so on. If one disregards these relations, it is not difficult to come up with a change to the design which makes it suitable for harsh environment operations.

One could of coarse aim for a conventional Spar design, with an increased draft and small hull diameter. With this design, the SEVAN unit would definitely have smaller heave motions, but loose too many of its benefits. As another option the waterline area and bilge box diameter could be respectively reduced and increased to achieve better performance in rough sea.

As an experiment the inside diameter (see Figure 20.4 for hull details) of the hull and bilge box diameter are changed to respectively 40 and 92 m, see Figure 17.16. This leads to a significantly higher operability in North Sea conditions. The increase in inside diameter reduces the waterline area from 3965 m^2 to 3125 m^2, thereby increasing the natural period in heave form 14 to 18 seconds. The enlarged bilge box also contributes to this increase by introducing additional added mass in heave. With the new design, the SEVAN unit achieves an all year operability of 93 % in the North Sea. An additional increase in operability is possible by further reducing the waterline area and increasing the bilge box diameter at the expense of deck load capacity, fluid capacity and stability.
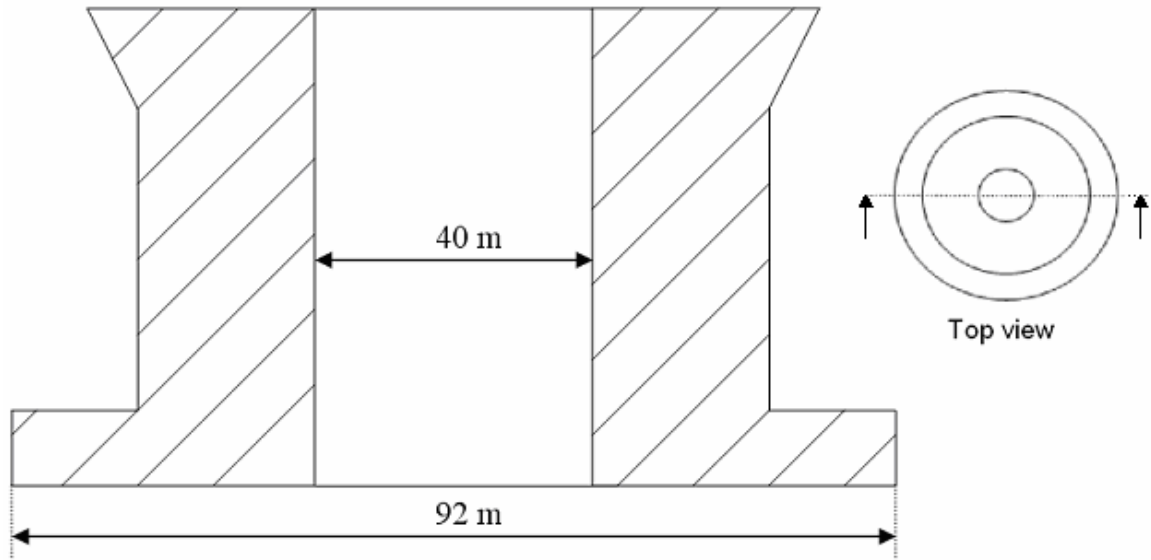
Figure 17.16 : *Cross section of a **modified** SEVAN drilling platform.*

18 Conclusion

Knowing the forces acting on arbitrary structures, it is possible to calculate the seaway motions of a floating vessel. Hydrodynamical load models and RAOs for the different drilling units have been established as well as long and short term prediction of the response. The operability in the GoM, the North Sea and the west coast of Africa has been calculated. As expected all units have a very high operability in the GoM and the west coast of Africa, which are characterized by relatively mild wave conditions. As anticipated, the Aker H6 has the highest operability in the North Sea, and can operate in 98.2 % of the sea states. The West Navigator also performs satisfactorily in North Sea conditions, with an operability of 96.4 %. The SEVAN unit is not suited for operation in the North Sea during the winter season, due to vertical resonance in severe weather.

All three units are marketed as ultra deep water and harsh environment units. Water depths exceeding 2000 m is a recognized definition of ultra deep water, whereas harsh environment is a relative term. *SEVAN MARINE* claims that their unit is tailored for both deepwater and harsh environments [18]. Harsh environment is as mentioned a relative term, but according to the hydrodynamical results in this report it would undoubtedly be more appropriate to classify the unit as a "medium environment" vessel. *Aker Drilling ASA* defines a "harsh environment drilling floater" as a vessel that can operate on the Norwegian continental shelf all year round. According to this definition, the SEVAN Deepsea Driller cannot be characterized as a harsh environment drilling platform, while the two other concepts can rightfully be referred to as harsh environment units.

A hull structure made for ultra-deep drilling, like the SEVAN unit, will typically focus on gaining a high variable deck load capacity at the lowest possible cost. This is usually achieved by increasing the waterplane area in order to gain higher stability restoring moment, and hence increase the variable deck load capacity of the rig. However a high water plane area negatively influences the vertical motion behavior in harsh environments, due to an unfavorable natural period in heave. The SEVAN Deepsea Driller is tailor made to suit the deck load capacity requirements of the buyer, and according to the analyses, one always has to make some compromises between load capacity/stability and motion performance.

Recommendations for further work are to study more carefully the influence of swells, by introducing a two peak wave spectrum. One must also take into consideration that swells could have a different direction than wind seas. Furthermore the interface of the developed excel program for prediction of short and long term response could have been made more user friendly. One could also look more into the costs involved with downtime caused by "waiting on weather", compared to the costs associated with transit, re-supply, day rates and so on.

19 References

/1/	Faltinsen O.M, "Sea Loads on ships and offshore structures", Cambridge University Press, 1990
/2/	Rao S. S, "Mechanical vibrations", Addison-Wesley Publishing Company, 2004
/3/	21st National Congress on Maritime Transportation, Ship Construction and Offshore Engineering, Rio de Janeiro, Brazil. 27th November to 1st December 2006
/4/	DNV RP-C 103 "Column-Stabilized Units", February 2005
/5/	DNV RP-F 205 "Global performance analysis of deepwater floating structures", October 2004
/6/	DNV RP-C 205, "Environmental conditions and environmental loads", april 2007
/7/	Arnfinn Nergaard, "Notat om bevegelse og respons", UiS
/8/	Markedsføringspresentasjon av Aker H-6e, Pareto-conference, september 2006.
/9/	Gunther Clauss, Eike Lehman and Carsten Østergaard, "Offshore Structures Volume 1, Conceptual Design and Hydromechanics" , Springer-Verlag, 1992
/10/	James F. Wilson ,"Dynamics of Offshore Structures" Second edition, John Wiley & Sons, 2003
/11/	Miljeteig Angunn, "Dynamic response of the Kvitebjørn jacket", UiS, 2006
/12/	Sørvaag Christian, " Dynamisk analyse av slanke konstruksjoner utsatt for bølgelast", UiS, 2003
/13/	Hooft J.P, "Hydrodynamic aspects of Semi-Submersible platforms", Wageningen, 1972
/14/	Jorde Jens H., "Hydrodynamikk", 1988
/15/	Larsen Carl M., " SIN 1015 – Marin dynamikk", 2000
/16/	Gudmestad O. T., "TE 6007 bølgeanalyser", 2002
/17/	Næss A., "Frequency domain analysis of dynamic response of drag dominated offshore structures", 1998
/18/	Offshore Magazine, August 2006
/19/	Scandinavian OIL-GAS MAGAZINE, NO. 7/8 2006
/20/	SEVAN Marine, Prospectus, November 2007

/21/	http://www.rigzone.com/news/insight/insight.asp?i_id=74 08.06.2008
/22/	MOSES reference guide, March 2007
/23/	RS Platou offshore, " The Platou report", 2008
/24/	Presentation Sevan Marine –NFLB conference, Bergen, February, 2007
/25/	Aker drilling ASA, Prospectus, 19 December 2006

20 Appendices

1. Verification of the West Navigator heave RAO

No information regarding the motion characteristics of the West Navigator is available, hence other similar vessels have to be used to verify the calculated RAOs. Most drill ships have conventional hull geometry, and the heave RAOs of different drill ships with equal displacement should compare quite well. *Gusto MSC* has published RAOs for drillships with various displacements, and the heave RAO for two drillships with 73 000 t (P 10 000) and 132 000 t (DP-FPSO) operational displacement are used to determine whether the West Navigators calculated RAO is reasonable or not.

Figure 20.1 shows the heave RAO for various drillships, with the green and the red curve representing the RAO of respectively the DP-FPSO and the P-10 000.
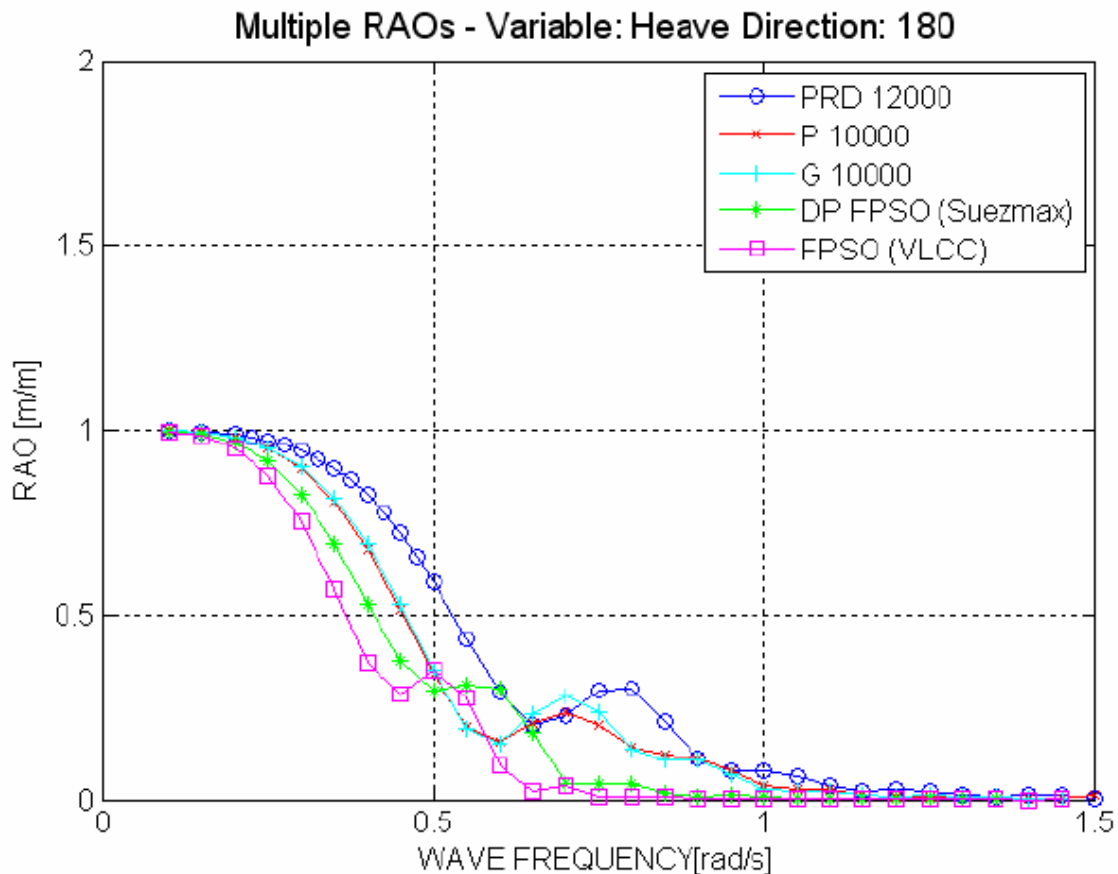
Figure 20.1: *Heave RAO of various drill ships as a function of angular frequency.*

West Navigator's RAO is in MOSES calculated as a function of wave *period*, and to compare this RAO with **Figure 20.1** a "middle curve" between the red and green in **Figure 20.1** is drawn as a function of wave *period* in **Figure 20.2**, based on the

conversions made in **Table 6**. **Figure 20.2** indicates that the calculated heave RAO for the West Navigator is reasonable, and is in accordance with results from similar vessels with equal displacement.
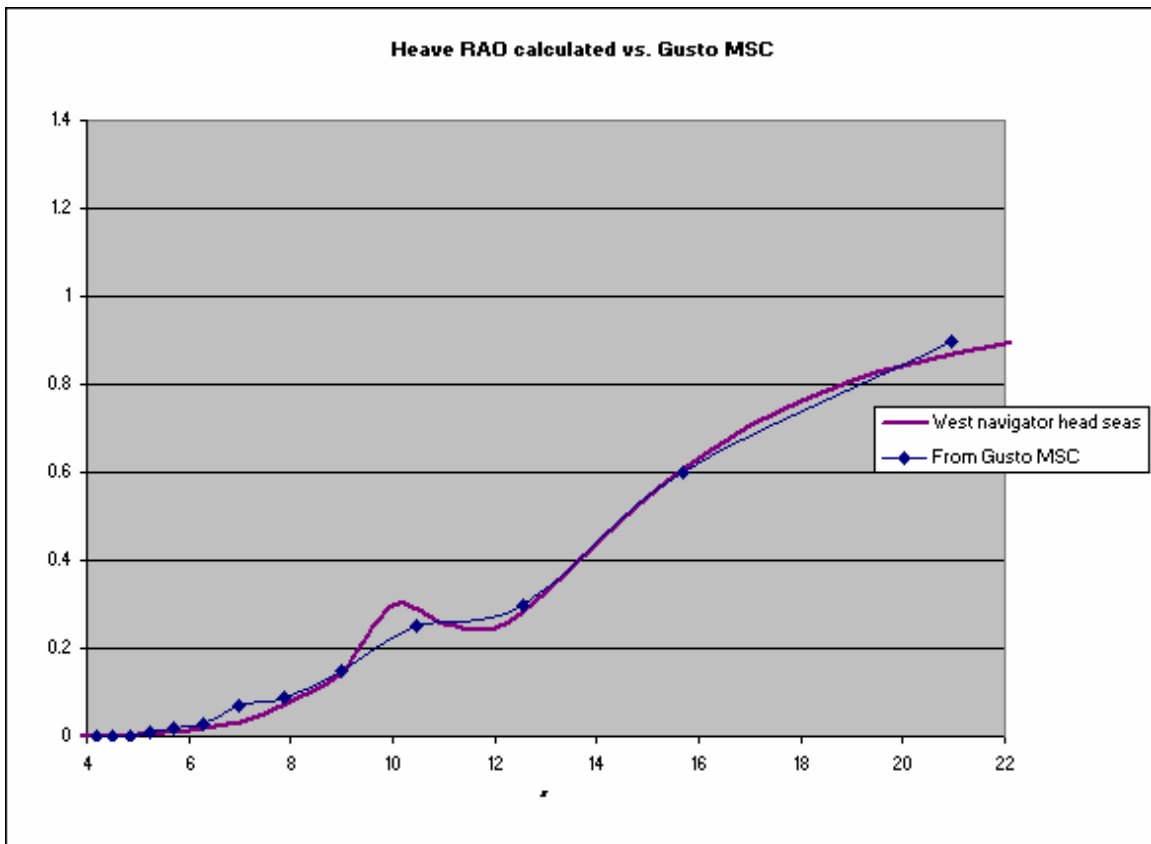
Figure 20.2: *Heave RAO calculated vs. average between P-10000 and DP-FPSO.*

Wave frequency (rad/s)	RAO value	Wave period (s)
0.1	1	62.83185307
0.2	1	31.41592654
0.3	0.9	20.94395102
0.4	0.6	15.70796327
0.5	0.3	12.56637061
0.6	0.25	10.47197551
0.7	0.15	8.97597901
0.8	0.09	7.853981634
0.9	0.07	6.981317008
1	0.03	6.283185307
1.1	0.02	5.711986643
1.2	0.01	5.235987756
1.3	0	4.833219467
1.4	0	4.487989505
1.5	0	4.188790205

Table 6: *Conversion of RAO values*

2. Relevant vessel geometry

SEVAN Driller:
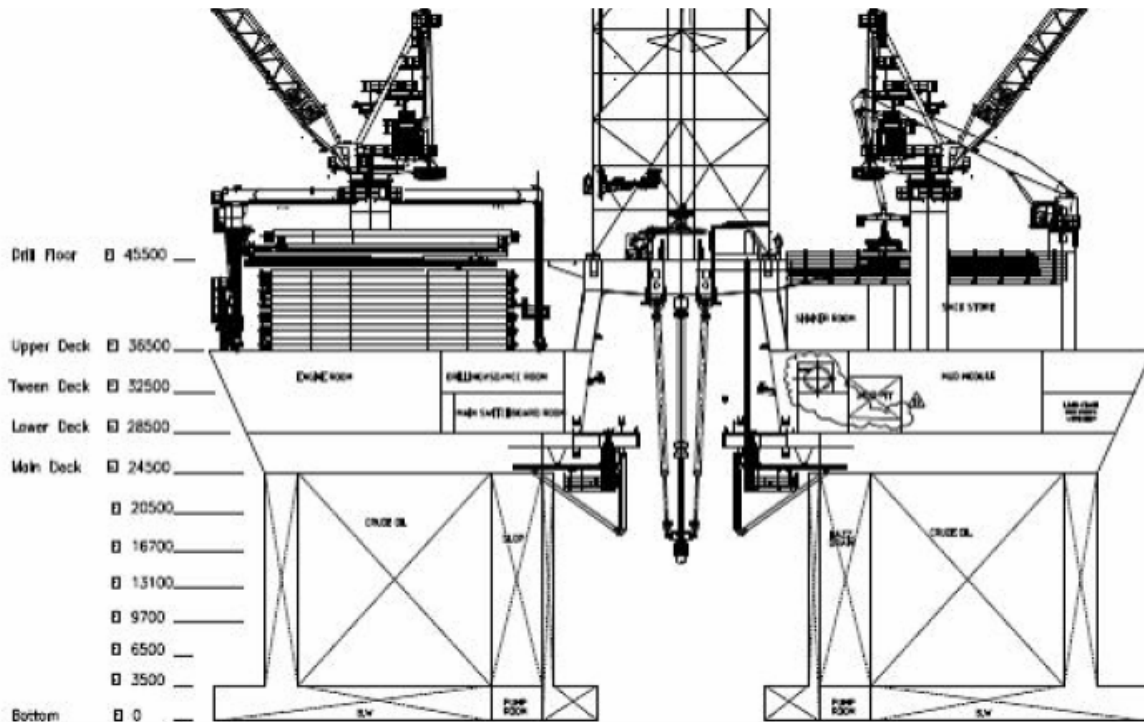
Figure 20.3: _The SEVAN Deepsea Driller – General arrangements, Profile in Midship View_

Hull diameter: …...…..75 m

Deck diameter: ……....80 m

Bilge box diameter:…..84 m

Bilge box height: …....3.5 m

Platform height: …...36.5 m

Waterplane area: ....3965 m^2

Figure 20.4: _The SEVAN Driller under construction in COSCO yard._

The moonpool in the SEVAN unit consists of a standard 12 x 20 m hole in the lower deck and the bottom hull. At elevations between 3.5 m and 28.5 m the moonpool is as indicated in **Figure 20.3** circular with a diameter of approximately 24 m. The circular section can also be seen in **Figure 20.4**. Moonpool dimensions are obtained from drafts and pictures like the above figures, but because of confidential detailed geometry, the dimensions are given with certain reservations.

West Navigator:
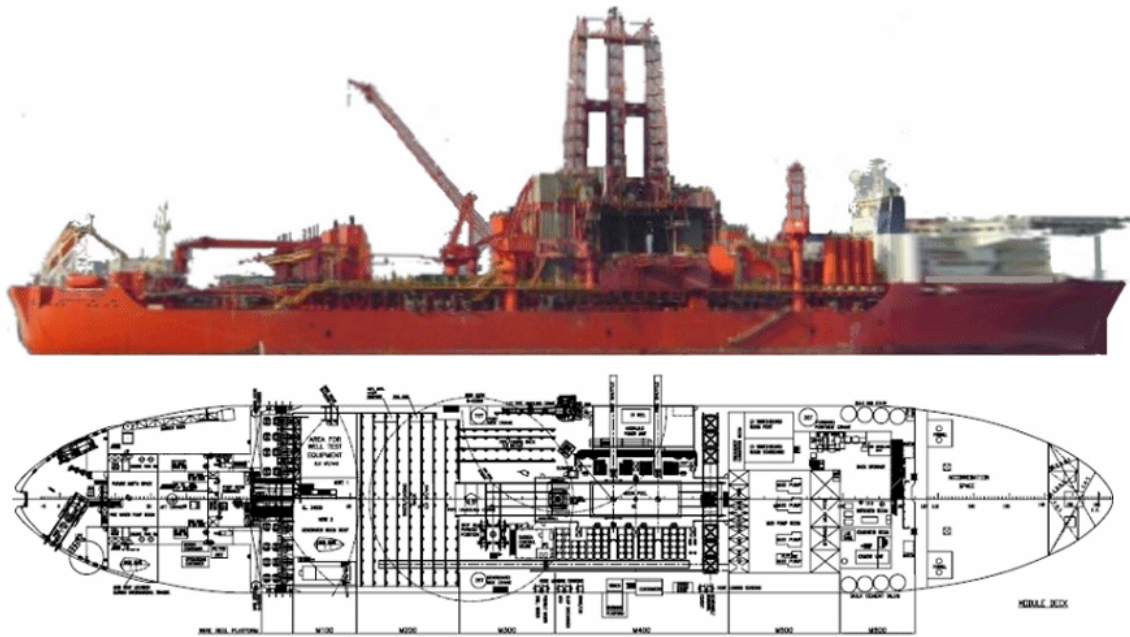
Figure 20.5: *The West Navigator – General arrangements, Profile in Top View*

Length:………………….………..…253 m   Moonpool width:………………....…12.5 m

Breath: …………………..…....….42 m   Moonpool length: ………………........20 m

Deck height: …………………….…....24 m   Waterplane area: ………………..…… 8317 m^2

Dist. from bow to center moonpool: 104 m

Aker H6:

Length main deck: ………………....90 m   Column height: ……………….…..….27.5 m

Breath main deck: ………..….……..70 m   Pontoon length: ………….……..….…120 m

Breath including columns: …….....…77 m   Pontoon beam: …………….....….……19.5 m

Column width:…………… ...…..…12.5 m   Pontoon height: ……………....……….10 m

Column length: …………..….…….12.5 m   Waterplane area: ……………..…….…..1222 m^2

3. Heave scatter diagrams

Aker H6 (Most probable largest heave single amplitude in meters):

Hs (m)	Spectral peak period (s)																					
	2.5	3.5	4.5	5.5	6.5	7.5	8.5	9.5	10.5	11.5	12.5	13.5	14.5	15.5	16.5	17.5	18.5	19.5	20.5	21.5	22.5	23.5
0.25	0.00	0.00	0.00	0.00	0.00	0.01	0.02	0.03	0.05	0.06	0.07	0.08	0.09	0.09	0.10	0.11	0.13	0.16	0.19	0.21	0.23	0.23
0.75	0.00	0.00	0.00	0.00	0.01	0.02	0.05	0.09	0.14	0.18	0.22	0.24	0.26	0.28	0.31	0.34	0.40	0.47	0.56	0.64	0.69	0.70
1.25	0.00	0.00	0.00	0.01	0.02	0.04	0.09	0.15	0.23	0.30	0.36	0.40	0.43	0.47	0.51	0.57	0.66	0.79	0.93	1.07	1.15	1.17
1.75	0.00	0.00	0.01	0.01	0.02	0.06	0.12	0.21	0.32	0.42	0.51	0.56	0.61	0.66	0.72	0.80	0.92	1.10	1.31	1.49	1.61	1.64
2.25	0.00	0.00	0.01	0.01	0.03	0.07	0.15	0.26	0.41	0.55	0.65	0.72	0.78	0.84	0.92	1.03	1.19	1.41	1.68	1.92	2.06	2.11
2.75	0.00	0.00	0.01	0.02	0.04	0.09	0.19	0.32	0.50	0.67	0.79	0.88	0.96	1.03	1.12	1.26	1.45	1.73	2.06	2.35	2.52	2.58
3.25	0.00	0.00	0.01	0.02	0.05	0.11	0.22	0.38	0.59	0.79	0.94	1.05	1.13	1.22	1.33	1.48	1.71	2.04	2.43	2.77	2.98	3.05
3.75	0.00	0.00	0.01	0.02	0.05	0.12	0.26	0.44	0.68	0.91	1.08	1.21	1.30	1.41	1.53	1.71	1.98	2.36	2.80	3.20	3.44	3.52
4.25	0.00	0.00	0.01	0.03	0.06	0.14	0.29	0.50	0.77	1.03	1.23	1.37	1.48	1.59	1.74	1.94	2.24	2.67	3.18	3.63	3.90	3.99
4.75	0.00	0.00	0.01	0.03	0.07	0.16	0.32	0.56	0.86	1.15	1.37	1.53	1.65	1.78	1.94	2.17	2.50	2.98	3.55	4.05	4.36	4.46
5.25	0.00	0.00	0.02	0.03	0.07	0.17	0.36	0.62	0.95	1.27	1.52	1.69	1.83	1.97	2.15	2.40	2.77	3.30	3.93	4.48	4.82	4.93
5.75	0.00	0.00	0.02	0.03	0.08	0.19	0.39	0.67	1.04	1.39	1.66	1.85	2.00	2.15	2.35	2.63	3.03	3.61	4.30	4.91	5.28	5.40
6.25	0.00	0.01	0.02	0.04	0.09	0.21	0.43	0.73	1.13	1.51	1.81	2.01	2.17	2.34	2.56	2.85	3.30	3.93	4.67	5.33	5.74	5.87
6.75	0.00	0.01	0.02	0.04	0.09	0.22	0.46	0.79	1.22	1.64	1.95	2.17	2.35	2.53	2.76	3.08	3.56	4.24	5.05	5.76	6.19	6.34
7.25	0.00	0.01	0.02	0.04	0.10	0.24	0.49	0.85	1.31	1.76	2.09	2.33	2.52	2.72	2.96	3.31	3.82	4.56	5.42	6.19	6.65	6.81
7.75	0.00	0.01	0.02	0.05	0.11	0.26	0.53	0.91	1.40	1.88	2.24	2.49	2.69	2.90	3.17	3.54	4.09	4.87	5.80	6.61	7.11	7.28
8.25	0.00	0.01	0.02	0.05	0.11	0.27	0.56	0.97	1.49	2.00	2.38	2.65	2.87	3.09	3.37	3.77	4.35	5.18	6.17	7.04	7.57	7.75
8.75	0.00	0.01	0.03	0.05	0.12	0.29	0.60	1.03	1.58	2.12	2.53	2.82	3.04	3.28	3.58	4.00	4.61	5.50	6.54	7.47	8.03	8.22
9.25	0.00	0.01	0.03	0.06	0.13	0.31	0.63	1.08	1.67	2.24	2.67	2.98	3.22	3.47	3.78	4.22	4.88	5.81	6.92	7.89	8.49	8.69
9.75	0.00	0.01	0.03	0.06	0.14	0.32	0.66	1.14	1.76	2.36	2.82	3.14	3.39	3.65	3.99	4.45	5.14	6.13	7.29	8.32	8.95	9.16
10.25	0.00	0.01	0.03	0.06	0.14	0.34	0.70	1.20	1.85	2.48	2.96	3.30	3.56	3.84	4.19	4.68	5.40	6.44	7.66	8.74	9.41	9.63
10.75	0.00	0.01	0.03	0.07	0.15	0.36	0.73	1.26	1.94	2.61	3.11	3.46	3.74	4.03	4.40	4.91	5.67	6.75	8.04	9.17	9.87	10.10
11.25	0.00	0.01	0.03	0.07	0.16	0.37	0.77	1.32	2.03	2.73	3.25	3.62	3.91	4.22	4.60	5.14	5.93	7.07	8.41	9.60	10.32	10.57
11.75	0.00	0.01	0.04	0.07	0.16	0.39	0.80	1.38	2.12	2.85	3.39	3.78	4.09	4.40	4.81	5.37	6.20	7.38	8.79	10.02	10.78	11.04
12.25	0.00	0.01	0.04	0.07	0.17	0.41	0.83	1.44	2.21	2.97	3.54	3.94	4.26	4.59	5.01	5.59	6.46	7.70	9.16	10.45	11.24	11.51
12.75	0.00	0.01	0.04	0.08	0.18	0.42	0.87	1.49	2.30	3.09	3.68	4.10	4.43	4.78	5.21	5.82	6.72	8.01	9.53	10.88	11.70	11.98

West Navigator:

Hs (m)	Spectral peak period (s)																					
	2.5	3.5	4.5	5.5	6.5	7.5	8.5	9.5	10.5	11.5	12.5	13.5	14.5	15.5	16.5	17.5	18.5	19.5	20.5	21.5	22.5	23.5
0.25	0.00	0.00	0.00	0.00	0.01	0.02	0.03	0.05	0.06	0.07	0.08	0.10	0.12	0.13	0.15	0.16	0.17	0.17	0.18	0.18	0.19	0.19
0.75	0.00	0.00	0.00	0.01	0.03	0.06	0.10	0.14	0.17	0.21	0.25	0.31	0.36	0.40	0.44	0.47	0.50	0.52	0.54	0.55	0.56	0.56
1.25	0.00	0.00	0.01	0.02	0.05	0.11	0.16	0.23	0.28	0.34	0.42	0.51	0.60	0.67	0.73	0.78	0.83	0.86	0.89	0.91	0.93	0.94
1.75	0.00	0.00	0.01	0.03	0.07	0.15	0.23	0.32	0.40	0.48	0.59	0.72	0.84	0.94	1.03	1.10	1.16	1.21	1.25	1.28	1.30	1.32
2.25	0.00	0.00	0.01	0.03	0.09	0.19	0.29	0.41	0.51	0.62	0.76	0.92	1.07	1.21	1.32	1.41	1.49	1.56	1.61	1.65	1.68	1.69
2.75	0.00	0.00	0.01	0.04	0.11	0.23	0.36	0.50	0.62	0.75	0.93	1.13	1.31	1.47	1.61	1.73	1.82	1.90	1.96	2.01	2.05	2.07
3.25	0.00	0.01	0.01	0.05	0.13	0.28	0.42	0.59	0.74	0.89	1.10	1.33	1.55	1.74	1.90	2.04	2.15	2.25	2.32	2.38	2.42	2.45
3.75	0.00	0.01	0.02	0.06	0.15	0.32	0.49	0.68	0.85	1.03	1.27	1.54	1.79	2.01	2.20	2.35	2.49	2.59	2.68	2.74	2.79	2.82
4.25	0.00	0.01	0.02	0.06	0.18	0.36	0.55	0.77	0.96	1.16	1.44	1.74	2.03	2.28	2.49	2.67	2.82	2.94	3.03	3.11	3.16	3.20
4.75	0.00	0.01	0.02	0.07	0.20	0.40	0.61	0.86	1.08	1.30	1.61	1.95	2.27	2.55	2.78	2.98	3.15	3.28	3.39	3.48	3.54	3.58
5.25	0.00	0.01	0.02	0.08	0.22	0.45	0.68	0.95	1.19	1.44	1.78	2.16	2.51	2.81	3.08	3.30	3.48	3.63	3.75	3.84	3.91	3.95
5.75	0.00	0.01	0.03	0.09	0.24	0.49	0.74	1.04	1.30	1.57	1.95	2.36	2.74	3.08	3.37	3.61	3.81	3.97	4.11	4.21	4.28	4.33
6.25	0.00	0.01	0.03	0.09	0.26	0.53	0.81	1.13	1.42	1.71	2.12	2.57	2.98	3.35	3.66	3.92	4.14	4.32	4.46	4.57	4.65	4.70
6.75	0.00	0.01	0.03	0.10	0.28	0.57	0.87	1.22	1.53	1.85	2.29	2.77	3.22	3.62	3.96	4.24	4.47	4.67	4.82	4.94	5.03	5.08
7.25	0.00	0.01	0.03	0.11	0.30	0.62	0.94	1.31	1.65	1.98	2.46	2.98	3.46	3.89	4.25	4.55	4.80	5.01	5.18	5.31	5.40	5.46
7.75	0.00	0.01	0.03	0.11	0.32	0.66	1.00	1.40	1.76	2.12	2.63	3.18	3.70	4.15	4.54	4.87	5.14	5.36	5.53	5.67	5.77	5.83
8.25	0.00	0.01	0.04	0.12	0.34	0.70	1.07	1.49	1.87	2.26	2.80	3.39	3.94	4.42	4.83	5.18	5.47	5.70	5.89	6.04	6.14	6.21
8.75	0.00	0.02	0.04	0.13	0.36	0.74	1.13	1.59	1.99	2.39	2.97	3.59	4.18	4.69	5.13	5.49	5.80	6.05	6.25	6.40	6.51	6.59
9.25	0.00	0.02	0.04	0.14	0.38	0.79	1.20	1.68	2.10	2.53	3.14	3.80	4.41	4.96	5.42	5.81	6.13	6.39	6.60	6.77	6.89	6.96
9.75	0.00	0.02	0.04	0.14	0.40	0.83	1.26	1.77	2.21	2.67	3.31	4.00	4.65	5.23	5.71	6.12	6.46	6.74	6.96	7.13	7.26	7.34
10.25	0.00	0.02	0.04	0.15	0.42	0.87	1.33	1.86	2.33	2.80	3.48	4.21	4.89	5.49	6.01	6.44	6.79	7.08	7.32	7.50	7.63	7.71
10.75	0.00	0.02	0.05	0.16	0.44	0.92	1.39	1.95	2.44	2.94	3.65	4.41	5.13	5.76	6.30	6.75	7.12	7.43	7.68	7.87	8.00	8.09
11.25	0.00	0.02	0.05	0.17	0.46	0.96	1.46	2.04	2.55	3.08	3.82	4.62	5.37	6.03	6.59	7.06	7.46	7.78	8.03	8.23	8.38	8.47
11.75	0.00	0.02	0.05	0.17	0.48	1.00	1.52	2.13	2.67	3.21	3.99	4.82	5.61	6.30	6.89	7.38	7.79	8.12	8.39	8.60	8.75	8.84
12.25	0.00	0.02	0.05	0.18	0.51	1.04	1.58	2.22	2.78	3.35	4.16	5.03	5.85	6.57	7.18	7.69	8.12	8.47	8.75	8.96	9.12	9.22
12.75	0.00	0.02	0.06	0.19	0.53	1.09	1.65	2.31	2.89	3.49	4.33	5.23	6.08	6.83	7.47	8.01	8.45	8.81	9.10	9.33	9.49	9.60

SEVAN Deepsea Driller:

Hs (m)	Spectral peak period (s)																					
	2.5	3.5	4.5	5.5	6.5	7.5	8.5	9.5	10.5	11.5	12.5	13.5	14.5	15.5	16.5	17.5	18.5	19.5	20.5	21.5	22.5	23.5
0.25	0.00	0.00	0.00	0.00	0.00	0.01	0.04	0.07	0.11	0.16	0.20	0.23	0.24	0.24	0.24	0.24	0.24	0.24	0.23	0.23	0.23	0.23
0.75	0.00	0.00	0.00	0.00	0.01	0.04	0.11	0.21	0.34	0.49	0.61	0.69	0.72	0.72	0.72	0.71	0.71	0.71	0.70	0.70	0.69	0.68
1.25	0.00	0.00	0.00	0.01	0.02	0.07	0.18	0.34	0.57	0.81	1.02	1.14	1.20	1.21	1.20	1.19	1.19	1.18	1.17	1.16	1.15	1.14
1.75	0.00	0.00	0.01	0.01	0.03	0.09	0.25	0.48	0.79	1.14	1.43	1.60	1.67	1.69	1.68	1.67	1.66	1.65	1.64	1.63	1.61	1.60
2.25	0.00	0.00	0.01	0.01	0.04	0.12	0.32	0.62	1.02	1.47	1.84	2.06	2.15	2.17	2.16	2.14	2.13	2.12	2.11	2.09	2.07	2.05
2.75	0.00	0.00	0.01	0.02	0.04	0.15	0.39	0.75	1.25	1.79	2.24	2.52	2.63	2.65	2.64	2.62	2.61	2.59	2.58	2.56	2.53	2.51
3.25	0.00	0.00	0.01	0.02	0.05	0.18	0.46	0.89	1.47	2.12	2.65	2.98	3.11	3.13	3.12	3.10	3.08	3.06	3.05	3.02	3.00	2.96
3.75	0.00	0.00	0.01	0.02	0.06	0.20	0.53	1.03	1.70	2.44	3.06	3.43	3.59	3.62	3.60	3.57	3.56	3.54	3.51	3.49	3.46	3.42
4.25	0.00	0.00	0.01	0.03	0.07	0.23	0.60	1.16	1.93	2.77	3.47	3.89	4.06	4.10	4.08	4.05	4.03	4.01	3.98	3.95	3.92	3.87
4.75	0.00	0.00	0.01	0.03	0.08	0.26	0.67	1.30	2.15	3.09	3.88	4.35	4.54	4.58	4.56	4.53	4.50	4.48	4.45	4.42	4.38	4.33
5.25	0.00	0.00	0.02	0.03	0.08	0.28	0.74	1.44	2.38	3.42	4.28	4.81	5.02	5.06	5.04	5.00	4.98	4.95	4.92	4.88	4.84	4.79
5.75	0.00	0.00	0.02	0.04	0.09	0.31	0.81	1.57	2.60	3.75	4.69	5.26	5.50	5.54	5.52	5.48	5.45	5.42	5.39	5.35	5.30	5.24
6.25	0.00	0.00	0.02	0.04	0.10	0.34	0.88	1.71	2.83	4.07	5.10	5.72	5.98	6.03	6.00	5.96	5.93	5.89	5.86	5.81	5.76	5.70
6.75	0.00	0.00	0.02	0.04	0.11	0.36	0.95	1.85	3.06	4.40	5.51	6.18	6.45	6.51	6.48	6.43	6.40	6.37	6.32	6.28	6.22	6.15
7.25	0.00	0.01	0.02	0.05	0.11	0.39	1.02	1.98	3.28	4.72	5.92	6.64	6.93	6.99	6.96	6.91	6.88	6.84	6.79	6.74	6.68	6.61
7.75	0.00	0.01	0.02	0.05	0.12	0.42	1.09	2.12	3.51	5.05	6.33	7.09	7.41	7.47	7.44	7.39	7.35	7.31	7.26	7.21	7.14	7.07
8.25	0.00	0.01	0.02	0.05	0.13	0.44	1.16	2.26	3.74	5.37	6.73	7.55	7.89	7.96	7.92	7.86	7.82	7.78	7.73	7.67	7.60	7.52
8.75	0.00	0.01	0.03	0.06	0.14	0.47	1.23	2.39	3.96	5.70	7.14	8.01	8.37	8.44	8.40	8.34	8.30	8.25	8.20	8.14	8.07	7.98
9.25	0.00	0.01	0.03	0.06	0.15	0.50	1.30	2.53	4.19	6.02	7.55	8.47	8.85	8.92	8.88	8.82	8.77	8.72	8.67	8.60	8.53	8.43
9.75	0.00	0.01	0.03	0.06	0.15	0.53	1.37	2.67	4.42	6.35	7.96	8.93	9.32	9.40	9.36	9.29	9.25	9.19	9.14	9.07	8.99	8.89
10.25	0.00	0.01	0.03	0.07	0.16	0.55	1.44	2.80	4.64	6.68	8.37	9.38	9.80	9.88	9.84	9.77	9.72	9.67	9.60	9.53	9.45	9.34
10.75	0.00	0.01	0.03	0.07	0.17	0.58	1.51	2.94	4.87	7.00	8.77	9.84	10.28	10.37	10.31	10.25	10.20	10.14	10.07	10.00	9.91	9.80
11.25	0.00	0.01	0.03	0.07	0.18	0.61	1.58	3.08	5.10	7.33	9.18	10.30	10.76	10.85	10.79	10.72	10.67	10.61	10.54	10.46	10.37	10.26
11.75	0.00	0.01	0.03	0.08	0.19	0.63	1.65	3.21	5.32	7.65	9.59	10.76	11.24	11.33	11.27	11.20	11.14	11.08	11.01	10.93	10.83	10.71
12.25	0.00	0.01	0.04	0.08	0.19	0.66	1.72	3.35	5.55	7.98	10.00	11.21	11.71	11.81	11.75	11.68	11.62	11.55	11.48	11.39	11.29	11.17
12.75	0.00	0.01	0.04	0.08	0.20	0.69	1.79	3.49	5.78	8.30	10.41	11.67	12.19	12.29	12.23	12.15	12.09	12.02	11.95	11.86	11.75	11.62

4. Appendix - Scatter tables

Average North Sea – All year:

Hs (m)	2.5	3.5	4.5	5.5	6.5	7.5	8.5	9.5	10.5	11.5	12.5	13.5	14.5	15.5	16.5	17.5	18.5	19.5	20.5	21.5	22.5	23.5
0.25	0	0	0	8	4	1	1	2	3	1	0	0	0	0	0	0	0	0	0	0	0	0
0.75	1	54	79	114	212	199	163	121	76	47	16	13	3	1	2	0	1	1	0	0	0	0
1.25	0	10	164	279	365	523	416	284	211	133	78	42	18	12	4	4	2	0	0	0	0	0
1.75	0	0	26	234	380	426	541	400	255	141	118	66	30	17	17	5	2	1	1	1	0	2
2.25	0	0	1	87	280	365	442	389	281	160	110	63	73	36	12	2	2	2	2	1	1	0
2.75	0	0	0	15	137	235	320	277	231	187	136	91	62	25	13	3	2	2	2	0	0	0
3.25	0	0	0	0	46	177	235	222	184	160	106	69	47	50	34	12	1	1	0	0	1	0
3.75	0	0	0	0	15	87	171	152	178	142	112	84	41	34	22	16	5	0	0	0	0	0
4.25	0	0	0	0	7	27	108	136	134	142	108	57	55	24	15	8	4	0	0	0	1	0
4.75	0	0	0	0	0	9	46	88	91	105	66	65	30	21	19	15	3	1	2	0	0	0
5.25	0	0	0	0	0	1	20	52	84	86	74	37	20	19	16	7	8	2	0	0	0	0
5.75	0	0	0	0	0	0	5	23	46	62	49	36	22	16	11	4	4	1	1	0	0	0
6.25	0	0	0	0	0	0	4	10	26	49	44	37	17	11	3	3	1	1	0	0	0	0
6.75	0	0	0	0	0	0	0	2	14	32	36	27	18	8	7	2	0	0	0	0	0	0
7.25	0	0	0	0	0	0	0	0	5	20	32	21	18	10	2	2	2	0	0	0	0	0
7.75	0	0	0	0	0	0	0	0	1	14	32	7	10	3	3	0	0	0	0	0	0	0
8.25	0	0	0	0	0	0	0	0	1	6	18	15	11	10	1	1	0	0	1	0	0	0
8.75	0	0	0	0	0	0	0	0	0	4	10	11	11	2	2	0	2	0	1	0	0	0
9.25	0	0	0	0	0	0	0	0	0	1	4	12	4	2	1	0	0	0	0	0	0	0
9.75	0	0	0	0	0	0	0	0	0	0	2	2	1	4	1	2	1	0	0	0	0	0
10.25	0	0	0	0	0	0	0	0	0	0	0	0	2	6	1	1	0	0	0	0	0	0
10.75	0	0	0	0	0	0	0	0	0	0	1	0	1	3	1	1	0	1	0	0	0	0
11.25	0	0	0	0	0	0	0	0	0	0	0	0	1	2	0	1	0	0	0	0	0	0
11.75	0	0	0	0	0	0	0	0	0	0	0	0	0	0	1	0	0	0	0	0	0	0
12.25	0	0	0	0	0	0	0	0	0	0	0	0	0	0	1	0	0	0	0	0	0	0
12.75	0	0	0	0	0	0	0	0	0	0	0	0	0	0	0	0	0	0	0	0	0	0

Average West Africa – All year:

Hs (m)	2.5	3.5	4.5	5.5	6.5	7.5	8.5	9.5	10.5	11.5	12.5	13.5	14.5	15.5	16.5	17.5	18.5	19.5	20.5	21.5	22.5	23.5
0.25	0	0	1	0	0	0	0	0	0	0	0	0	0	0	0	0	0	0	0	0	0	0
0.75	0	0	0	12	46	47	71	71	22	22	0	0	0	0	0	0	0	0	0	0	0	0
1.25	0	0	0	2	23	23	104	104	109	108	28	28	2	1	0	0	0	0	0	0	0	0
1.75	0	0	0	0	1	1	12	12	36	35	27	27	6	5	1	0	0	0	0	0	0	0
2.25	0	0	0	0	0	0	0	0	1	2	3	3	1	1	1	0	0	0	0	0	0	0
2.75	0	0	0	0	0	0	0	0	0	0	0	0	1	0	0	0	0	0	0	0	0	0
3.25	0	0	0	0	0	0	0	0	0	0	0	0	0	0	0	0	0	0	0	0	0	0
3.75	0	0	0	0	0	0	0	0	0	0	0	0	0	0	0	0	0	0	0	0	0	0
4.25	0	0	0	0	0	0	0	0	0	0	0	0	0	0	0	0	0	0	0	0	0	0
4.75	0	0	0	0	0	0	0	0	0	0	0	0	0	0	0	0	0	0	0	0	0	0
5.25	0	0	0	0	0	0	0	0	0	0	0	0	0	0	0	0	0	0	0	0	0	0
5.75	0	0	0	0	0	0	0	0	0	0	0	0	0	0	0	0	0	0	0	0	0	0
6.25	0	0	0	0	0	0	0	0	0	0	0	0	0	0	0	0	0	0	0	0	0	0
6.75	0	0	0	0	0	0	0	0	0	0	0	0	0	0	0	0	0	0	0	0	0	0
7.25	0	0	0	0	0	0	0	0	0	0	0	0	0	0	0	0	0	0	0	0	0	0
7.75	0	0	0	0	0	0	0	0	0	0	0	0	0	0	0	0	0	0	0	0	0	0
8.25	0	0	0	0	0	0	0	0	0	0	0	0	0	0	0	0	0	0	0	0	0	0
8.75	0	0	0	0	0	0	0	0	0	0	0	0	0	0	0	0	0	0	0	0	0	0
9.25	0	0	0	0	0	0	0	0	0	0	0	0	0	0	0	0	0	0	0	0	0	0
9.75	0	0	0	0	0	0	0	0	0	0	0	0	0	0	0	0	0	0	0	0	0	0
10.25	0	0	0	0	0	0	0	0	0	0	0	0	0	0	0	0	0	0	0	0	0	0
10.75	0	0	0	0	0	0	0	0	0	0	0	0	0	0	0	0	0	0	0	0	0	0
11.25	0	0	0	0	0	0	0	0	0	0	0	0	0	0	0	0	0	0	0	0	0	0
11.75	0	0	0	0	0	0	0	0	0	0	0	0	0	0	0	0	0	0	0	0	0	0
12.25	0	0	0	0	0	0	0	0	0	0	0	0	0	0	0	0	0	0	0	0	0	0
12.75	0	0	0	0	0	0	0	0	0	0	0	0	0	0	0	0	0	0	0	0	0	0

Southern Green Canyon - GoM – All year

Hs (m)	2.5	3.5	4.5	5.5	6.5	7.5	8.5	9.5	10.5	11.5	12.5	13.5	14.5	15.5	16.5	17.5	18.5	19.5	20.5	21.5	22.5	23.5
0.25	0	0	0	0	0	0	0	0	0	0	0	0	0	0	0	0	0	0	0	0	0	0
0.75	0	223.8	347.4	13.2	86	0	0.6	0	0	0	0	0	0	0	0	0	0	0	0	0	0	0
1.25	0	0	1430	1358	64.8	3	0	0	0	0	0	0	0	0	0	0	0	0	0	0	0	0
1.75	0	0.011	4.23	1533	837	13.24	0.01	0	0	0	0	0	0	0	0	0	0	0	0	0	0	0
2.25	0	0	0.144	10.678	1140.777	133.222	8.433	0.122	0.233	0.033	0.022	0	0	0	0	0	0	0	0	0	0	0
2.75	0	0	0.011	0.311	134.966	555.6	28.4	1	0.2	0.178	0.077	0	0	0	0.011	0	0	0	0	0	0	0
3.25	0	0	0	0.033	0.9	259	158.7	3.888	0.9	0.166	0.145	0.122	0.022	0.011	0.011	0	0	0	0	0	0	0
3.75	0	0	0	0	0.022	8.4	177.577	8.7	0.788	0.199	0.056	0.211	0.055	0.022	0	0	0	0	0	0	0	0
4.25	0	0	0	0	0	0.211	38.6	65.9	0.932	0.266	0.245	0.1	0.033	0.022	0	0	0	0	0	0	0	0
4.75	0	0	0	0	0	0.067	1.678	52.9	4.2	0.1	0.03	0.256	0.066	0	0	0	0	0	0	0	0	0
5.25	0	0	0	0	0	0	0.254	9.4	9.3	0.133	0.055	0.122	0.122	0	0	0	0	0	0	0	0	0
5.75	0	0	0	0	0	0	0.033	0.411	13.66	0.833	0.111	0.01	0.089	0.011	0.011	0	0	0	0	0	0	0
6.25	0	0	0	0	0	0	0	0.2	1.9	3.9	0.011	0.044	0.022	0.011	0	0	0	0	0	0	0	0
6.75	0	0	0	0	0	0	0	0.044	0.36	0.989	0.022	0.044	0.011	0.044	0	0	0	0	0	0	0	0
7.25	0	0	0	0	0	0	0	0.022	0.245	0.444	0.1	0.033	0.022	0.044	0	0	0	0	0	0	0	0
7.75	0	0	0	0	0	0	0	0	0.188	0.356	0.122	0.056	0	0.011	0	0	0	0	0	0	0	0
8.25	0	0	0	0	0	0	0	0	0.055	0.333	0.189	0.011	0	0.011	0	0	0	0	0	0	0	0
8.75	0	0	0	0	0	0	0	0	0.055	0.111	0.1	0.011	0	0.011	0	0	0	0	0	0	0	0
9.25	0	0	0	0	0	0	0	0	0.011	0.178	0.122	0.011	0.022	0.022	0	0	0	0	0	0	0	0
9.75	0	0	0	0	0	0	0	0	0	0.066	0.077	0.055	0	0.011	0	0	0	0	0	0	0	0
10.25	0	0	0	0	0	0	0	0	0	0.033	0.077	0.066	0	0	0	0	0	0	0	0	0	0
10.75	0	0	0	0	0	0	0	0	0	0.022	0.088	0.077	0	0	0	0	0	0	0	0	0	0
11.25	0	0	0	0	0	0	0	0	0	0	0.055	0.011	0	0	0	0	0	0	0	0	0	0
11.75	0	0	0	0	0	0	0	0	0	0	0.044	0	0	0	0	0	0	0	0	0	0	0
12.25	0	0	0	0	0	0	0	0	0	0	0	0.022	0	0	0	0	0	0	0	0	0	0
12.75	0	0	0	0	0	0	0	0	0	0	0	0	0	0	0	0	0	0	0	0	0	0

Ormen Lange – All year

Hs (m)	Spectral peak period (s)																					
	2.5	3.5	4.5	5.5	6.5	7.5	8.5	9.5	10.5	11.5	12.5	13.5	14.5	15.5	16.5	17.5	18.5	19.5	20.5	21.5	22.5	23.5
0.25	83	734	2300	3836	4332	3816	2857	1917	1194	707	404	225	124	67	36	20	11	6	7	0	0	0
0.75	83	734	2300	3836	4332	3816	2857	1917	1194	707	404	225	124	67	36	20	11	6	7	0	0	0
1.25	9	319	2435	7725	13998	17408	16665	13251	9251	5813	3413	1901	1019	531	271	137	68	34	33	0	0	0
1.75	9	319	2435	7725	13998	17408	16665	13251	9251	5813	3413	1901	1019	531	271	137	68	34	33	0	0	0
2.25	0	5	161	1399	5181	10734	14711	14911	12083	8279	4996	2738	1394	672	310	139	61	26	19	0	0	0
2.75	0	5	161	1399	5181	10734	14711	14911	12083	8279	4996	2738	1394	672	310	139	61	26	19	0	0	0
3.25	0	0	2	61	620	2660	6162	9023	9330	7386	4756	2609	1263	555	226	87	32	11	6	0	0	0
3.75	0	0	2	61	620	2660	6162	9023	9330	7386	4756	2609	1263	555	226	87	32	11	6	0	0	0
4.25	0	0	0	1	26	301	1465	3679	5552	5624	4162	2402	1138	461	165	53	16	5	2	0	0	0
4.75	0	0	0	1	26	301	1465	3679	5552	5624	4162	2402	1138	461	165	53	16	5	2	0	0	0
5.25	0	0	0	0	0	13	174	910	2343	3451	3251	2137	1051	409	132	37	9	2	1	0	0	0
5.75	0	0	0	0	0	13	174	910	2343	3451	3251	2137	1051	409	132	37	9	2	1	0	0	0
6.25	0	0	0	0	0	0	8	113	589	1457	1973	1638	911	366	112	28	6	1	0	0	0	0
6.75	0	0	0	0	0	0	8	113	589	1457	1973	1638	911	366	112	28	6	1	0	0	0	0
7.25	0	0	0	0	0	0	0	7	82	392	862	1009	702	318	101	24	4	1	0	0	0	0
7.75	0	0	0	0	0	0	0	7	82	392	862	1009	702	318	101	24	4	1	0	0	0	0
8.25	0	0	0	0	0	0	0	0	6	65	256	466	447	252	91	22	4	1	0	0	0	0
8.75	0	0	0	0	0	0	0	0	6	65	256	466	447	252	91	22	4	1	0	0	0	0
9.25	0	0	0	0	0	0	0	0	0	7	51	155	222	168	75	21	4	1	0	0	0	0
9.75	0	0	0	0	0	0	0	0	0	7	51	155	222	168	75	21	4	1	0	0	0	0
10.25	0	0	0	0	0	0	0	0	0	0	7	37	83	90	53	19	4	1	0	0	0	0
10.75	0	0	0	0	0	0	0	0	0	0	7	37	83	90	53	19	4	1	0	0	0	0
11.25	0	0	0	0	0	0	0	0	0	0	1	7	23	37	31	14	4	1	0	0	0	0
11.75	0	0	0	0	0	0	0	0	0	0	1	7	23	37	31	14	4	1	0	0	0	0
12.25	0	0	0	0	0	0	0	0	0	0	0	1	5	12	14	9	3	1	0	0	0	0
12.75	0	0	0	0	0	0	0	0	0	0	0	0	1	4	7	7	4	1	0	0	0	0

Ormen Lange – January

Hs (m)	Spectral peak period (s)																					
	2.5	3.5	4.5	5.5	6.5	7.5	8.5	9.5	10.5	11.5	12.5	13.5	14.5	15.5	16.5	17.5	18.5	19.5	20.5	21.5	22.5	23.5
0.25	5	20	39	51	53	47	39	30	22	16	11	8	6	4	3	2	1	1	2	0	0	0
0.75	5	20	39	51	53	47	39	30	22	16	11	8	6	4	3	2	1	1	2	0	0	0
1.25	3	34	136	305	467	554	551	484	389	293	210	146	98	65	43	28	18	11	20	0	0	0
1.75	3	34	136	305	467	554	551	484	389	293	210	146	98	65	43	28	18	11	20	0	0	0
2.25	0	2	24	127	355	647	869	932	847	679	495	335	215	132	79	46	26	15	18	0	0	0
2.75	0	2	24	127	355	647	869	932	847	679	495	335	215	132	79	46	26	15	18	0	0	0
3.25	0	0	0	9	65	236	519	787	895	817	628	422	255	142	74	37	18	8	7	0	0	0
3.75	0	0	0	9	65	236	519	787	895	817	628	422	255	142	74	37	18	8	7	0	0	0
4.25	0	0	0	0	3	29	139	367	615	718	630	440	256	129	58	24	9	3	2	0	0	0
4.75	0	0	0	0	3	29	139	367	615	718	630	440	256	129	58	24	9	3	2	0	0	0
5.25	0	0	0	0	0	1	16	93	283	499	566	449	266	125	49	16	5	1	0	0	0	0
5.75	0	0	0	0	0	1	16	93	283	499	566	449	266	125	49	16	5	1	0	0	0	0
6.25	0	0	0	0	0	0	1	11	73	231	392	398	264	124	44	12	3	1	0	0	0	0
6.75	0	0	0	0	0	0	1	11	73	231	392	398	264	124	44	12	3	1	0	0	0	0
7.25	0	0	0	0	0	0	0	1	10	64	188	276	230	119	42	11	2	0	0	0	0	0
7.75	0	0	0	0	0	0	0	1	10	64	188	276	230	119	42	11	2	0	0	0	0	0
8.25	0	0	0	0	0	0	0	0	1	11	60	141	163	104	40	10	2	0	0	0	0	0
8.75	0	0	0	0	0	0	0	0	1	11	60	141	163	104	40	10	2	0	0	0	0	0
9.25	0	0	0	0	0	0	0	0	0	1	13	53	90	77	36	10	2	0	0	0	0	0
9.75	0	0	0	0	0	0	0	0	0	1	13	53	90	77	36	10	2	0	0	0	0	0
10.25	0	0	0	0	0	0	0	0	0	0	2	15	38	45	28	10	2	0	0	0	0	0
10.75	0	0	0	0	0	0	0	0	0	0	2	15	38	45	28	10	2	0	0	0	0	0
11.25	0	0	0	0	0	0	0	0	0	0	0	3	13	22	18	8	2	0	0	0	0	0
11.75	0	0	0	0	0	0	0	0	0	0	0	3	13	22	18	8	2	0	0	0	0	0
12.25	0	0	0	0	0	0	0	0	0	0	0	1	4	8	9	5	2	0	0	0	0	0
12.75	0	0	0	0	0	0	0	0	0	0	0	0	1	4	5	5	2	0	0	0	0	0

Ormen Lange – February

Hs (m)	Spectral peak period (s)																					
	2.5	3.5	4.5	5.5	6.5	7.5	8.5	9.5	10.5	11.5	12.5	13.5	14.5	15.5	16.5	17.5	18.5	19.5	20.5	21.5	22.5	23.5
0.25	0	3	9	16	21	22	19	16	12	8	6	4	3	2	1	1	0	0	1	0	0	0
0.75	0	3	9	16	21	22	19	16	12	8	6	4	3	2	1	1	0	0	1	0	0	0
1.25	0	9	60	187	353	477	511	465	376	279	194	129	82	51	31	19	11	7	10	0	0	0
1.75	0	9	60	187	353	477	511	465	376	279	194	129	82	51	31	19	11	7	10	0	0	0
2.25	0	1	17	113	364	717	1001	1086	980	769	544	355	218	128	72	40	21	11	12	0	0	0
2.75	0	1	17	113	364	717	1001	1086	980	769	544	355	218	128	72	40	21	11	12	0	0	0
3.25	0	0	1	13	94	324	675	969	1049	916	678	441	260	141	72	35	17	8	6	0	0	0
3.75	0	0	1	13	94	324	675	969	1049	916	678	441	260	141	72	35	17	8	6	0	0	0
4.25	0	0	0	0	8	61	229	498	719	756	618	416	239	122	56	24	10	4	2	0	0	0
4.75	0	0	0	0	8	61	229	498	719	756	618	416	239	122	56	24	10	4	2	0	0	0
5.25	0	0	0	0	0	5	40	156	345	486	477	352	206	100	42	16	5	2	1	0	0	0
5.75	0	0	0	0	0	5	40	156	345	486	477	352	206	100	42	16	5	2	1	0	0	0
6.25	0	0	0	0	0	0	3	29	116	250	327	288	183	90	35	12	3	1	0	0	0	0
6.75	0	0	0	0	0	0	3	29	116	250	327	288	183	90	35	12	3	1	0	0	0	0
7.25	0	0	0	0	0	0	0	3	23	87	170	197	148	78	31	9	2	1	0	0	0	0
7.75	0	0	0	0	0	0	0	3	23	87	170	197	148	78	31	9	2	1	0	0	0	0
8.25	0	0	0	0	0	0	0	0	3	19	61	103	101	63	26	8	2	0	0	0	0	0
8.75	0	0	0	0	0	0	0	0	3	19	61	103	101	63	26	8	2	0	0	0	0	0
9.25	0	0	0	0	0	0	0	0	0	2	15	39	54	43	21	7	2	0	0	0	0	0
9.75	0	0	0	0	0	0	0	0	0	2	15	39	54	43	21	7	2	0	0	0	0	0
10.25	0	0	0	0	0	0	0	0	0	0	2	11	22	24	15	6	2	0	0	0	0	0
10.75	0	0	0	0	0	0	0	0	0	0	2	11	22	24	15	6	2	0	0	0	0	0
11.25	0	0	0	0	0	0	0	0	0	0	0	2	7	10	9	4	1	0	0	0	0	0
11.75	0	0	0	0	0	0	0	0	0	0	0	2	7	10	9	4	1	0	0	0	0	0
12.25	0	0	0	0	0	0	0	0	0	0	0	0	1	3	4	3	1	0	0	0	0	0
12.75	0	0	0	0	0	0	0	0	0	0	0	0	1	1	2	1	0	0	0	0	0	0

Ormen Lange – March

Hs (m)	Spectral peak period (s)																					
	2.5	3.5	4.5	5.5	6.5	7.5	8.5	9.5	10.5	11.5	12.5	13.5	14.5	15.5	16.5	17.5	18.5	19.5	20.5	21.5	22.5	23.5
0.25	0	4	17	36	51	57	54	45	34	25	17	12	8	5	3	2	1	1	1	0	0	0
0.75	0	4	17	36	51	57	54	45	34	25	17	12	8	5	3	2	1	1	1	0	0	0
1.25	0	8	65	235	490	705	786	729	593	438	301	196	123	75	44	26	15	9	11	0	0	0
1.75	0	8	65	235	490	705	786	729	593	438	301	196	123	75	44	26	15	9	11	0	0	0
2.25	0	0	12	98	361	776	1134	1254	1126	865	591	369	216	119	63	33	17	8	8	0	0	0
2.75	0	0	12	98	361	776	1134	1254	1126	865	591	369	216	119	63	33	17	8	8	0	0	0
3.25	0	0	0	8	73	288	647	956	1028	867	607	368	199	99	46	20	8	3	2	0	0	0
3.75	0	0	0	8	73	288	647	956	1028	867	607	368	199	99	46	20	8	3	2	0	0	0
4.25	0	0	0	0	5	49	208	480	698	705	537	327	167	74	29	11	4	1	1	0	0	0
4.75	0	0	0	0	5	49	208	480	698	705	537	327	167	74	29	11	4	1	1	0	0	0
5.25	0	0	0	0	0	3	35	152	344	467	423	276	139	57	20	6	2	0	0	0	0	0
5.75	0	0	0	0	0	3	35	152	344	467	423	276	139	57	20	6	2	0	0	0	0	0
6.25	0	0	0	0	0	0	2	24	102	214	258	198	106	42	13	3	1	0	0	0	0	0
6.75	0	0	0	0	0	0	2	24	102	214	258	198	106	42	13	3	1	0	0	0	0	0
7.25	0	0	0	0	0	0	0	2	17	62	112	114	71	30	9	2	0	0	0	0	0	0
7.75	0	0	0	0	0	0	0	2	17	62	112	114	71	30	9	2	0	0	0	0	0	0
8.25	0	0	0	0	0	0	0	0	1	11	32	48	39	19	6	1	0	0	0	0	0	0
8.75	0	0	0	0	0	0	0	0	1	11	32	48	39	19	6	1	0	0	0	0	0	0
9.25	0	0	0	0	0	0	0	0	0	1	6	14	16	11	4	1	0	0	0	0	0	0
9.75	0	0	0	0	0	0	0	0	0	1	6	14	16	11	4	1	0	0	0	0	0	0
10.25	0	0	0	0	0	0	0	0	0	0	1	3	5	4	2	1	0	0	0	0	0	0
10.75	0	0	0	0	0	0	0	0	0	0	1	3	5	4	2	1	0	0	0	0	0	0
11.25	0	0	0	0	0	0	0	0	0	0	0	0	1	1	1	0	0	0	0	0	0	0
11.75	0	0	0	0	0	0	0	0	0	0	0	0	1	1	1	0	0	0	0	0	0	0
12.25	0	0	0	0	0	0	0	0	0	0	0	0	0	0	0	0	0	0	0	0	0	0
12.75	0	0	0	0	0	0	0	0	0	0	0	0	0	0	0	0	0	0	0	0	0	0

Ormen Lange – April

Hs (m)	Spectral peak period (s)																					
	2.5	3.5	4.5	5.5	6.5	7.5	8.5	9.5	10.5	11.5	12.5	13.5	14.5	15.5	16.5	17.5	18.5	19.5	20.5	21.5	22.5	23.5
0.25	3	29	108	210	279	289	255	201	147	101	67	44	28	17	11	7	4	2	4	0	0	0
0.75	3	29	108	210	279	289	255	201	147	101	67	44	28	17	11	7	4	2	4	0	0	0
1.25	1	23	175	565	1066	1401	1433	1228	927	637	410	250	148	85	48	27	15	8	10	0	0	0
1.75	1	23	175	565	1066	1401	1433	1228	927	637	410	250	148	85	48	27	15	8	10	0	0	0
2.25	0	1	17	134	465	929	1253	1271	1044	733	457	261	139	71	34	16	8	3	3	0	0	0
2.75	0	1	17	134	465	929	1253	1271	1044	733	457	261	139	71	34	16	8	3	3	0	0	0
3.25	0	0	0	8	66	256	548	754	744	569	358	194	93	41	17	7	2	1	0	0	0	0
3.75	0	0	0	8	66	256	548	754	744	569	358	194	93	41	17	7	2	1	0	0	0	0
4.25	0	0	0	0	3	32	140	317	436	407	280	152	68	26	9	3	1	0	0	0	0	0
4.75	0	0	0	0	3	32	140	317	436	407	280	152	68	26	9	3	1	0	0	0	0	0
5.25	0	0	0	0	0	1	17	80	185	246	210	125	56	20	6	1	0	0	0	0	0	0
5.75	0	0	0	0	0	1	17	80	185	246	210	125	56	20	6	1	0	0	0	0	0	0
6.25	0	0	0	0	0	0	1	9	44	100	123	93	47	17	5	1	0	0	0	0	0	0
6.75	0	0	0	0	0	0	1	9	44	100	123	93	47	17	5	1	0	0	0	0	0	0
7.25	0	0	0	0	0	0	0	0	5	23	49	55	36	15	4	1	0	0	0	0	0	0
7.75	0	0	0	0	0	0	0	0	5	23	49	55	36	15	4	1	0	0	0	0	0	0
8.25	0	0	0	0	0	0	0	0	3	12	22	22	12	4	1	0	0	0	0	0	0	0
8.75	0	0	0	0	0	0	0	0	3	12	22	22	12	4	1	0	0	0	0	0	0	0
9.25	0	0	0	0	0	0	0	0	0	1	5	9	8	4	1	0	0	0	0	0	0	0
9.75	0	0	0	0	0	0	0	0	0	1	5	9	8	4	1	0	0	0	0	0	0	0
10.25	0	0	0	0	0	0	0	0	0	0	1	2	3	2	1	0	0	0	0	0	0	0
10.75	0	0	0	0	0	0	0	0	0	0	1	2	3	2	1	0	0	0	0	0	0	0
11.25	0	0	0	0	0	0	0	0	0	0	0	0	1	1	1	0	0	0	0	0	0	0
11.75	0	0	0	0	0	0	0	0	0	0	0	0	0	0	0	0	0	0	0	0	0	0
12.25	0	0	0	0	0	0	0	0	0	0	0	0	0	0	0	0	0	0	0	0	0	0
12.75	0	0	0	0	0	0	0	0	0	0	0	0	0	0	0	0	0	0	0	0	0	0

Ormen Lange – May

Hs (m)	Spectral peak period (s)																					
	2.5	3.5	4.5	5.5	6.5	7.5	8.5	9.5	10.5	11.5	12.5	13.5	14.5	15.5	16.5	17.5	18.5	19.5	20.5	21.5	22.5	23.5
0.25	47	239	540	728	719	584	419	277	173	105	62	36	21	12	7	4	2	1	2	0	0	0
0.75	47	239	540	728	719	584	419	277	173	105	62	36	21	12	7	4	2	1	2	0	0	0
1.25	3	83	493	1314	2083	2306	1977	1413	886	506	271	138	69	33	16	8	4	2	2	0	0	0
1.75	3	83	493	1314	2083	2306	1977	1413	886	506	271	138	69	33	16	8	4	2	2	0	0	0
2.25	0	0	11	121	498	1042	1330	1169	775	416	191	78	30	11	4	1	0	0	0	0	0	0
2.75	0	0	11	121	498	1042	1330	1169	775	416	191	78	30	11	4	1	0	0	0	0	0	0
3.25	0	0	0	1	23	151	419	596	501	279	113	36	9	2	0	0	0	0	0	0	0	0
3.75	0	0	0	1	23	151	419	596	501	279	113	36	9	2	0	0	0	0	0	0	0	0
4.25	0	0	0	0	0	5	50	162	229	164	68	18	3	1	0	0	0	0	0	0	0	0
4.75	0	0	0	0	0	5	50	162	229	164	68	18	3	1	0	0	0	0	0	0	0	0
5.25	0	0	0	0	0	0	2	17	55	66	36	10	2	0	0	0	0	0	0	0	0	0
5.75	0	0	0	0	0	0	2	17	55	66	36	10	2	0	0	0	0	0	0	0	0	0
6.25	0	0	0	0	0	0	1	6	15	14	5	1	0	0	0	0	0	0	0	0	0	0
6.75	0	0	0	0	0	0	1	6	15	14	5	1	0	0	0	0	0	0	0	0	0	0
7.25	0	0	0	0	0	0	0	0	2	3	2	1	0	0	0	0	0	0	0	0	0	0
7.75	0	0	0	0	0	0	0	0	2	3	2	1	0	0	0	0	0	0	0	0	0	0
8.25	0	0	0	0	0	0	0	0	0	0	0	0	0	0	0	0	0	0	0	0	0	0
8.75	0	0	0	0	0	0	0	0	0	0	0	0	0	0	0	0	0	0	0	0	0	0
9.25	0	0	0	0	0	0	0	0	0	0	0	0	0	0	0	0	0	0	0	0	0	0
9.75	0	0	0	0	0	0	0	0	0	0	0	0	0	0	0	0	0	0	0	0	0	0
10.25	0	0	0	0	0	0	0	0	0	0	0	0	0	0	0	0	0	0	0	0	0	0
10.75	0	0	0	0	0	0	0	0	0	0	0	0	0	0	0	0	0	0	0	0	0	0
11.25	0	0	0	0	0	0	0	0	0	0	0	0	0	0	0	0	0	0	0	0	0	0
11.75	0	0	0	0	0	0	0	0	0	0	0	0	0	0	0	0	0	0	0	0	0	0
12.25	0	0	0	0	0	0	0	0	0	0	0	0	0	0	0	0	0	0	0	0	0	0
12.75	0	0	0	0	0	0	0	0	0	0	0	0	0	0	0	0	0	0	0	0	0	0

Ormen Lange – June

Hs (m)	Spectral peak period (s)																					
	2.5	3.5	4.5	5.5	6.5	7.5	8.5	9.5	10.5	11.5	12.5	13.5	14.5	15.5	16.5	17.5	18.5	19.5	20.5	21.5	22.5	23.5
0.25	6	77	285	518	611	548	412	274	169	98	55	30	16	8	4	2	1	1	1	0	0	0
0.75	6	77	285	518	611	548	412	274	169	98	55	30	16	8	4	2	1	1	1	0	0	0
1.25	1	45	402	1346	2398	2766	2352	1611	947	499	244	113	50	22	9	4	2	1	1	0	0	0
1.75	1	45	402	1346	2398	2766	2352	1611	947	499	244	113	50	22	9	4	2	1	1	0	0	0
2.25	0	0	13	150	624	1254	1490	1199	722	350	145	53	18	6	2	1	0	0	0	0	0	0
2.75	0	0	13	150	624	1254	1490	1199	722	350	145	53	18	6	2	1	0	0	0	0	0	0
3.25	0	0	0	2	31	172	410	513	388	199	75	23	6	1	0	0	0	0	0	0	0	0
3.75	0	0	0	2	31	172	410	513	388	199	75	23	6	1	0	0	0	0	0	0	0	0
4.25	0	0	0	0	0	5	39	109	143	102	44	13	3	0	0	0	0	0	0	0	0	0
4.75	0	0	0	0	0	5	39	109	143	102	44	13	3	0	0	0	0	0	0	0	0	0
5.25	0	0	0	0	0	0	1	6	21	29	20	8	2	0	0	0	0	0	0	0	0	0
5.75	0	0	0	0	0	0	1	6	21	29	20	8	2	0	0	0	0	0	0	0	0	0
6.25	0	0	0	0	0	0	0	0	1	3	4	3	1	0	0	0	0	0	0	0	0	0
6.75	0	0	0	0	0	0	0	0	1	3	4	3	1	0	0	0	0	0	0	0	0	0
7.25	0	0	0	0	0	0	0	0	0	0	0	0	0	0	0	0	0	0	0	0	0	0
7.75	0	0	0	0	0	0	0	0	0	0	0	0	0	0	0	0	0	0	0	0	0	0
8.25	0	0	0	0	0	0	0	0	0	0	0	0	0	0	0	0	0	0	0	0	0	0
8.75	0	0	0	0	0	0	0	0	0	0	0	0	0	0	0	0	0	0	0	0	0	0
9.25	0	0	0	0	0	0	0	0	0	0	0	0	0	0	0	0	0	0	0	0	0	0
9.75	0	0	0	0	0	0	0	0	0	0	0	0	0	0	0	0	0	0	0	0	0	0
10.25	0	0	0	0	0	0	0	0	0	0	0	0	0	0	0	0	0	0	0	0	0	0
10.75	0	0	0	0	0	0	0	0	0	0	0	0	0	0	0	0	0	0	0	0	0	0
11.25	0	0	0	0	0	0	0	0	0	0	0	0	0	0	0	0	0	0	0	0	0	0
11.75	0	0	0	0	0	0	0	0	0	0	0	0	0	0	0	0	0	0	0	0	0	0
12.25	0	0	0	0	0	0	0	0	0	0	0	0	0	0	0	0	0	0	0	0	0	0
12.75	0	0	0	0	0	0	0	0	0	0	0	0	0	0	0	0	0	0	0	0	0	0

Ormen Lange – July

Hs (m)	Spectral peak period (s)																					
	2.5	3.5	4.5	5.5	6.5	7.5	8.5	9.5	10.5	11.5	12.5	13.5	14.5	15.5	16.5	17.5	18.5	19.5	20.5	21.5	22.5	23.5
0.25	40	263	689	1017	1060	889	647	429	268	160	93	53	30	17	10	5	3	2	2	0	0	0
0.75	40	263	689	1017	1060	889	647	429	268	160	93	53	30	17	10	5	3	2	2	0	0	0
1.25	2	66	499	1524	2576	2856	2332	1528	857	432	203	91	40	17	7	3	1	1	0	0	0	0
1.75	2	66	499	1524	2576	2856	2332	1528	857	432	203	91	40	17	7	3	1	1	0	0	0	0
2.25	0	0	4	73	407	964	1204	917	478	188	61	17	4	1	0	0	0	0	0	0	0	0
2.75	0	0	4	73	407	964	1204	917	478	188	61	17	4	1	0	0	0	0	0	0	0	0
3.25	0	0	0	0	8	83	275	367	236	85	19	3	0	0	0	0	0	0	0	0	0	0
3.75	0	0	0	0	8	83	275	367	236	85	19	3	0	0	0	0	0	0	0	0	0	0
4.25	0	0	0	0	0	1	15	59	74	37	9	1	0	0	0	0	0	0	0	0	0	0
4.75	0	0	0	0	0	1	15	59	74	37	9	1	0	0	0	0	0	0	0	0	0	0
5.25	0	0	0	0	0	0	0	3	9	9	4	1	0	0	0	0	0	0	0	0	0	0
5.75	0	0	0	0	0	0	0	3	9	9	4	1	0	0	0	0	0	0	0	0	0	0
6.25	0	0	0	0	0	0	0	0	0	1	1	0	0	0	0	0	0	0	0	0	0	0
6.75	0	0	0	0	0	0	0	0	0	1	1	0	0	0	0	0	0	0	0	0	0	0
7.25	0	0	0	0	0	0	0	0	0	0	0	0	0	0	0	0	0	0	0	0	0	0
7.75	0	0	0	0	0	0	0	0	0	0	0	0	0	0	0	0	0	0	0	0	0	0
8.25	0	0	0	0	0	0	0	0	0	0	0	0	0	0	0	0	0	0	0	0	0	0
8.75	0	0	0	0	0	0	0	0	0	0	0	0	0	0	0	0	0	0	0	0	0	0
9.25	0	0	0	0	0	0	0	0	0	0	0	0	0	0	0	0	0	0	0	0	0	0
9.75	0	0	0	0	0	0	0	0	0	0	0	0	0	0	0	0	0	0	0	0	0	0
10.25	0	0	0	0	0	0	0	0	0	0	0	0	0	0	0	0	0	0	0	0	0	0
10.75	0	0	0	0	0	0	0	0	0	0	0	0	0	0	0	0	0	0	0	0	0	0
11.25	0	0	0	0	0	0	0	0	0	0	0	0	0	0	0	0	0	0	0	0	0	0
11.75	0	0	0	0	0	0	0	0	0	0	0	0	0	0	0	0	0	0	0	0	0	0
12.25	0	0	0	0	0	0	0	0	0	0	0	0	0	0	0	0	0	0	0	0	0	0
12.75	0	0	0	0	0	0	0	0	0	0	0	0	0	0	0	0	0	0	0	0	0	0

Ormen Lange – August

Hs (m)	Spectral peak period (s)																					
	2.5	3.5	4.5	5.5	6.5	7.5	8.5	9.5	10.5	11.5	12.5	13.5	14.5	15.5	16.5	17.5	18.5	19.5	20.5	21.5	22.5	23.5
0.25	3	63	319	709	943	902	695	461	276	154	82	42	21	10	5	2	1	1	1	0	0	0
0.75	3	63	319	709	943	902	695	461	276	154	82	42	21	10	5	2	1	1	1	0	0	0
1.25	0	20	245	1023	2116	2717	2497	1810	1106	597	295	136	60	26	11	4	2	1	1	0	0	0
1.75	0	20	245	1023	2116	2717	2497	1810	1106	597	295	136	60	26	11	4	2	1	1	0	0	0
2.25	0	0	6	87	408	911	1194	1057	700	373	169	68	25	9	3	1	0	0	0	0	0	0
2.75	0	0	6	87	408	911	1194	1057	700	373	169	68	25	9	3	1	0	0	0	0	0	0
3.25	0	0	0	1	23	122	293	383	315	181	79	28	8	2	1	0	0	0	0	0	0	0
3.75	0	0	0	1	23	122	293	383	315	181	79	28	8	2	1	0	0	0	0	0	0	0
4.25	0	0	0	0	0	7	39	96	119	86	41	14	4	1	0	0	0	0	0	0	0	0
4.75	0	0	0	0	0	7	39	96	119	86	41	14	4	1	0	0	0	0	0	0	0	0
5.25	0	0	0	0	0	0	2	12	27	30	18	7	2	0	0	0	0	0	0	0	0	0
5.75	0	0	0	0	0	0	2	12	27	30	18	7	2	0	0	0	0	0	0	0	0	0
6.25	0	0	0	0	0	0	0	1	3	6	6	3	1	0	0	0	0	0	0	0	0	0
6.75	0	0	0	0	0	0	0	1	3	6	6	3	1	0	0	0	0	0	0	0	0	0
7.25	0	0	0	0	0	0	0	0	0	1	1	1	0	0	0	0	0	0	0	0	0	0
7.75	0	0	0	0	0	0	0	0	0	1	1	1	0	0	0	0	0	0	0	0	0	0
8.25	0	0	0	0	0	0	0	0	0	0	0	0	0	0	0	0	0	0	0	0	0	0
8.75	0	0	0	0	0	0	0	0	0	0	0	0	0	0	0	0	0	0	0	0	0	0
9.25	0	0	0	0	0	0	0	0	0	0	0	0	0	0	0	0	0	0	0	0	0	0
9.75	0	0	0	0	0	0	0	0	0	0	0	0	0	0	0	0	0	0	0	0	0	0
10.25	0	0	0	0	0	0	0	0	0	0	0	0	0	0	0	0	0	0	0	0	0	0
10.75	0	0	0	0	0	0	0	0	0	0	0	0	0	0	0	0	0	0	0	0	0	0
11.25	0	0	0	0	0	0	0	0	0	0	0	0	0	0	0	0	0	0	0	0	0	0
11.75	0	0	0	0	0	0	0	0	0	0	0	0	0	0	0	0	0	0	0	0	0	0
12.25	0	0	0	0	0	0	0	0	0	0	0	0	0	0	0	0	0	0	0	0	0	0
12.75	0	0	0	0	0	0	0	0	0	0	0	0	0	0	0	0	0	0	0	0	0	0

Ormen Lange – September

Hs (m)	Spectral peak period (s)																					
	2.5	3.5	4.5	5.5	6.5	7.5	8.5	9.5	10.5	11.5	12.5	13.5	14.5	15.5	16.5	17.5	18.5	19.5	20.5	21.5	22.5	23.5
0.25	3	33	130	255	331	330	276	205	141	91	57	34	20	12	7	4	2	1	2	0	0	0
0.75	3	33	130	255	331	330	276	205	141	91	57	34	20	12	7	4	2	1	2	0	0	0
1.25	1	23	198	687	1333	1745	1735	1419	1009	648	386	218	118	62	32	16	8	4	4	0	0	0
1.75	1	23	198	687	1333	1745	1735	1419	1009	648	386	218	118	62	32	16	8	4	4	0	0	0
2.25	0	0	13	127	496	1046	1421	1400	1086	705	401	206	98	44	19	8	3	1	1	0	0	0
2.75	0	0	13	127	496	1046	1421	1400	1086	705	401	206	98	44	19	8	3	1	1	0	0	0
3.25	0	0	0	5	53	236	540	747	703	494	277	130	54	20	7	2	1	0	0	0	0	0
3.75	0	0	0	5	53	236	540	747	703	494	277	130	54	20	7	2	1	0	0	0	0	0
4.25	0	0	0	0	2	22	113	271	365	313	188	85	31	10	3	1	0	0	0	0	0	0
4.75	0	0	0	0	2	22	113	271	365	313	188	85	31	10	3	1	0	0	0	0	0	0
5.25	0	0	0	0	0	1	12	61	144	177	130	63	22	6	1	0	0	0	0	0	0	0
5.75	0	0	0	0	0	1	12	61	144	177	130	63	22	6	1	0	0	0	0	0	0	0
6.25	0	0	0	0	0	0	7	33	70	73	44	16	4	1	0	0	0	0	0	0	0	0
6.75	0	0	0	0	0	0	7	33	70	73	44	16	4	1	0	0	0	0	0	0	0	0
7.25	0	0	0	0	0	0	0	0	4	17	30	25	12	3	1	0	0	0	0	0	0	0
7.75	0	0	0	0	0	0	0	0	4	17	30	25	12	3	1	0	0	0	0	0	0	0
8.25	0	0	0	0	0	0	0	0	0	2	8	11	7	3	1	0	0	0	0	0	0	0
8.75	0	0	0	0	0	0	0	0	0	2	8	11	7	3	1	0	0	0	0	0	0	0
9.25	0	0	0	0	0	0	0	0	0	0	1	3	3	2	1	0	0	0	0	0	0	0
9.75	0	0	0	0	0	0	0	0	0	0	1	3	3	2	1	0	0	0	0	0	0	0
10.25	0	0	0	0	0	0	0	0	0	0	1	1	1	0	0	0	0	0	0	0	0	0
10.75	0	0	0	0	0	0	0	0	0	0	1	1	1	0	0	0	0	0	0	0	0	0
11.25	0	0	0	0	0	0	0	0	0	0	0	0	0	0	0	0	0	0	0	0	0	0
11.75	0	0	0	0	0	0	0	0	0	0	0	0	0	0	0	0	0	0	0	0	0	0
12.25	0	0	0	0	0	0	0	0	0	0	0	0	0	0	0	0	0	0	0	0	0	0
12.75	0	0	0	0	0	0	0	0	0	0	0	0	0	0	0	0	0	0	0	0	0	0

Ormen Lange – October

Hs (m)	Spectral peak period (s)																					
	2.5	3.5	4.5	5.5	6.5	7.5	8.5	9.5	10.5	11.5	12.5	13.5	14.5	15.5	16.5	17.5	18.5	19.5	20.5	21.5	22.5	23.5
0.25	0	4	20	47	68	72	63	47	32	20	12	7	4	2	1	1	0	0	0	0	0	0
0.75	0	4	20	47	68	72	63	47	32	20	12	7	4	2	1	1	0	0	0	0	0	0
1.25	0	6	64	273	618	908	988	869	655	441	273	159	88	47	25	13	6	3	3	0	0	0
1.75	0	6	64	273	618	908	988	869	655	441	273	159	88	47	25	13	6	3	3	0	0	0
2.25	0	0	10	97	398	897	1324	1435	1240	903	578	335	181	92	45	21	10	4	3	0	0	0
2.75	0	0	10	97	398	897	1324	1435	1240	903	578	335	181	92	45	21	10	4	3	0	0	0
3.25	0	0	0	8	74	299	675	986	1041	857	583	342	179	85	38	16	6	3	2	0	0	0
3.75	0	0	0	8	74	299	675	986	1041	857	583	342	179	85	38	16	6	3	2	0	0	0
4.25	0	0	0	0	6	48	193	425	598	594	450	275	142	64	26	10	3	1	1	0	0	0
4.75	0	0	0	0	6	48	193	425	598	594	450	275	142	64	26	10	3	1	1	0	0	0
5.25	0	0	0	0	0	4	33	126	264	345	311	209	111	49	18	6	2	1	0	0	0	0
5.75	0	0	0	0	0	4	33	126	264	345	311	209	111	49	18	6	2	1	0	0	0	0
6.25	0	0	0	0	0	0	3	25	88	166	193	152	87	38	14	4	1	0	0	0	0	0
6.75	0	0	0	0	0	0	3	25	88	166	193	152	87	38	14	4	1	0	0	0	0	0
7.25	0	0	0	0	0	0	0	3	19	57	94	93	61	29	10	3	1	0	0	0	0	0
7.75	0	0	0	0	0	0	0	3	19	57	94	93	61	29	10	3	1	0	0	0	0	0
8.25	0	0	0	0	0	0	0	0	3	14	34	46	37	20	8	2	0	0	0	0	0	0
8.75	0	0	0	0	0	0	0	0	3	14	34	46	37	20	8	2	0	0	0	0	0	0
9.25	0	0	0	0	0	0	0	0	0	2	9	18	19	12	5	2	0	0	0	0	0	0
9.75	0	0	0	0	0	0	0	0	0	2	9	18	19	12	5	2	0	0	0	0	0	0
10.25	0	0	0	0	0	0	0	0	0	0	2	5	8	6	3	1	0	0	0	0	0	0
10.75	0	0	0	0	0	0	0	0	0	0	2	5	8	6	3	1	0	0	0	0	0	0
11.25	0	0	0	0	0	0	0	0	0	0	1	2	3	2	1	0	0	0	0	0	0	0
11.75	0	0	0	0	0	0	0	0	0	0	1	2	3	2	1	0	0	0	0	0	0	0
12.25	0	0	0	0	0	0	0	0	0	0	0	1	1	1	0	0	0	0	0	0	0	0
12.75	0	0	0	0	0	0	0	0	0	0	0	1	1	1	0	0	0	0	0	0	0	0

Ormen Lange – November

Hs (m)	Spectral peak period (s)																					
	2.5	3.5	4.5	5.5	6.5	7.5	8.5	9.5	10.5	11.5	12.5	13.5	14.5	15.5	16.5	17.5	18.5	19.5	20.5	21.5	22.5	23.5
0.25	0	3	13	27	39	43	39	32	24	17	12	8	5	3	2	1	1	0	1	0	0	0
0.75	0	3	13	27	39	43	39	32	24	17	12	8	5	3	2	1	1	0	1	0	0	0
1.25	0	8	70	250	511	722	788	716	571	413	278	178	109	65	38	22	12	7	9	0	0	0
1.75	0	8	70	250	511	722	788	716	571	413	278	178	109	65	38	22	12	7	9	0	0	0
2.25	0	1	17	125	434	888	1248	1338	1174	888	600	372	216	119	63	33	17	8	8	0	0	0
2.75	0	1	17	125	434	888	1248	1338	1174	888	600	372	216	119	63	33	17	8	8	0	0	0
3.25	0	0	1	13	98	349	725	1014	1053	873	608	371	203	103	49	22	10	4	3	0	0	0
3.75	0	0	1	13	98	349	725	1014	1053	873	608	371	203	103	49	22	10	4	3	0	0	0
4.25	0	0	0	0	8	62	225	470	641	628	477	296	156	73	31	12	4	2	1	0	0	0
4.75	0	0	0	0	8	62	225	470	641	628	477	296	156	73	31	12	4	2	1	0	0	0
5.25	0	0	0	0	0	5	38	140	287	371	333	223	119	52	20	7	2	1	0	0	0	0
5.75	0	0	0	0	0	5	38	140	287	371	333	223	119	52	20	7	2	1	0	0	0	0
6.25	0	0	0	0	0	0	3	26	93	180	212	167	96	42	15	4	1	0	0	0	0	0
6.75	0	0	0	0	0	0	3	26	93	180	212	167	96	42	15	4	1	0	0	0	0	0
7.25	0	0	0	0	0	0	0	2	18	60	103	106	72	34	12	3	1	0	0	0	0	0
7.75	0	0	0	0	0	0	0	2	18	60	103	106	72	34	12	3	1	0	0	0	0	0
8.25	0	0	0	0	0	0	0	0	2	12	35	52	46	26	10	3	1	0	0	0	0	0
8.75	0	0	0	0	0	0	0	0	2	12	35	52	46	26	10	3	1	0	0	0	0	0
9.25	0	0	0	0	0	0	0	0	0	1	8	19	23	17	8	2	1	0	0	0	0	0
9.75	0	0	0	0	0	0	0	0	0	1	8	19	23	17	8	2	1	0	0	0	0	0
10.25	0	0	0	0	0	0	0	0	0	0	1	4	9	9	5	2	1	0	0	0	0	0
10.75	0	0	0	0	0	0	0	0	0	0	1	4	9	9	5	2	1	0	0	0	0	0
11.25	0	0	0	0	0	0	0	0	0	0	0	1	2	3	3	1	0	0	0	0	0	0
11.75	0	0	0	0	0	0	0	0	0	0	0	1	2	3	3	1	0	0	0	0	0	0
12.25	0	0	0	0	0	0	0	0	0	0	0	0	1	1	1	0	0	0	0	0	0	0
12.75	0	0	0	0	0	0	0	0	0	0	0	0	1	1	1	0	0	0	0	0	0	0

Ormen Lange – December

Hs (m)	Spectral peak period (s)																					
	2.5	3.5	4.5	5.5	6.5	7.5	8.5	9.5	10.5	11.5	12.5	13.5	14.5	15.5	16.5	17.5	18.5	19.5	20.5	21.5	22.5	23.5
0.25	0	1	6	12	18	21	21	18	15	12	9	7	5	3	2	2	1	1	2	0	0	0
0.75	0	1	6	12	18	21	21	18	15	12	9	7	5	3	2	2	1	1	2	0	0	0
1.25	0	6	43	148	303	442	509	496	428	338	250	176	119	78	51	32	20	13	20	0	0	0
1.75	0	6	43	148	303	442	509	496	428	338	250	176	119	78	51	32	20	13	20	0	0	0
2.25	0	1	14	97	328	673	977	1100	1027	834	609	410	260	157	91	52	29	16	18	0	0	0
2.75	0	1	14	97	328	673	977	1100	1027	834	609	410	260	157	91	52	29	16	18	0	0	0
3.25	0	0	1	13	91	320	674	973	1057	924	684	445	262	143	73	36	17	8	6	0	0	0
3.75	0	0	1	13	91	320	674	973	1057	924	684	445	262	143	73	36	17	8	6	0	0	0
4.25	0	0	0	0	9	66	243	519	730	743	587	380	210	103	46	19	7	3	1	0	0	0
4.75	0	0	0	0	9	66	243	519	730	743	587	380	210	103	46	19	7	3	1	0	0	0
5.25	0	0	0	0	0	6	47	177	373	494	453	310	168	75	29	10	3	1	0	0	0	0
5.75	0	0	0	0	0	6	47	177	373	494	453	310	168	75	29	10	3	1	0	0	0	0
6.25	0	0	0	0	0	0	4	36	136	268	319	252	143	62	22	6	2	0	0	0	0	0
6.75	0	0	0	0	0	0	4	36	136	268	319	252	143	62	22	6	2	0	0	0	0	0
7.25	0	0	0	0	0	0	0	4	28	97	171	175	115	52	18	5	1	0	0	0	0	0
7.75	0	0	0	0	0	0	0	4	28	97	171	175	115	52	18	5	1	0	0	0	0	0
8.25	0	0	0	0	0	0	0	0	3	21	63	94	80	42	15	4	1	0	0	0	0	0
8.75	0	0	0	0	0	0	0	0	3	21	63	94	80	42	15	4	1	0	0	0	0	0
9.25	0	0	0	0	0	0	0	0	0	3	15	36	44	30	13	4	1	0	0	0	0	0
9.75	0	0	0	0	0	0	0	0	0	3	15	36	44	30	13	4	1	0	0	0	0	0
10.25	0	0	0	0	0	0	0	0	0	0	2	9	17	17	10	3	1	0	0	0	0	0
10.75	0	0	0	0	0	0	0	0	0	0	2	9	17	17	10	3	1	0	0	0	0	0
11.25	0	0	0	0	0	0	0	0	0	0	0	1	5	7	6	3	1	0	0	0	0	0
11.75	0	0	0	0	0	0	0	0	0	0	0	1	5	7	6	3	1	0	0	0	0	0
12.25	0	0	0	0	0	0	0	0	0	0	0	0	1	2	2	2	1	0	0	0	0	0
12.75	0	0	0	0	0	0	0	0	0	0	0	0	0	0	1	1	0	0	0	0	0	0

5. Monthly operability Ormen Lange

January:

Operability drilling/tripping:			Ormen January
	Heave	Rotation	Total
Aker H6:	0.969	0.999	0.969
SEVAN:	0.653	0.999	0.653
West Navigator:	0.919	0.966	0.919

Operability running casing:			Ormen January
	Heave	Rotation	Total
Aker H6:	0.956	0.999	0.956
SEVAN:	0.628	0.999	0.628
West Navigator:	0.893	0.960	0.893

Operability logging:			Ormen January
	Heave	Rotation	Total
Aker H6:	0.956	0.999	0.956
SEVAN:	0.628	0.999	0.628
West Navigator:	0.893	0.960	0.893

Operability miscellaneous:			Ormen January
	Heave	Rotation	Total
Aker H6:	0.969	0.999	0.969
SEVAN:	0.653	0.999	0.653
West Navigator:	0.919	0.960	0.919

Operability running BOP/riser:			Ormen January
	Heave	Rotation	Total
Aker H6:	0.708	0.863	0.708
SEVAN:	0.399	0.911	0.399
West Navigator:	0.622	0.723	0.622

Operability cementing:			Ormen January
	Heave	Rotation	Total
Aker H6:	0.879	0.994	0.879
SEVAN:	0.511	0.996	0.511
West Navigator:	0.805	0.926	0.805

Operability TOTAL:			Ormen January
	Heave	Rotation	Total
Aker H6:	0.936	0.985	0.936
SEVAN:	0.615	0.990	0.615
West Navigator:	0.878	0.938	0.878

Downtime TOTAL:			Ormen January
	Heave	Rotation	Total
Aker H6:	0.064	0.015	0.064
SEVAN:	0.385	0.010	0.385
West Navigator:	0.122	0.062	0.122

February:

Operability drilling/tripping:			Ormen February
	Heave	Rotation	Total
Aker H6:	0.981	1.000	0.981
SEVAN:	0.698	1.000	0.698
West Navigator:	0.945	0.979	0.945

Operability running casing:			Ormen February
	Heave	Rotation	Total
Aker H6:	0.972	1.000	0.972
SEVAN:	0.671	1.000	0.671
West Navigator:	0.925	0.975	0.925

Operability logging:			Ormen February
	Heave	Rotation	Total
Aker H6:	0.972	1.000	0.972
SEVAN:	0.671	1.000	0.671
West Navigator:	0.925	0.975	0.925

Operability miscellaneous:			Ormen February
	Heave	Rotation	Total
Aker H6:	0.981	1.000	0.981
SEVAN:	0.698	1.000	0.698
West Navigator:	0.945	0.975	0.945

Operability running BOP/riser:			Ormen February
	Heave	Rotation	Total
Aker H6:	0.758	0.898	0.758
SEVAN:	0.414	0.938	0.414
West Navigator:	0.666	0.769	0.666

Operability cementing:			Ormen February
	Heave	Rotation	Total
Aker H6:	0.914	0.997	0.914
SEVAN:	0.544	0.998	0.544
West Navigator:	0.849	0.949	0.849

Operability TOTAL:			Ormen February
	Heave	Rotation	Total
Aker H6:	0.953	0.989	0.953
SEVAN:	0.656	0.993	0.656
West Navigator:	0.908	0.955	0.908

Downtime TOTAL:			Ormen February
	Heave	Rotation	Total
Aker H6:	0.047	0.011	0.047
SEVAN:	0.344	0.007	0.344
West Navigator:	0.092	0.045	0.092

March:

Operability drilling/tripping:			Ormen March		Operability running casing:			Ormen March
	Heave	Rotation	Total			Heave	Rotation	Total
Aker H6:	0.995	1.000	0.995		Aker H6:	0.992	1.000	0.992
SEVAN:	0.783	1.000	0.783		SEVAN:	0.758	1.000	0.758
West Navigator:	0.978	0.995	0.978		West Navigator:	0.966	0.992	0.966

Operability logging:			Ormen March		Operability miscellaneous:			Ormen March
	Heave	Rotation	Total			Heave	Rotation	Total
Aker H6:	0.992	1.000	0.992		Aker H6:	0.995	1.000	0.995
SEVAN:	0.758	1.000	0.758		SEVAN:	0.783	1.000	0.783
West Navigator:	0.966	0.992	0.966		West Navigator:	0.978	0.992	0.978

Operability running BOP/riser:			Ormen March		Operability cementing:			Ormen March
	Heave	Rotation	Total			Heave	Rotation	Total
Aker H6:	0.834	0.944	0.834		Aker H6:	0.959	1.000	0.959
SEVAN:	0.497	0.973	0.497		SEVAN:	0.635	1.000	0.635
West Navigator:	0.753	0.841	0.753		West Navigator:	0.913	0.979	0.913

Operability TOTAL:			Ormen March		Downtime TOTAL:			Ormen March
	Heave	Rotation	Total			Heave	Rotation	Total
Aker H6:	0.977	0.994	0.977		Aker H6:	0.023	0.006	0.023
SEVAN:	0.742	0.997	0.742		SEVAN:	0.258	0.003	0.258
West Navigator:	0.950	0.978	0.950		West Navigator:	0.050	0.022	0.050

April:

Operability drilling/tripping:			Ormen April		Operability running casing:			Ormen April
	Heave	Rotation	Total			Heave	Rotation	Total
Aker H6:	0.997	1.000	0.997		Aker H6:	0.996	1.000	0.996
SEVAN:	0.895	1.000	0.895		SEVAN:	0.882	1.000	0.882
West Navigator:	0.990	0.997	0.990		West Navigator:	0.985	0.996	0.985

Operability logging:			Ormen April		Operability miscellaneous:			Ormen April
	Heave	Rotation	Total			Heave	Rotation	Total
Aker H6:	0.996	1.000	0.996		Aker H6:	0.997	1.000	0.997
SEVAN:	0.882	1.000	0.882		SEVAN:	0.895	1.000	0.895
West Navigator:	0.985	0.996	0.985		West Navigator:	0.990	0.996	0.990

Operability running BOP/riser:			Ormen April		Operability cementing:			Ormen April
	Heave	Rotation	Total			Heave	Rotation	Total
Aker H6:	0.923	0.974	0.923		Aker H6:	0.981	1.000	0.981
SEVAN:	0.693	0.987	0.693		SEVAN:	0.803	1.000	0.803
West Navigator:	0.879	0.926	0.879		West Navigator:	0.962	0.990	0.962

Operability TOTAL:			Ormen April		Downtime TOTAL:			Ormen April
	Heave	Rotation	Total			Heave	Rotation	Total
Aker H6:	0.989	0.997	0.989		Aker H6:	0.011	0.003	0.011
SEVAN:	0.867	0.999	0.867		SEVAN:	0.133	0.001	0.133
West Navigator:	0.976	0.989	0.976		West Navigator:	0.024	0.011	0.024

May:

Operability drilling/tripping: Ormen May

	Heave	Rotation	Total
Aker H6:	1.000	1.000	1.000
SEVAN:	0.983	1.000	0.983
West Navigator:	1.000	1.000	1.000

Operability running casing: Ormen May

	Heave	Rotation	Total
Aker H6:	1.000	1.000	1.000
SEVAN:	0.979	1.000	0.979
West Navigator:	1.000	1.000	1.000

Operability logging: Ormen May

	Heave	Rotation	Total
Aker H6:	1.000	1.000	1.000
SEVAN:	0.979	1.000	0.979
West Navigator:	1.000	1.000	1.000

Operability miscellaneous: Ormen May

	Heave	Rotation	Total
Aker H6:	1.000	1.000	1.000
SEVAN:	0.983	1.000	0.983
West Navigator:	1.000	1.000	1.000

Operability running BOP/riser: Ormen May

	Heave	Rotation	Total
Aker H6:	0.991	0.999	0.991
SEVAN:	0.887	1.000	0.887
West Navigator:	0.980	0.991	0.980

Operability cementing: Ormen May

	Heave	Rotation	Total
Aker H6:	1.000	1.000	1.000
SEVAN:	0.949	1.000	0.949
West Navigator:	0.998	1.000	0.998

Operability TOTAL: Ormen May

	Heave	Rotation	Total
Aker H6:	0.999	1.000	0.999
SEVAN:	0.971	1.000	0.971
West Navigator:	0.998	0.999	0.998

Downtime TOTAL: Ormen May

	Heave	Rotation	Total
Aker H6:	0.001	0.000	0.001
SEVAN:	0.029	0.000	0.029
West Navigator:	0.002	0.001	0.002

June:

Operability drilling/tripping: Ormen June

	Heave	Rotation	Total
Aker H6:	1.000	1.000	1.000
SEVAN:	0.990	1.000	0.990
West Navigator:	1.000	1.000	1.000

Operability running casing: Ormen June

	Heave	Rotation	Total
Aker H6:	1.000	1.000	1.000
SEVAN:	0.988	1.000	0.988
West Navigator:	1.000	1.000	1.000

Operability logging: Ormen June

	Heave	Rotation	Total
Aker H6:	1.000	1.000	1.000
SEVAN:	0.988	1.000	0.988
West Navigator:	1.000	1.000	1.000

Operability miscellaneous: Ormen June

	Heave	Rotation	Total
Aker H6:	1.000	1.000	1.000
SEVAN:	0.990	1.000	0.990
West Navigator:	1.000	1.000	1.000

Operability running BOP/riser: Ormen June

	Heave	Rotation	Total
Aker H6:	0.995	1.000	0.995
SEVAN:	0.920	1.000	0.920
West Navigator:	0.989	0.996	0.989

Operability cementing: Ormen June

	Heave	Rotation	Total
Aker H6:	1.000	1.000	1.000
SEVAN:	0.968	1.000	0.968
West Navigator:	0.999	1.000	0.999

Operability TOTAL: Ormen June

	Heave	Rotation	Total
Aker H6:	1.000	1.000	1.000
SEVAN:	0.982	1.000	0.982
West Navigator:	0.999	1.000	0.999

Downtime TOTAL: Ormen June

	Heave	Rotation	Total
Aker H6:	0.000	0.000	0.000
SEVAN:	0.018	0.000	0.018
West Navigator:	0.001	0.000	0.001

July:

Operability drilling/tripping: Ormen July

	Heave	Rotation	Total
Aker H6:	1.000	1.000	1.000
SEVAN:	0.998	1.000	0.998
West Navigator:	1.000	1.000	1.000

Operability running casing: Ormen July

	Heave	Rotation	Total
Aker H6:	1.000	1.000	1.000
SEVAN:	0.997	1.000	0.997
West Navigator:	1.000	1.000	1.000

Operability logging: Ormen July

	Heave	Rotation	Total
Aker H6:	1.000	1.000	1.000
SEVAN:	0.997	1.000	0.997
West Navigator:	1.000	1.000	1.000

Operability miscellaneous: Ormen July

	Heave	Rotation	Total
Aker H6:	1.000	1.000	1.000
SEVAN:	0.998	1.000	0.998
West Navigator:	1.000	1.000	1.000

Operability running BOP/riser: Ormen July

	Heave	Rotation	Total
Aker H6:	0.999	1.000	0.999
SEVAN:	0.960	1.000	0.960
West Navigator:	0.997	0.999	0.997

Operability cementing: Ormen July

	Heave	Rotation	Total
Aker H6:	1.000	1.000	1.000
SEVAN:	0.989	1.000	0.989
West Navigator:	1.000	1.000	1.000

Operability TOTAL: Ormen July

	Heave	Rotation	Total
Aker H6:	1.000	1.000	1.000
SEVAN:	0.993	1.000	0.993
West Navigator:	1.000	1.000	1.000

Downtime TOTAL: Ormen July

	Heave	Rotation	Total
Aker H6:	0.000	0.000	0.000
SEVAN:	0.007	0.000	0.007
West Navigator:	0.000	0.000	0.000

August:

Operability drilling/tripping: Ormen August

	Heave	Rotation	Total
Aker H6:	1.000	1.000	1.000
SEVAN:	0.990	1.000	0.990
West Navigator:	1.000	1.000	1.000

Operability running casing: Ormen August

	Heave	Rotation	Total
Aker H6:	1.000	1.000	1.000
SEVAN:	0.988	1.000	0.988
West Navigator:	1.000	1.000	1.000

Operability logging: Ormen August

	Heave	Rotation	Total
Aker H6:	1.000	1.000	1.000
SEVAN:	0.988	1.000	0.988
West Navigator:	1.000	1.000	1.000

Operability miscellaneous: Ormen August

	Heave	Rotation	Total
Aker H6:	1.000	1.000	1.000
SEVAN:	0.990	1.000	0.990
West Navigator:	1.000	1.000	1.000

Operability running BOP/riser: Ormen August

	Heave	Rotation	Total
Aker H6:	0.995	0.999	0.995
SEVAN:	0.919	1.000	0.919
West Navigator:	0.988	0.995	0.988

Operability cementing: Ormen August

	Heave	Rotation	Total
Aker H6:	1.000	1.000	1.000
SEVAN:	0.967	1.000	0.967
West Navigator:	0.999	1.000	0.999

Operability TOTAL: Ormen August

	Heave	Rotation	Total
Aker H6:	0.999	1.000	0.999
SEVAN:	0.981	1.000	0.981
West Navigator:	0.999	1.000	0.999

Downtime TOTAL: Ormen August

	Heave	Rotation	Total
Aker H6:	0.001	0.000	0.001
SEVAN:	0.019	0.000	0.019
West Navigator:	0.001	0.000	0.001

September:

Operability drilling/tripping:	Heave	Rotation	Total	Ormen September
Aker H6:	0.999	1.000		0.999
SEVAN:	0.937	1.000		0.937
West Navigator:	0.997	0.999		0.997

Operability running casing:	Heave	Rotation	Total	Ormen September
Aker H6:	0.999	1.000		0.999
SEVAN:	0.928	1.000		0.928
West Navigator:	0.994	0.999		0.994

Operability logging:	Heave	Rotation	Total	Ormen September
Aker H6:	0.999	1.000		0.999
SEVAN:	0.928	1.000		0.928
West Navigator:	0.994	0.999		0.994

Operability miscellaneous:	Heave	Rotation	Total	Ormen September
Aker H6:	0.999	1.000		0.999
SEVAN:	0.937	1.000		0.937
West Navigator:	0.997	0.999		0.997

Operability running BOP/riser:	Heave	Rotation	Total	Ormen September
Aker H6:	0.958	0.987		0.958
SEVAN:	0.765	0.995		0.765
West Navigator:	0.927	0.959		0.927

Operability cementing:	Heave	Rotation	Total	Ormen September
Aker H6:	0.992	1.000		0.992
SEVAN:	0.864	1.000		0.864
West Navigator:	0.983	0.996		0.983

Operability TOTAL:	Heave	Rotation	Total	Ormen September
Aker H6:	0.995	0.999		0.995
SEVAN:	0.914	0.999		0.914
West Navigator:	0.989	0.995		0.989

Downtime TOTAL:	Heave	Rotation	Total	Ormen September
Aker H6:	0.005	0.001		0.005
SEVAN:	0.086	0.001		0.086
West Navigator:	0.011	0.005		0.011

October:

Operability drilling/tripping:	Heave	Rotation	Total	Ormen October
Aker H6:	0.994	1.000		0.994
SEVAN:	0.817	1.000		0.817
West Navigator:	0.979	0.993		0.979

Operability running casing:	Heave	Rotation	Total	Ormen October
Aker H6:	0.990	1.000		0.990
SEVAN:	0.796	1.000		0.796
West Navigator:	0.969	0.991		0.969

Operability logging:	Heave	Rotation	Total	Ormen October
Aker H6:	0.990	1.000		0.990
SEVAN:	0.796	1.000		0.796
West Navigator:	0.969	0.991		0.969

Operability miscellaneous:	Heave	Rotation	Total	Ormen October
Aker H6:	0.994	1.000		0.994
SEVAN:	0.817	1.000		0.817
West Navigator:	0.979	0.991		0.979

Operability running BOP/riser:	Heave	Rotation	Total	Ormen October
Aker H6:	0.864	0.951		0.864
SEVAN:	0.554	0.974		0.554
West Navigator:	0.794	0.869		0.794

Operability cementing:	Heave	Rotation	Total	Ormen October
Aker H6:	0.962	0.999		0.962
SEVAN:	0.686	0.999		0.686
West Navigator:	0.926	0.979		0.926

Operability TOTAL:	Heave	Rotation	Total	Ormen October
Aker H6:	0.979	0.995		0.979
SEVAN:	0.780	0.997		0.780
West Navigator:	0.955	0.980		0.955

Downtime TOTAL:	Heave	Rotation	Total	Ormen October
Aker H6:	0.021	0.005		0.021
SEVAN:	0.220	0.003		0.220
West Navigator:	0.045	0.020		0.045

November:

Operability drilling/tripping:			Ormen November
	Heave	Rotation	Total
Aker H6:	0.992	1.000	0.992
SEVAN:	0.800	1.000	0.800
West Navigator:	0.975	0.992	0.975

Operability running casing:			Ormen November
	Heave	Rotation	Total
Aker H6:	0.988	1.000	0.988
SEVAN:	0.778	1.000	0.778
West Navigator:	0.964	0.989	0.964

Operability logging:			Ormen November
	Heave	Rotation	Total
Aker H6:	0.988	1.000	0.988
SEVAN:	0.778	1.000	0.778
West Navigator:	0.964	0.989	0.964

Operability miscellaneous:			Ormen November
	Heave	Rotation	Total
Aker H6:	0.992	1.000	0.992
SEVAN:	0.800	1.000	0.800
West Navigator:	0.975	0.989	0.975

Operability running BOP/riser:			Ormen November
	Heave	Rotation	Total
Aker H6:	0.849	0.945	0.849
SEVAN:	0.521	0.970	0.521
West Navigator:	0.773	0.857	0.773

Operability cementing:			Ormen November
	Heave	Rotation	Total
Aker H6:	0.957	0.999	0.957
SEVAN:	0.658	0.999	0.658
West Navigator:	0.917	0.976	0.917

Operability TOTAL:			Ormen November
	Heave	Rotation	Total
Aker H6:	0.976	0.994	0.976
SEVAN:	0.760	0.997	0.760
West Navigator:	0.950	0.977	0.950

Downtime TOTAL:			Ormen November
	Heave	Rotation	Total
Aker H6:	0.024	0.006	0.024
SEVAN:	0.240	0.003	0.240
West Navigator:	0.050	0.023	0.050

December:

Operability drilling/tripping:			Ormen December
	Heave	Rotation	Total
Aker H6:	0.987	1.000	0.987
SEVAN:	0.723	1.000	0.723
West Navigator:	0.959	0.986	0.959

Operability running casing:			Ormen December
	Heave	Rotation	Total
Aker H6:	0.980	1.000	0.980
SEVAN:	0.696	1.000	0.696
West Navigator:	0.942	0.981	0.942

Operability logging:			Ormen December
	Heave	Rotation	Total
Aker H6:	0.980	1.000	0.980
SEVAN:	0.696	1.000	0.696
West Navigator:	0.942	0.981	0.942

Operability miscellaneous:			Ormen December
	Heave	Rotation	Total
Aker H6:	0.987	1.000	0.987
SEVAN:	0.723	1.000	0.723
West Navigator:	0.959	0.981	0.959

Operability running BOP/riser:			Ormen December
	Heave	Rotation	Total
Aker H6:	0.781	0.912	0.781
SEVAN:	0.418	0.950	0.418
West Navigator:	0.686	0.793	0.686

Operability cementing:			Ormen December
	Heave	Rotation	Total
Aker H6:	0.931	0.998	0.931
SEVAN:	0.558	0.999	0.558
West Navigator:	0.872	0.959	0.872

Operability TOTAL:			Ormen December
	Heave	Rotation	Total
Aker H6:	0.962	0.991	0.962
SEVAN:	0.679	0.995	0.679
West Navigator:	0.924	0.964	0.924

Downtime TOTAL:			Ormen December
	Heave	Rotation	Total
Aker H6:	0.038	0.009	0.038
SEVAN:	0.321	0.005	0.321
West Navigator:	0.076	0.036	0.076

6. Response Amplitude Operators

Aker H6, 0 deg off bow wave heading:
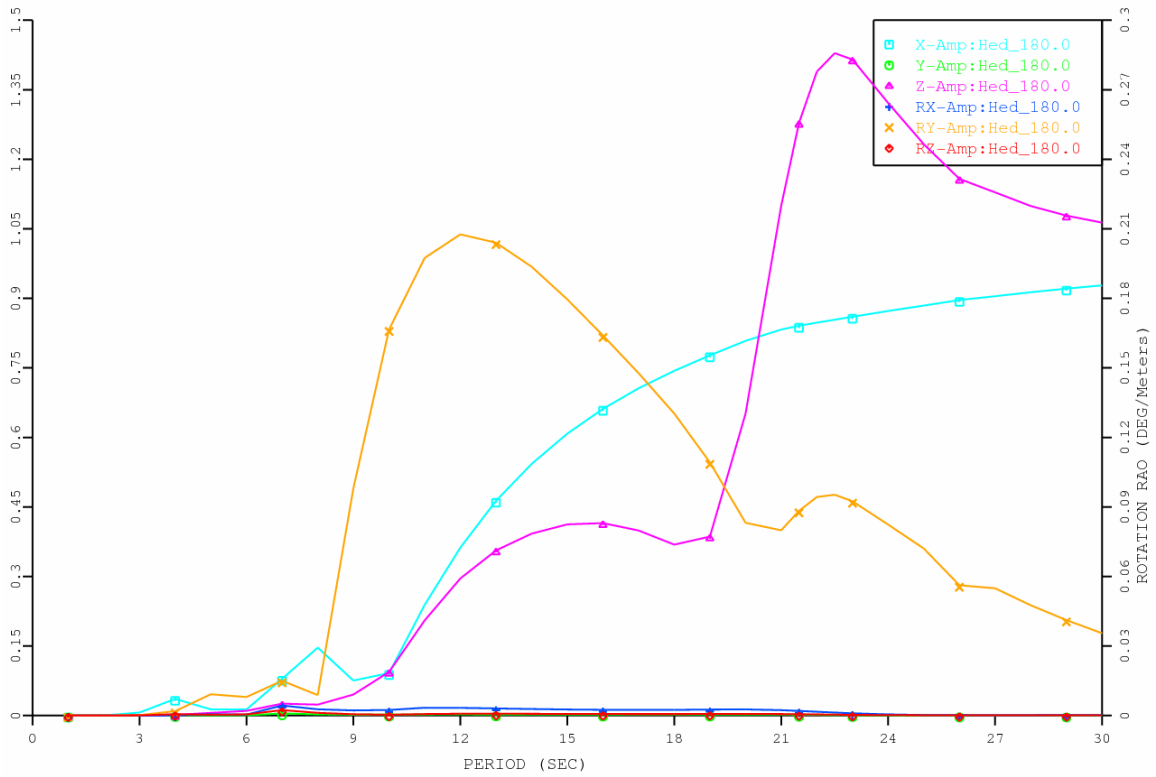
Aker H6, 45 deg off bow wave heading:
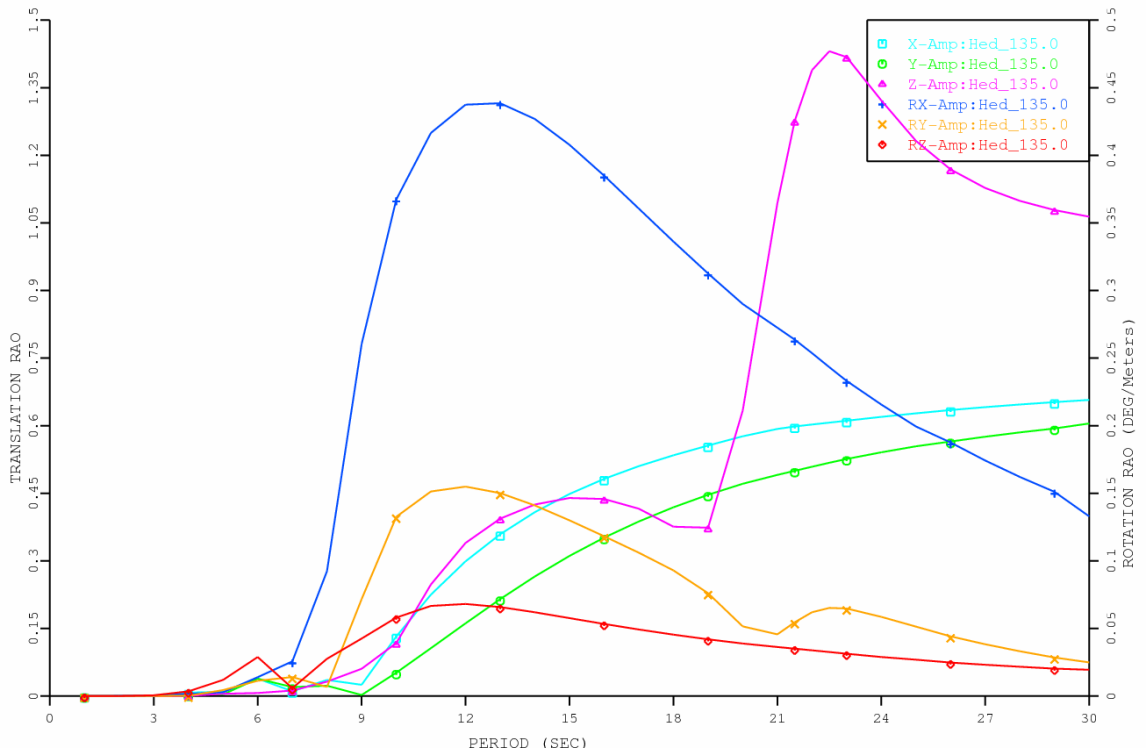
Aker H6, 90 deg off bow wave heading:
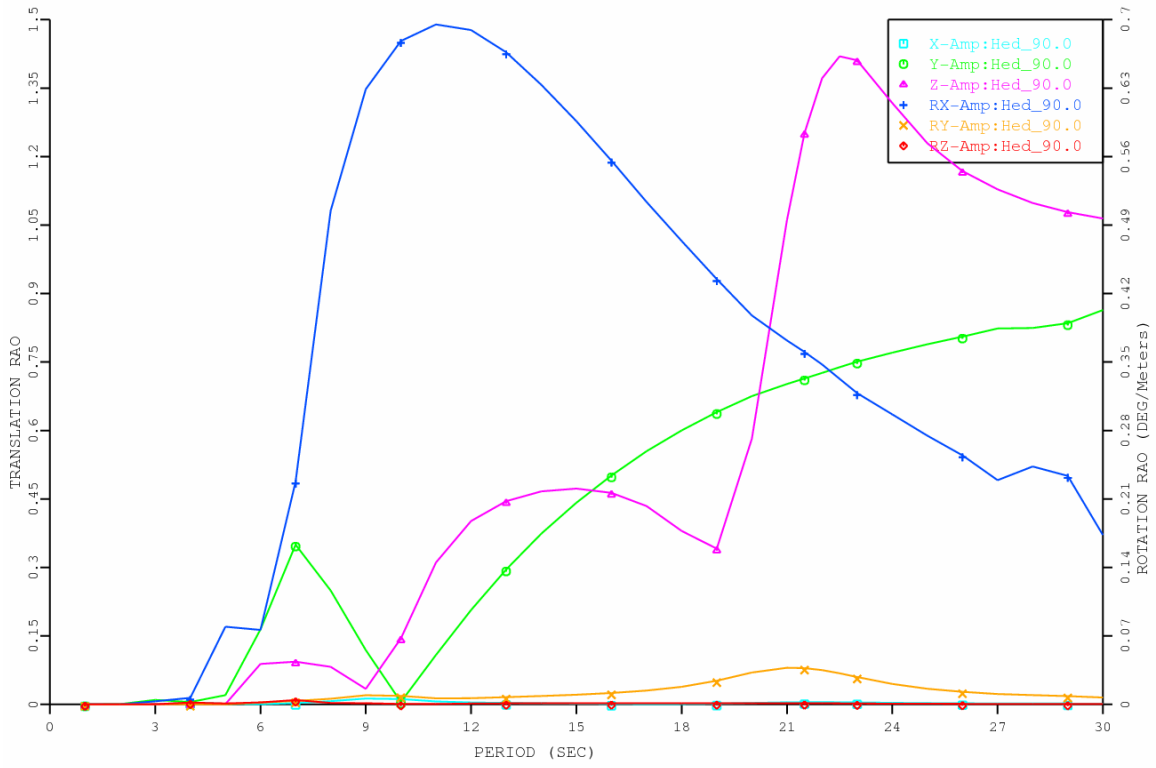
West Navigator, 0 deg off bow wave heading:
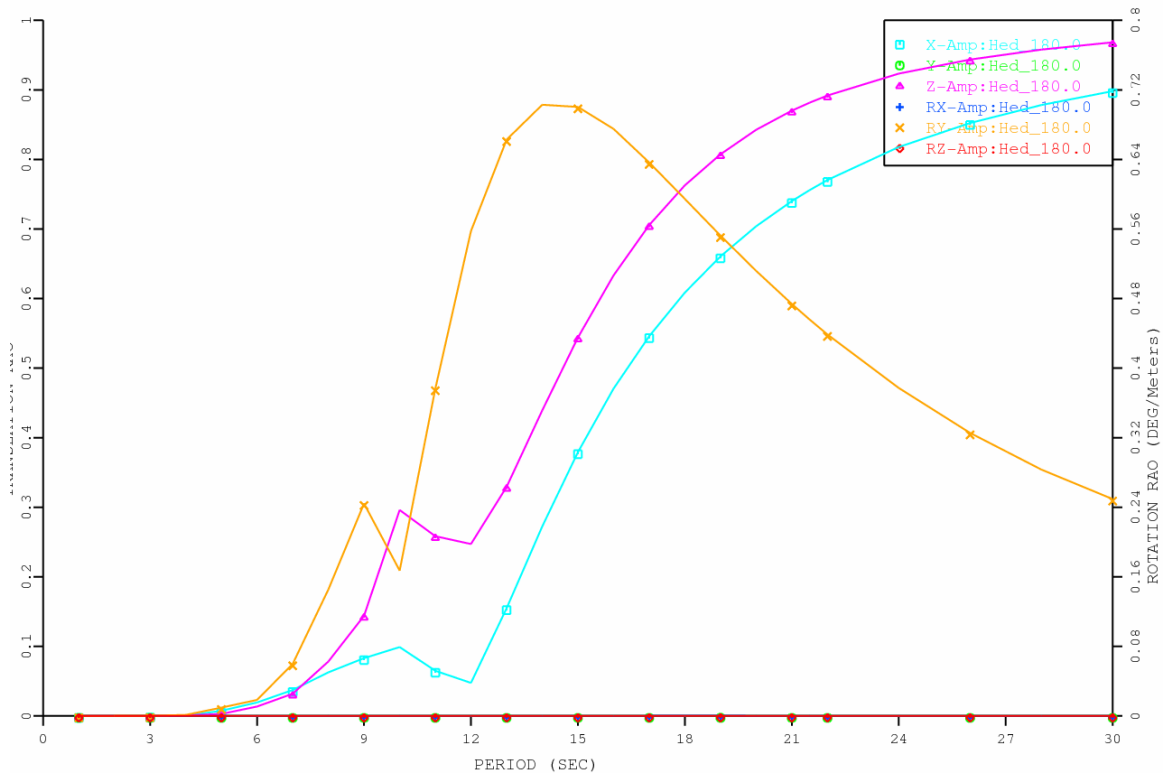
West Navigator, 15 deg off bow wave heading:
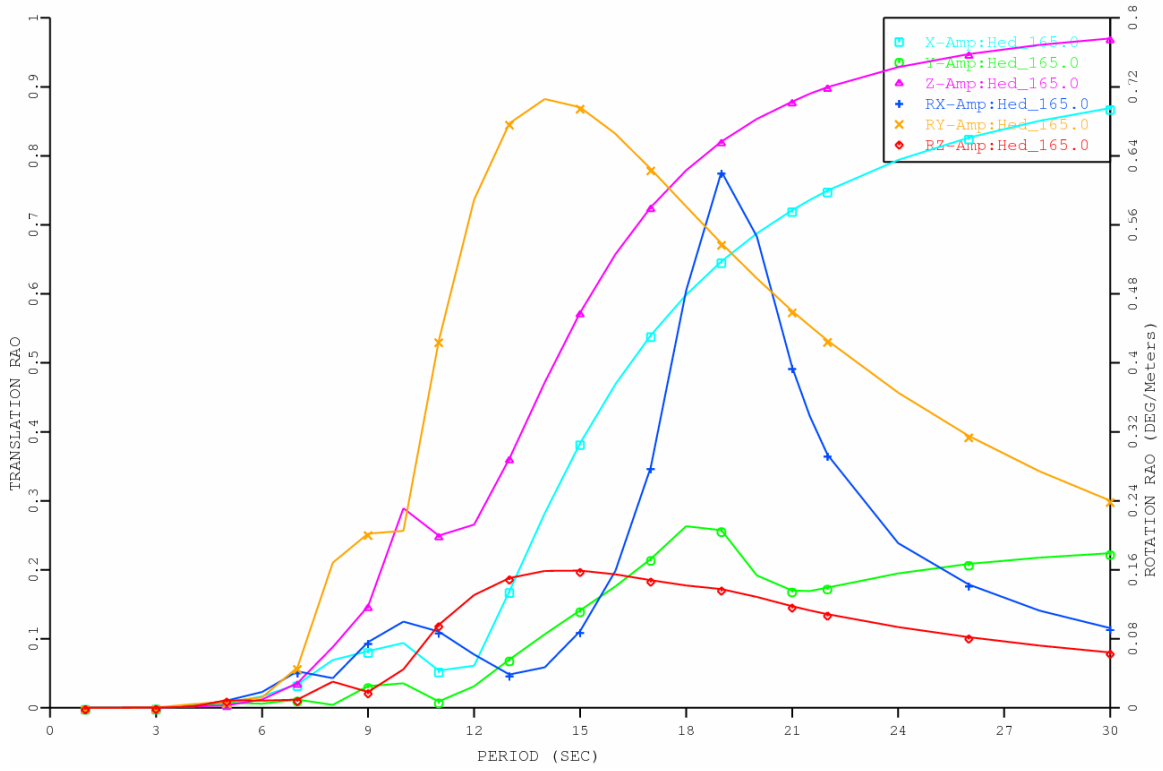
West Navigator, 25 deg off bow wave heading:
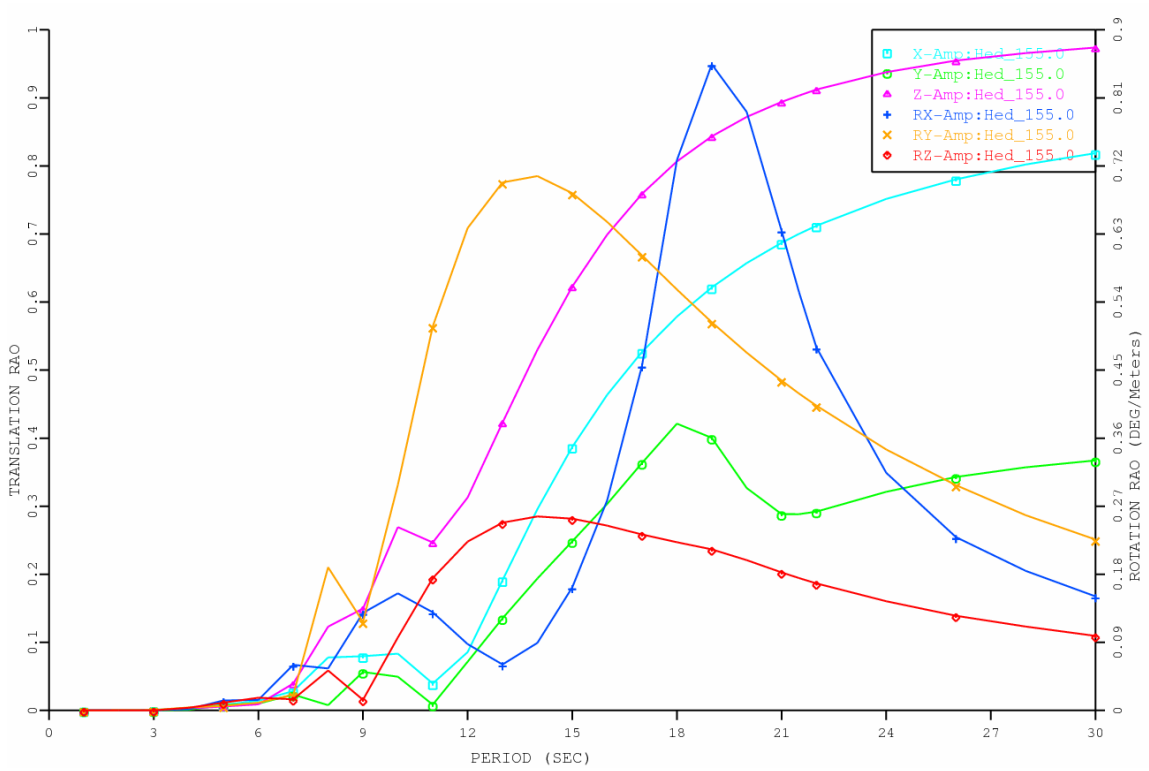
West Navigator, 45 deg off bow wave heading:
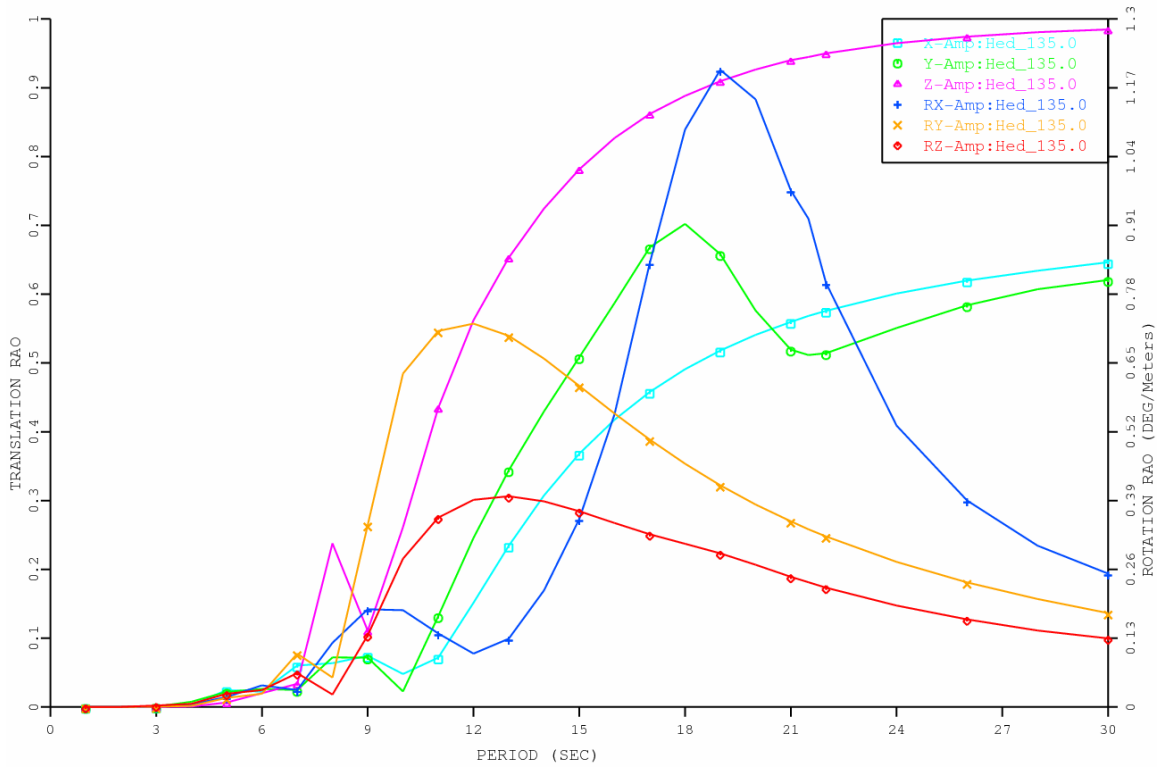
West Navigator, 90 deg off bow wave heading:
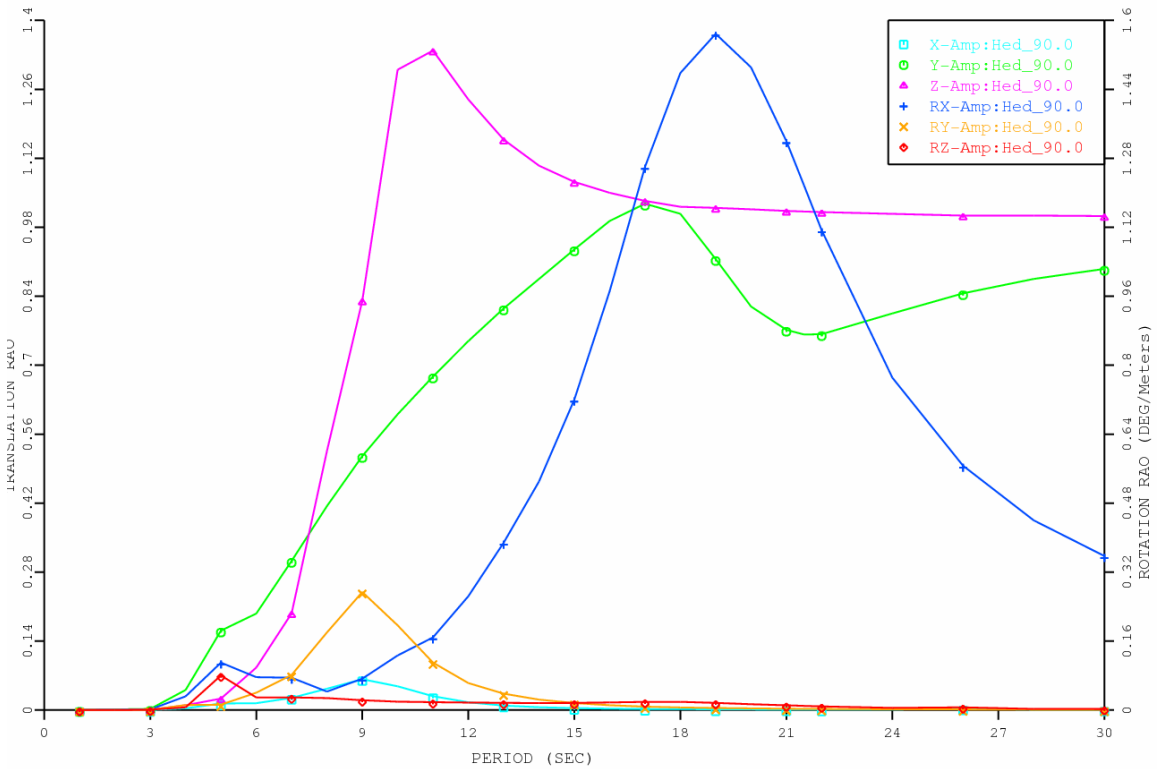
SEVAN Deepsea Driller, All wave headings:
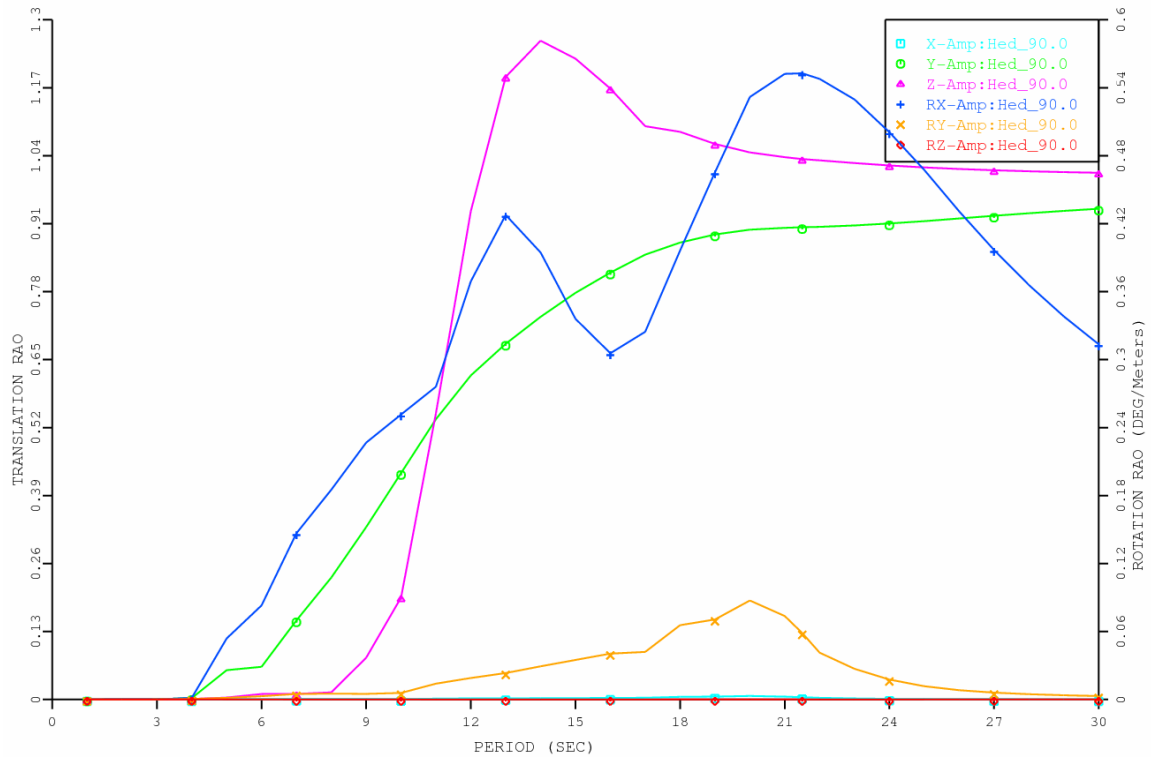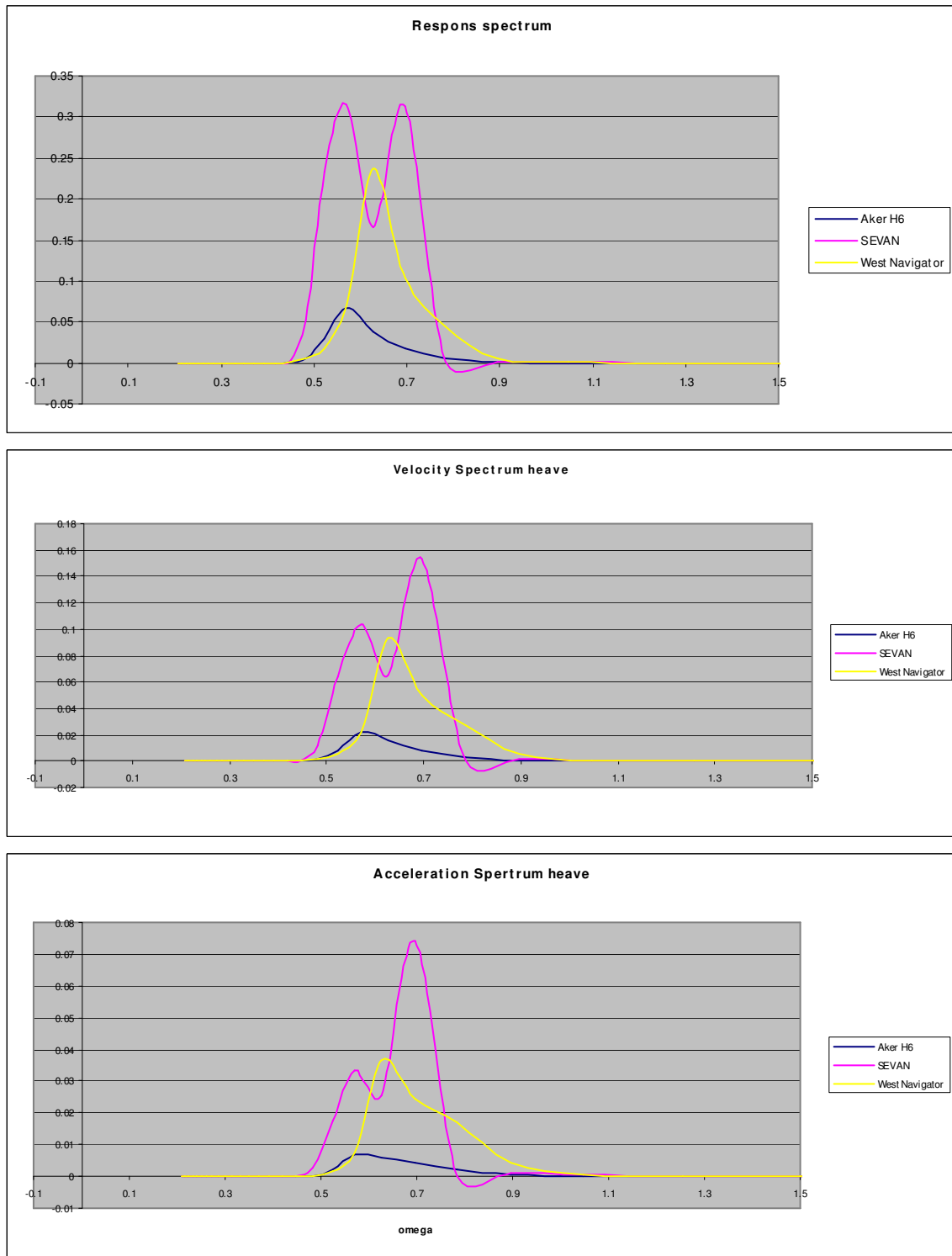
7. Motion, velocity and acceleration spectra

Figure 20.6: *Heave motion, velocity and acceleration response spectra for Tp=8, Hs=7*

8. Calculation of the heave RAO for the Aker H6

Geometry Aker H6:

$l_{deck} := 90m$ — Main deck length

$b_{deck} := 70m$ — Main deck breath

$h_{pont} := 10m$ — Height pontoon

$w_{pont} := 19.5m$ — Width pontoon

$l_{pont} := 120m$ — length pontoon

$l_{pont.eq} := l_{pont} - \left(1 - \dfrac{\pi}{4}\right) \cdot w_{pont} = 115.815m$ — Equivalent length of pontoon, considering that they are rounded fore and aft with a radius of w_{pont}. This corrected length is use in calculation of hull volume and forces.

$draft_{H6} := 23 \cdot m$

$h_c := draft_{H6} - h_{pont} = 13m$ — Distance from waterline to top of pontoon

$w_c := 12.5 \cdot m$ — Width column

$b_c := 12.5m$ — Breath column

$A_c := w_c \cdot b_c = 156.25m^2$ — Cross section area column

$A_{cw} := 152\,m^2$ — Corrected due to rounded corners. Calculated in MOSES.

$b_0 := 59\,m$ — Distance from center to center hulls

$d_{brace} := 3.0m$ — Average diameter of braces

$l_{b.eqv} := 6 \cdot \left(b_{deck} - 2 \cdot b_c\right) = 270m$ — Approximate total length of all transverse braces and k-braces

$n_0 := 4$ — Columns per hull

$\theta(\omega) = k \cdot \dfrac{b_0}{2} - \omega \cdot t$

Force on columns

$$V_{col} := A_c \cdot h_c = 1.976 \times 10^3 \cdot m^3$$

Volume of column

$$F_{3c}(\omega) := \rho \cdot g \cdot A_c \cdot \zeta_a \cdot e^{\frac{-\omega^2}{g} \cdot h_c}$$

Vertical excitation force on column, according to equation 3.1

$$G_{\zeta a} := 2 \cdot n_0 \cdot \rho \cdot g \cdot \zeta_a \cdot A_c$$

Normalizing reference force, [9]

$$F_{3c.nor}(\omega) := \frac{F_{3c}(\omega)}{G_{\zeta a}}$$

Normalized excitation force

Vertical force on 1 column

$F_{3c.nor}(\omega)$
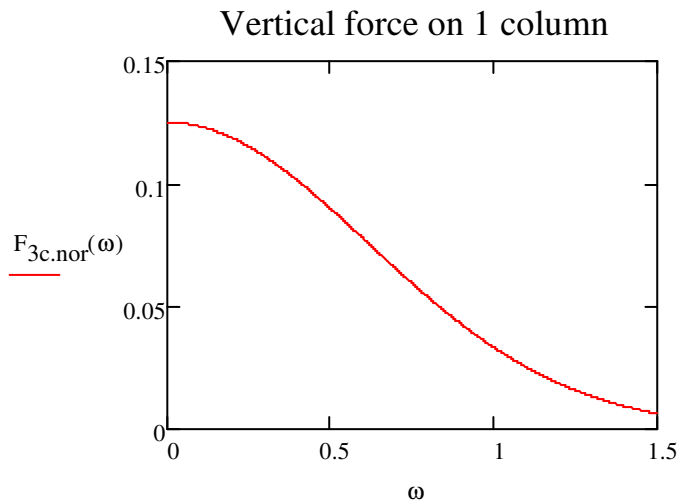
$$F_{3c}(\omega) = n_0 \cdot \rho \cdot g \cdot A_c \cdot \zeta_a \cdot e^{\frac{-\omega^2}{g} \cdot h_c} \cdot \cos\left(\frac{b_0 \cdot \omega^2}{g \cdot 2} - \omega \cdot t\right)$$

Reference force with phase taken into account.

Port and starbord vertical force:

$$F_{vc}(\omega) = n_0 \cdot \rho \cdot g \cdot A_c \cdot \zeta_a \cdot e^{\frac{-\omega^2}{g} \cdot h_c} \cdot \left[\cos\left(\frac{b_0 \cdot \omega^2}{2 \cdot g} - \omega \cdot t\right) + \cos\left(-\frac{b_0 \cdot \omega^2}{2 \cdot g} - \omega \cdot t\right)\right]$$

$$F_{vc}(\omega) = n_0 \cdot 2\rho \cdot g \cdot A_c \cdot \zeta_a \cdot e^{\frac{-\omega^2}{g} \cdot h_c} \cdot \left(\cos\left(\frac{\omega^2 \cdot b_0}{2 \cdot g}\right) \cdot \cos(\omega \cdot t)\right)$$

$$\frac{F_{vc}(\omega)}{G_{\zeta a}} = F_{vc.nor} \cdot \cos(\omega \cdot t)$$

$$F_{vc.nor}(\omega) := \frac{n_0 \cdot 2\rho \cdot g \cdot A_c \cdot \zeta_a \cdot e^{\frac{-\omega^2}{g} \cdot h_c} \cdot \cos\left(\frac{\omega^2 \cdot b_0}{2 \cdot g}\right)}{G_{\zeta a}}$$

Vertical force on all columns

Vertical force on 8 columns

$F_{vc.nor}(\omega)$
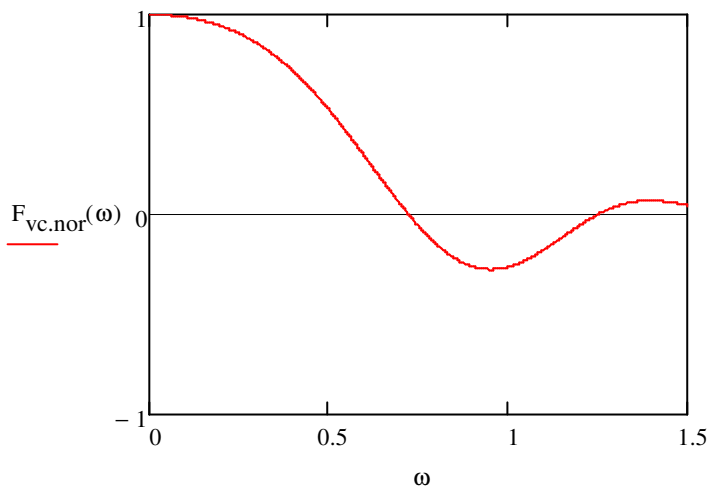
Force on pontoons

$$V_{hull} := h_{pont} \cdot w_{pont} \cdot l_{pont.eq} = 2.258 \times 10^4 \cdot m^3$$

Volume hull

$$C_m := 1 + C_a = 2.8$$

Value obtained from
[9], page 228

$$F_{3h}(\omega) := -C_m \cdot \rho \cdot V_{hull} \cdot \zeta_a \cdot \omega^2 \cdot e^{\frac{-\omega^2}{g}(h_c + h_{pont})}$$

Force on one hull according to
equation 3.3

$$F_{3h.nor}(\omega) := \frac{F_{3h}(\omega)}{G_{\zeta a}}$$

Normalized force on one hull

Vertical force on 1 hull
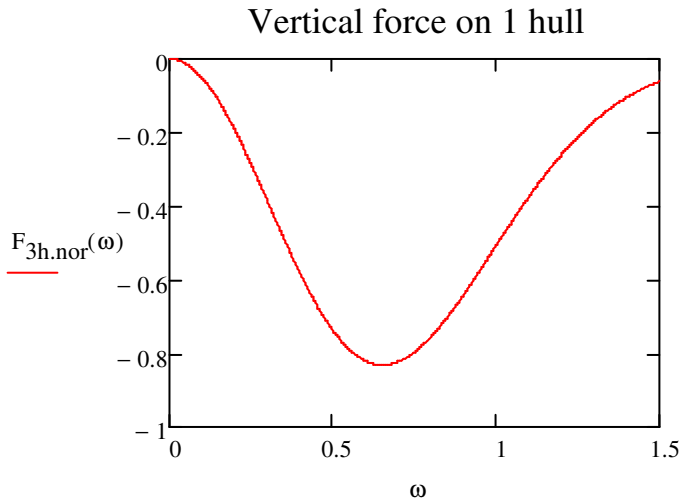
$$F_{3h}(\omega) = -C_m \cdot \rho \cdot V_{hull} \cdot \zeta_a \cdot \omega^2 \cdot e^{\frac{-\omega^2}{g}(h_c+R)} \cdot \cos\left(k \cdot \frac{b_0}{2} - \omega \cdot t\right)$$

Force with phase taken into account

Port and starboard vertical force:

$$F_{vh}(\omega) = -C_m \cdot \rho \cdot V_{hull} \cdot \zeta_a \cdot \omega^2 \cdot e^{\frac{-\omega^2}{g}(h_c+R)} \cdot \left[\cos\left(\frac{b_0 \cdot \omega^2}{2 \cdot g} - \omega \cdot t\right) + \cos\left(-\frac{b_0 \cdot \omega^2}{2 \cdot g} - \omega \cdot t\right)\right]$$

$$F_{vh}(\omega) = -C_m \cdot 2 \cdot \rho \cdot V_{hull} \cdot \zeta_a \cdot \omega^2 \cdot e^{\frac{-\omega^2}{g}(h_c+R)} \cdot \left(\cos\left(\frac{\omega^2 \cdot b_0}{2 \cdot g}\right) \cdot \cos(\omega \cdot t)\right)$$

$$\frac{F_{vh}(\omega)}{G_{\zeta.a}} = F_{vh.nor} \cdot \cos(\omega t)$$

$$F_{vh.nor}(\omega) := \frac{-C_m \cdot 2 \cdot \rho \cdot V_{hull} \cdot \zeta_a \cdot \omega^2 \cdot e^{\frac{-\omega^2}{g}(h_c+h_{pont})} \cdot \cos\left(\frac{\omega^2 \cdot b_0}{2 \cdot g}\right)}{G_{\zeta.a}}$$

Vertical force on 2 hulls
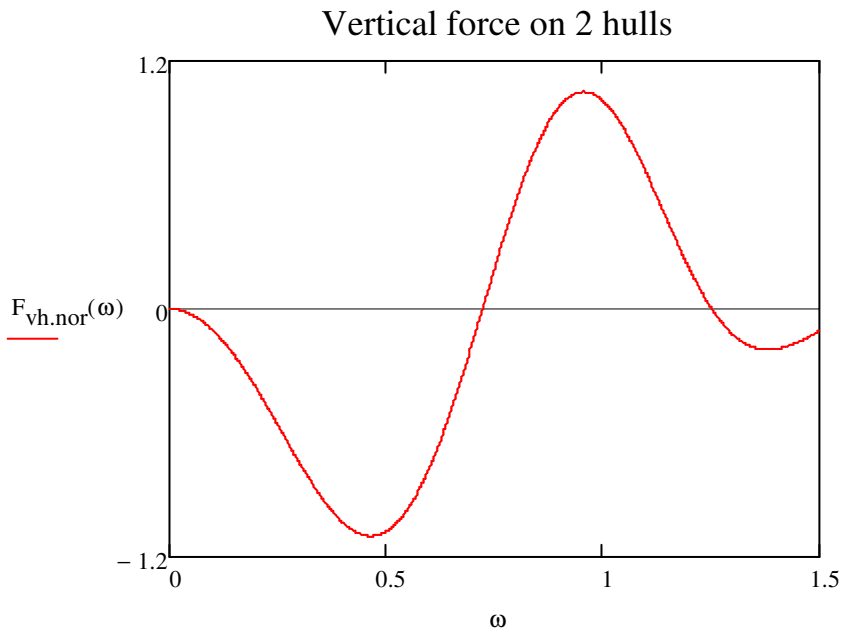
$F_{vh.nor}(\omega)$

Total vertical force

Vertical forces on one side of the semisubmersible:

$$F_{v.port}(\omega) := F_{3c.nor}(\omega) + F_{3h.nor}(\omega)$$

Vertical force on 2 columns and 1 hull

$F_{v.port}(\omega)$
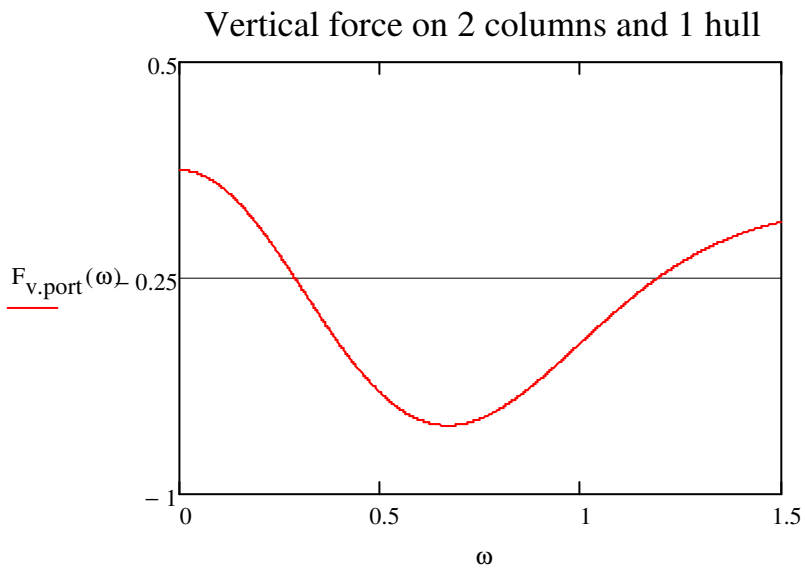
Total vertical force on semisubmersible:

$$F_v(\omega) := F_{vc.nor}(\omega) + F_{vh.nor}(\omega)$$

Vertical force on 4 columns and 2 hulls
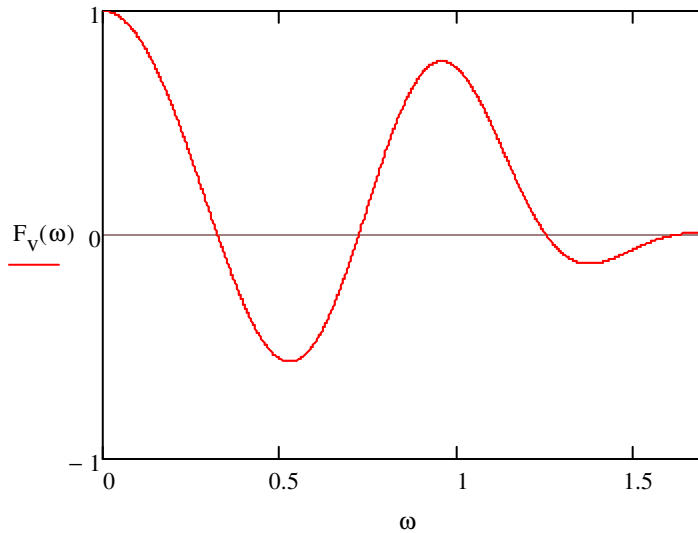
$$\omega_c := \sqrt{\frac{g}{h_c} \cdot \frac{n_0 \cdot V_{col}}{C_m \cdot V_{hull}}} = 0.307 \frac{1}{s} \cdot rad$$

Cancellation frequency according to ref [9]

$$V_{braces} := \frac{\pi}{4} \cdot l_{b.eqv} \cdot d_{brace}^2 = 1.909 \times 10^3 \cdot m^3$$

Total volume of braces

$$C_{A.brace} := 1$$

According to DNV RP-C205

$$V_{semi} := V_{hull} \cdot 2 + V_{col} \cdot n_0 \cdot 2 + V_{braces} = 6.288 \times 10^4 \cdot m^3$$

$$Depl_{semi} := V_{semi} \cdot \rho = 6.446 \times 10^7 \, kg$$

Displacement of semi including braces

$$\rho \cdot V_{semi} + m_{33} = 2 \cdot \left(n_0 \cdot \rho \cdot V_{col} + C_m \cdot \rho \cdot V_{hull} \right)$$

$$c_{33} := 2 \cdot n_0 \cdot \rho \cdot g \cdot A_c = 1.222 \times 10^7 \cdot \frac{N}{m}$$

Restoring term

$$\omega_R = \sqrt{\frac{c_{33}}{\rho \cdot V_{semi} + A_{33}}}$$

Natural frequency

$$\omega_R := \sqrt{\frac{c_{33}}{\left(V_{semi} \cdot \rho + C_a \cdot V_{hull} \cdot 2 \cdot \rho + V_{braces} \cdot \rho \cdot C_{A.brace} \right)}} = 0.286 \frac{1}{s}$$

$$A_{33} := C_a \cdot V_{hull} \cdot 2 \cdot \rho + V_{braces} \cdot \rho \cdot C_{A.brace} = 8.529 \times 10^7 \, kg$$

$$T_R := \frac{2\pi}{\omega_R} = 22\,s \qquad\qquad\qquad \text{Natural period}$$

The transfer function can in a complex form be given as:

$$H_{3z}(\omega) = \frac{s_{3a}(\omega)}{\zeta_a(\omega)} \cdot e^{i\cdot\varepsilon\cdot\omega}$$

$$\Omega = \frac{\omega}{\omega_R} \qquad\qquad\qquad \text{Frequency ratio}$$

$$DAF = \frac{1}{\sqrt{\left(1 - \Omega^2\right)^2 + (2\cdot\delta\cdot\Omega)^2}} \qquad\qquad\qquad \text{Dynamic amplification factor}$$

From the total vertical force, the transfer function of the undamped heave motion can be obtained with the two above given equations:

$$H_{3z}(\omega) = \frac{z_a(\omega)}{\zeta_a(\omega)} \cdot e^{i\cdot\varepsilon(\omega)} = \frac{F_V}{c_{33}\cdot\zeta_a} \cdot DAF \cdot e^{i\cdot\varepsilon\cdot\omega}$$

The transfer function can, if combined with the cancellation frequency, be expressed as [9]:

$$H_{3z}(\omega) := \left[\frac{1 - \left(\dfrac{\omega}{\omega_c}\right)^2}{1 - \left(\dfrac{\omega}{\omega_R}\right)^2} \cdot e^{\frac{-\omega^2}{g}\cdot h_c} \cdot \cos\left(\frac{\dfrac{\omega^2}{g}\cdot b_0}{2}\right) \right]$$
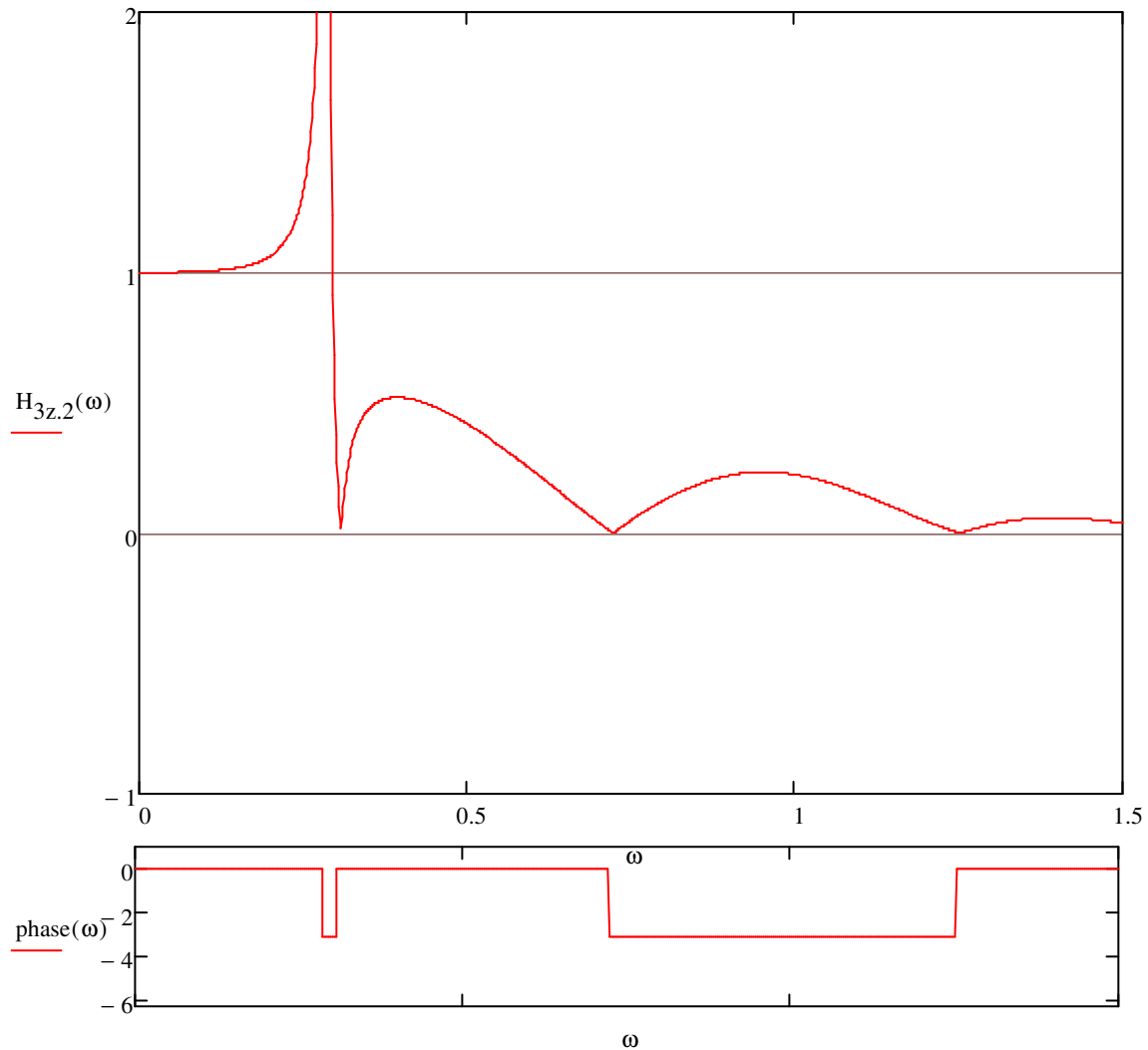
The numerical value of the transfer function can be obtained as:

$$H_{3z.2}(\omega) := \sqrt{\left[\frac{1 - \left(\dfrac{\omega}{\omega_c}\right)^2}{1 - \left(\dfrac{\omega}{\omega_R}\right)^2} \cdot e^{\frac{-\omega^2}{g}\cdot h_c} \cdot \cos\left(\frac{\dfrac{\omega^2}{g}\cdot b_0}{2}\right) \right]^2}$$

$$\underset{\sim\sim\sim\sim\sim}{\text{phase}}(\omega) := \begin{Vmatrix} 0 & \text{if} \ H_{3z}(\omega) > 0 \\ \\ (-\pi) & \text{if} \ H_{3z}(\omega) < 0 \end{Vmatrix}$$

If the transfer function is positive, then the motion is in phase with the wave elevation.
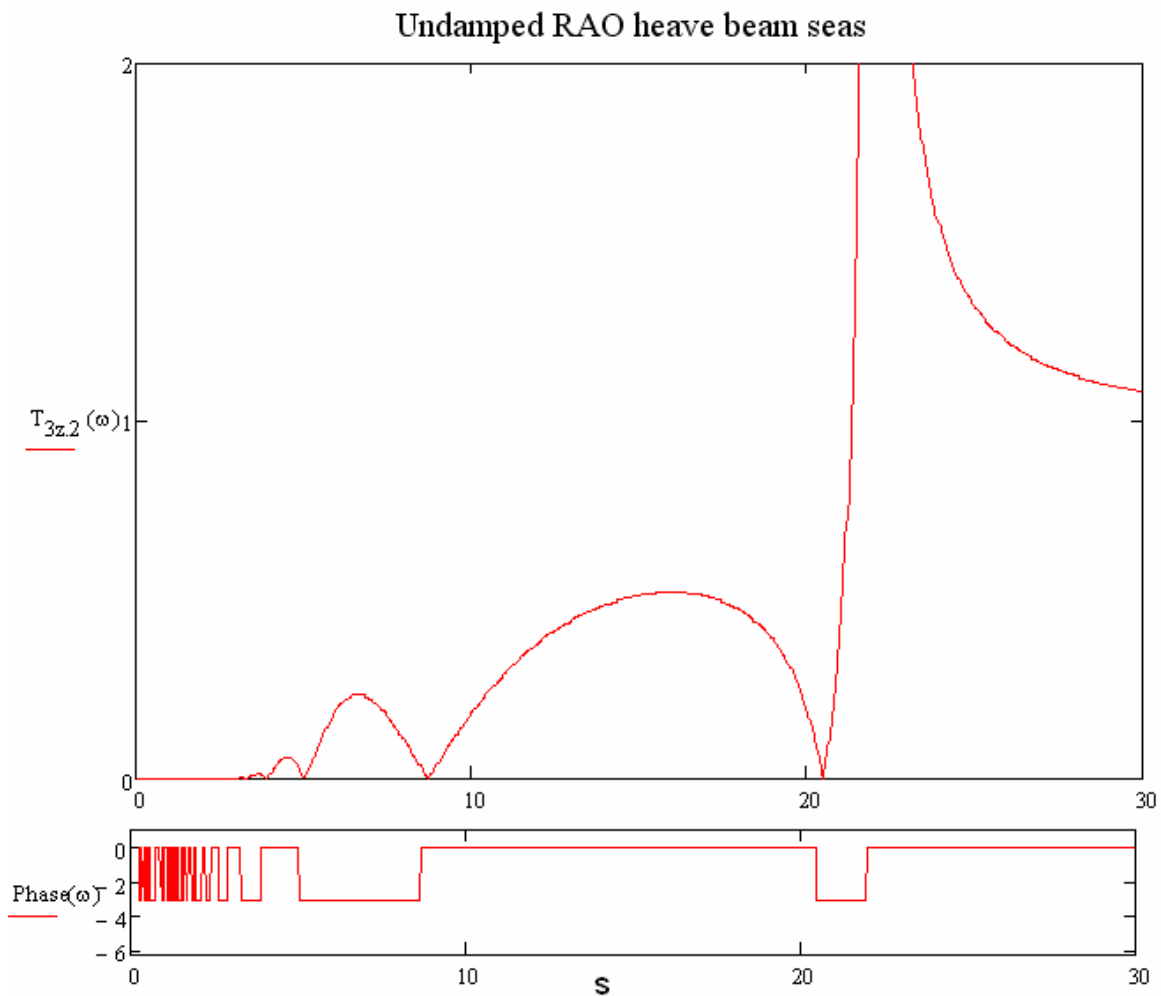
RAO heave

$$t(\omega) := \frac{2\pi}{\omega}$$

$$T_{3z.2}(t) := H_{3z.2}\left(\frac{2 \cdot \pi}{t}\right)$$

$$\text{Phase}(\omega) := \text{phase}\left(\frac{2 \cdot \pi}{\omega}\right)$$

$$\text{Phase}(\omega) := \text{phase}\left(\frac{2 \cdot \pi}{\omega}\right)$$

Undamped RAO heave beam seas

To calculate damped natural period dampening is introduced:

$\zeta := 0.3$

With a maximum dynamic amplification of 1.42, the dampening level is 0.3 according to figure 6.3 in the report.

$$\omega_d := \omega_R \cdot \sqrt{1 - \zeta^2}$$

Damped natural frequency

$$T_d := \frac{2 \cdot \pi}{\omega_d} = 23.054s$$

Damped natural period